Calibration study of Seekonk-Narragansett Bay (SNB) ROMS Model for Bullocks Reach section of the Providence River, RI

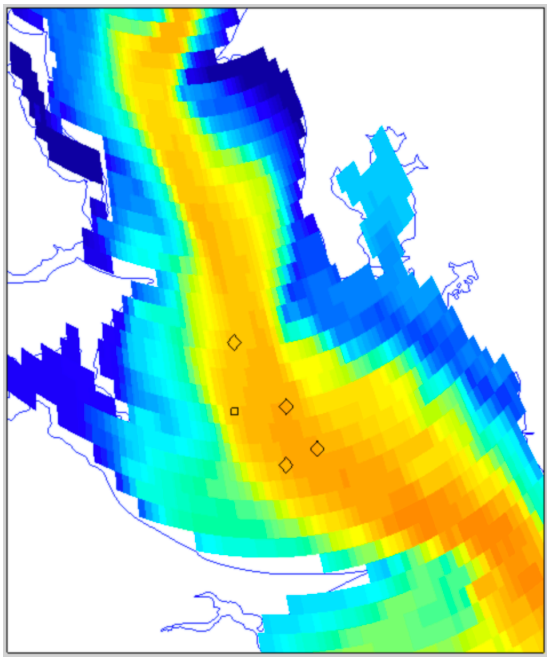

Report to the Narragansett Bay Commission
April 20, 2018

Prepared by Chris Kincaid, PhD

Professor, Graduate School of Oceanography, URI

1.0 Introduction

RI coastal waters are stressed by factors such as bacteria, invasive species, warming waters, low oxygen conditions and threats due to suspension and transport of chemicals of emerging concern residing in riverine sediments. Strategies to manage these and other estuarine stresses require improved modeling tools, capable of accurate representation of both hydrodynamics and ecosystem processes. At the foundation of these efforts are the physical processes that move, mix and flush the internal biogeochemical constituents to the water column. For more than two decades, systematic improvements have been made to modeling tools (Figure 1) for coastal physics through a combination of better, spatially and temporally detailed data sets (Figure 2) and improved modeling tools. This often involves picking sections of the estuary where models struggle to match observations, and performing a targeted data-modeling study in that region. This data-model cycle has been employed in numerous regions of the Bay, using the fixed buoy network (Figure 2) and using shorter term acoustic Doppler current profiler (ADCP) deployments and spatially-temporally detailed tilt current meter (TCM) deployments (Figure 2) (Kincaid, 2001a-c; Bergondo and Kincaid, 2005; Kincaid, 2012a,b). Results of these efforts have led to significant improvements in the ROMS modeling tools for Narragansett Bay. A number of acronyms are used throughout the report, such as ADCP. These are summarized in Table 1.

We present results from a targeted data-model study aimed at improving the Seekonk River – Narragansett Bay ROMS model (or SNB-ROMS) in the region of Bullocks Reach (Figure 2) and within the Seekonk River. Prior work comparing results with the fixed-site buoy network has shown the ROMS model has the most difficulty in matching hydrographic (T: Temperature; S: Salinity) values at the Bullocks Reach buoy (Tables 2-4; Figure 3). We combine moored ADCP and conductivity-temperature-depth sensor (CTD) (Figures 4-7) data with simulations using the high resolution SNB-ROMS (Kincaid, 2012) to improve understanding for conditions in this area that may provide a foundation for improving the model here, and throughout the estuary. Model results are also compared with time series data from another one of the fixed-site buoy locations, the Phillipsdale buoy located in the upper Seekonk River.

Results show the Bullocks Reach area is a smaller, but similar hydrographic system to the more studied Edgewood Shoals area. The Bullocks Reach buoy sits in a transitional zone for flow and hydrography between the artificially deeper, more dynamic shipping channel (>10m deep) and a shallow, western shoal (2-5m depth). Just as at Edgewood, dredging actions have created a strong mismatch in bathymetry between the channel and the shoals that accentuates hydrodynamic differences between the sub-regions. The Bullocks Reach buoy sits exactly within a transitional zone (6-9m depth) between these sub-regions. Data-model comparisons show the SNB-ROMS simulations do an exceptional job at matching sub-tidal flows and show that hydrographic mismatches between the Bullocks Reach buoy and the models can be due in part to strong lateral gradients that exist in this region. Where modeled T-S values differ from data at the buoy location, near-perfect matches can be found moving as little as 300m east or west from the buoy site. A series of sensitivity-parameter tests show that changes in modeled winds and river output can slightly alter T-S comparisons, but that these are small

compared with the persistent lateral differences in T-S that exist in the area. The largest parameter effect was found for changing the background vertical mixing coefficient. We only altered this very complex parameter in a very simple way (e.g., changing the constant background value). The size of the impact for this parameter in influencing flow and hydrography in this area, and the fact that vertical mixing relies in such a non-linear fashion on flow and stratification, warrants further study. Results also show the model has difficulty in matching hydrographic values observed within the Seekonk River, most notably under-predicting the salinity. Additional observational work is needed at the mouth of the Seekonk to determine how much of the mismatch is due to missed residual return flow into the Seekonk in the model, versus under-predicted salt flux.

2.0 Prior Work

A combination of current meter observations (Figure 2) and ROMS modeling (Figure 1) has led to an improved understanding of Narragansett Bay (NB) circulation (Rosenberger, 2001; Kincaid, 2001a-c; Kincaid et al., 2003; Bergondo, 2004; Kincaid, 2006, Bergondo and Kincaid, 2007; Kincaid and Bergondo, 2005; Kincaid et al, 2008; Rogers, 2008; Kremer et al., 2010; Pfeiffer-Herbert, 2012; Kincaid 2012a,b; Pfeiffer-Herbert et al., 2015). This work builds from basic circulation patterns defined in these prior studies. NB has been shown to circulate predominantly in a counterclockwise sense, with residual (or net non-tidal) flow up the East Passage and down, or out, the West Passage of the estuary. This large scale gyre stalls and spins up with northward and southward blowing winds, respectively. There are also counterclockwise sub-gyres within each passage (Kincaid et al., 2003). These persistent residual circulation patterns tend to carry water entering at any point (latitude) along the eastern side of the East Passage well northward into the system, as far as the Mt. Hope Bay, the Providence River or around the north end of Prudence Island and into the upper West Passage. It is important to note that this background style of flow in the Bay can be upset and altered by prevailing winds and runoff patterns.

In addition to these basin-scale flow patterns, a series of underway ADCP measurements (Kincaid, 2001a-c), moored ADCP deployments (Kincaid and Bergondo, 2005) and tilt current meter deployments (Kincaid, 2012a) supported by the NBC have documented localized circulation trends in the Providence River estuary. Targeted data circulation observational studies have also been carried out in other embayments, such as Greenwich Bay (Balt, 2013), Mt. Hope Bay (Kincaid, 2006; Deleo, 2003) and Bristol Harbor (Kincaid, 2014) (Figure 2). Results within the northern Providence River show the flow is characterized by a strong residual outflow along the western edge of the shipping channel and a strong residual inflow of deeper water along the eastern side of the shipping channel with weak, reversed flow of water in the shallow regions adjacent to the shipping channel. The most notable of these counter-rotating gyres, or eddies, occupies the shallow region of the Edgewood Shoals, west and south of Fields Point and west of the local trend of the shipping channel. However, underway ADCP data also show circulation gyres near Sabin and Gaspee Points, where flow is clockwise or counterclockwise for regions west and east of the channel, respectively. NBC funded bottom mounted ADCPs in the shipping channel and on the shoal near Edgewood reveal time characteristics of these prevailing subtidal flows (Kincaid and Bergondo, 2005).

The two-layer sub-tidal (or residual) flow in the shipping channel (surface out and deep in) is remarkably persistent. Moreover, time series data also show persistent layered flows can occur even on the shallow shoals. The moored ADCP and TCMs on Edgewood Shoals show the gyre is exceptionally stable, even to large forcing events like the 2010 flood, and that it exhibits surprisingly strong vertical structure. Surface water motion oscillates with the wind (Kincaid and Bergondo, 2005), but mid-water and bottom water subtidal flow continues a slow clockwise motion in the gyre (speeds of ~ 1-2 cm/s) (Kincaid and Bergondo, 2005, Kincaid, 2012a). Such slow, stable flow features imply water retention times are exceedingly high in such features. Experience with Edgewood Shoals spawned a hypothesis that the Bullocks Reach region, that also has a deep shipping channel and a shallow western shoal, can be expected to behave in a similar fashion.

While data provide an essential constraint on local circulation, it is the combination of these data with modeling results that enable us to build toward accurate predictive tools for managing the estuary. A benefit of model development in the upper Narragansett Bay is the extensive data available for comparisons. When modeled and observed hydrodynamic behavior compare well it improves the hydrodynamic foundation on which the ecological model rests. A number of studies have considered how well ROMS simulations do in matching both flow and hydrographic data collected in the Bay (Rogers, 2008; Kremer et al., 2010; Balt, 2014). Early coarse grid models produced instantaneous (or tidal) flows and sub-tidal flows that did not match the current meter observations in key areas such as the Edgewood Shoals (Kincaid, 2012). Solutions that could not match the flow data showing gyre recirculation incorrectly suggested this region was well flushed. An improved version of ROMS was developed, with a higher resolution and that included the Seekonk River. With ~30 m horizontal grid spacing (vs. > 150 m spacing in prior models), the SNB-ROMS was able to reproduce key aspects of the circulation, including the clockwise gyre on the Edgewood Shoals. Willmott model skill values for instantaneous data-model records (e.g., including tidal responses) are typically >0.9 for surface elevations, water currents and hydrographic parameters (salinity, temperature) (Balt, 2014), often exceeding 0.95. Subtidal flow patterns that are most important for controlling long-term biogeochemical transport and flushing processes are challenging to match well because they are significantly lower energy than instantaneous or tidal variations. A dye circulation study with the SNB- ROMS shows that the model does well at simulating residual flows recorded by TCMs, even given the extreme discharges from the 2010 sampling period. Willmott skills of >0.8 are calculated for periods before, during and after the 2010 flood (Kincaid, 2012a).

A primary motivation for this study comes from a recent skill assessment performed by D. Ullman (URI-GSO) that compared ROMS predicted tidal elevations (Table 2), currents (Table 3) and hydrographic parameters (temperature and salinity) (Table 4, Figure 3). The comparison was performed using 2006-2007 data for tidal elevations from NOAA-PORT and currents from moored ADCPs in the West Passage and East Passage, near the north end of Prudence Island. In line with other studies (e.g., Rogers, 2008), ROMS Willmott skill values are very high at over 0.9 for tidal water levels (Table 2). Instantaneous currents (without the tides filtered out) are also well represented in models

(skills > 0.8) (Table 3). More challenging are the residual or subtidal currents. As summarized above, the SNB-ROMS model generates higher subtidal circulation skills within the Providence River (Kincaid, 2012a). The final part of the recent skill assessment was for hydrography. Here SNB-ROMS output was compared with T-S data from the fixed buoy network in the Bay. Table 4 shows the model does exceptionally well with all buoys except Bullocks Reach, where the bottom salinity skill is low. Figure 3 shows the time series data-model comparison at this site, where ROMS bottom salinity is clearly too fresh and bottom temperature is also tending to be too warm. A goal of this work is to further explore why there is a persistent mismatch between ROMS output and the Bullocks Reach buoy.

The process of calibrating the ROMS model with data from TCMs greatly improves the usefulness of the models in quantitatively mapping relationships between flow, flushing and transport in the estuary and how these impact ecosystem processes. The SNB-ROMS model was subsequently used to study dye transport/dispersion for distinct dye fields representing each major river and major WWTF releasing to Narragansett Bay for the spring-summer 2010 period (Kincaid, 2012b). Dye inputs were used to document transport/flushing pathways for each source, given a range of environmental forcing conditions. Results from these simulations show 3-D circulation leads to often unexpected patterns: 1) deep northward transport carries Taunton River dye well into the Providence River, 2) Edgewood Shoals is supplied primarily with chemical inputs from the Blackstone and Pawtuxet Rivers, 3) the Pawtuxet River chemical plume bifurcates into distinct regions, a surface plume that advects south along the western Providence River, an intermediate depth plume that moves onto Edgewood Shoals, and a deep plume that moves northward in the shipping channel (Kincaid, 2012b). Most recently, the SNB-ROMS model has been combined with a Franks-NPZD (N=nitrogen, P=phytoplankton, Z=zooplankton, D=detritus) to study ecosystem dynamics in the Bay (Kincaid, 2018). The study focused on a major bloom in the summer of 2010. The model was able to reproduce the timing and magnitude of the bloom. An interesting outcome of the work was that phytoplankton blooms tended to initiate in the mid-Bay (Greenwich Bay, Ohio Ledge, Mt. Hope Bay) and progress northward. This occurred when phytoplankton fields were carried northward into the Providence River in the northward (inward) residual flow, accessing the higher nutrient concentrations of this sub-region. A detailed ecosystem parameter sensitivity analysis was conducted that showed which factors most controlled the magnitude of the 2010 bloom event. Key factors included phytoplankton growth rate, zooplankton grazing rate and light extinction coefficients. Models also tested how simulated nutrient release levels from waste water treatment facilities (WWTFs) compared with these factors and other environmental forcing factors (winds, tides, runoff) (Kincaid, 2018). WWTF reductions in total nitrogen from 15 to 5 mg/l produced a noticeable impact on the size and duration of the simulated blooms, albeit smaller than the parameters controlling phytoplankton growth/death. Reductions from 5 to 3 mg/l and 3 to 0 mg/l had very minor impacts on bloom magnitude.

3.0 Methods

Work on this project involved comparing new SNB-ROMS models with new ADCP/CTD data (Figures 4-7) and Bullocks Reach buoy data collected in summer-fall of

2016.

Observations:
A goal of this work is to test the solutions for the SNB-ROMS model in the vicinity of the Bullocks Reach buoy (Figure 5). A bottom moored, upward looking 600 kHz RD Instruments ADCP was deployed in a trawl resistant mount at latitude 41.7324 and longitude -71.3688, just south of the Bullocks Reach buoy on 7/29/16 (Figure 4). The ADCP transducer sat 0.5m above the bottom and data were recorded in 0.5m vertical bins until recovery on 10/27/16. Mounted within this frame was an internally recording Seabird CTD. The instrument package was placed in the water at a depth of 7 to 8m. Both the ADCP/CTD mooring and the Bullocks Reach buoy lie in a transitional bathymetric zone, between the relatively deep, dredged shipping channel (>10m depth) and a broader, shallow (<2m deep) shoal to the west (Figure 5). The width of this region is roughly 300-400m, or similar to the width of the channel.

SNB-ROMS Model: To simulate coastal circulation patterns, we use the three-dimensional (3-D) Regional Ocean Modeling System (ROMS) hydrodynamic model (Shchepetkin and McWilliams, 2003; 2005). ROMS is a split-explicit, free-surface, primitive equation model with curvilinear and terrain-following coordinates. Using the curvilinear capabilities of the grid, the original NB-ROMS model utilized a computational grid for the full extent of Narragansett Bay which focused resolution towards the northern end of the estuary (Figure 1). Horizontal spacing of grids varied from 300m in the south, near the Bay mouth, to roughly 30m in the vicinity of Fields Point, RI. Fifteen vertical (or sigma) layers in the model resulted in a vertical resolution that varied locally with the water depth (e.g., water depth divided by 15 vertical levels). The use of sigma coordinates in ROMS allows for modeling circulation in the presence of varying bathymetry.

Simulations using the SNB-ROMS model are run for 2016 environmental conditions, coinciding with when the ADCP and CTD were deployed just south of the Bullocks Reach buoy (Figure 5). Freshwater discharge applied at primary river sites of the Blackstone, Pawtuxet, Taunton, Ten Mile, Woonasquatucket, Moshassuck, Palmer, and Hunt/Green. Two Greenwich Bay rivers are included, Harding Brook and the Muskerchug River. Winds and atmospheric air-sea flux conditions are applied at the surface and conditions on water velocity, temperature and salinity applied along the open ocean boundary of the model (e.g., the mouth of Narragansett Bay). A nesting procedure is used to apply conditions at the mouth of the estuary. Values for water velocity, temperature and salinity are applied along this boundary from information supplied from the coarser, but spatially larger Rhode Island Sound (RIS) ROMS model (Figure 1) (Rogers, 2008; Pfeiffer-Herbert, 2012) that covers all of RIS. The RIS ROMS model is, in turn, forced at its open boundaries by information provided from the ROMS-ESPRESSO model of the Mid-Atlantic Bight (http://www.myroms.org/espresso/) (2016). As recommended by Janekovic and Powell (2012), separate applications of tidal forcing were applied around the RIS ROMS boundary using tidal harmonics from the ADCIRC model of the U. S. East Coast (Mukai et al., 2002; http://www.unc.edu/ims/ccats/tides/tides.htm)(2016).

Models are spun up from June 27, 2016 (day 180), where an initial T-S conditions file for the SNB-ROMS grid was produced from simplified salinity (S) and temperature (T) averaged for this time period from 2010 model output. This represents a representative early summer hydrographic state. A 30-day simulation was run from this point with 2016 forcing (Figures 8-11) to bring the model into a representative 2016 starting condition on day 210, or the start of the ADCP/CTD record (Figure 8). Wind forcing for the RIS-ROMS is applied from meteorological data from the Buzzards Bay monitoring station (www.ndbc.noaa.gov/station=buzm3) (2016). Wind forcing for the SNB-ROMS grid covering Narragansett Bay is constructed by taking an average of wind speed and direction at three real-time physical oceanographic real-time system sites (PORTS) (http://tidesandcurrents.noaa.gov/ports.html) (2016), including Providence (RI), Quonset Point (RI) and Newport (RI) (Figure 9). Air temperature (Figure 8) is taken from the Providence station, as this is closer to the region of interest. Radiative surface heat flux and relative humidity data used in forcing ROMS were obtained from the North American Regional Reanalysis data set (http:/www.emc.ncep.noaa.gov/mmb/rreanl/). Precipitation data were gathered from T.F. Green International Airport (Station ID GHCND:USW00014765, http://www.ncdc.noaa.gov/cdo-web/search) (2016).

Model runs use information on runoff temperature from a NOAA PORTS water temperature record (Figure 10) and runoff volume flow from the United States Geological Survey records (http://waterdata.usgs.gov/nwis/dv) (2016) (Figure 11). River temperature data are from the Providence station surface water temperature. A data gap at the start of the sampling period was filled by interpolating 2016 river temperatures for the missing period that are guided by the seasonal bounds of the 2010 record for this same period. In the development of ROMS for Narragansett Bay, an analysis has been done to correct river discharge values by determining the extend of un-gauged drainage areas, below the last gauging station and correcting published data values by a scale factor (Kremer et al., 2010). River transport for systems without gauged data is produced using watershed area ratios between these and the gauged Blackstone River. A river transport time series for an ungauged river is then produced for 2016 based on the watershed ratios and the measured 2016 Blackstone curve (Figure 11).

Air temperatures during this deployment period increase from 20°C to ~30°C in mid-August. After this period there is a steady decline in average air temperature to ~15°C in early October (Figure 8). Winds are predominantly blowing northeastward during this period, with significant oscillations about this average (Figure 9). There are a number of events involving rapid change from northward to southward blowing winds, such as an event on day 235. There is also a period of strong, sustained southwestward winds in early September, around day 250. Runoff is very low (<10 m^3s^{-1} in the Blackstone River) for the majority of the deployment period (Figure 11).

To best characterize how data and models compare, and how local spatial-temporal processes might influence data-model comparisons, a new SNB-ROMS stations file was developed. ROMS output involves 3-D velocity, temperature and salinity, along with numerous other parameters, such as turbulent mixing factors, water level, etc.

Information is output on the full grid (350x175x15 nodes) at sparse time intervals (every 6 hours) based on available memory restrictions. This same information is output at a select number of locations, called "stations", at much higher frequency to provide better temporal data coverage (30 minute sampling). A new stations file was produced for these runs that includes a dense grid of SNB-ROMS output locations in the Bullocks Reach area (Figures 12-13), with a new station added for model information at the location of the Phillipsdale buoy in the Seekonk River. Much of the analysis and discussion of results is focused on a select number of these stations, shown in Figure 14. The ROMS station at the ADCP/CTD/Bullocks Reach buoy site is 253. Key additional stations run in a channel-perpendicular orientation through the ADCP/buoy site, from 254 located in the channel, to 252 and 251 on the shallow western shoal. Stations 246 and 260 are oriented in the same bathymetric transition zone as station 253, but in a channel-parallel orientation that is down-estuary and up-estuary, respectively.

4.0 Results:

Results are presented from SNB-ROMS model simulations for summer-fall 2016 that coincide with an ADCP-CTD deployment at the Bullocks Reach buoy site (Bullocks Reach buoy). Data-model comparisons are first made for hydrographic parameters (salinity/temperature) and circulation patterns for a reference case, which utilized the best representation of the environmental forcing values for this period (Figures 8-11). Results are then presented from a series of model runs that explore how changes in wind, runoff and mixing factors alter both hydrography and flow in the region, and how these in turn influence the match between data and model output.

4.1 Reference Case Results

Temperature and salinity plots are summarized for the SNB-ROMS simulation period of days 210- 250 (7/27/16-9/5/16) in Figures 15 and 16. Shown as colored lines are modeled near-surface, mid-water column and near-bottom temperatures and salinities. Surface water is warmer and fresher, exhibiting stronger oscillations than deeper water. Prior to day 235, there is a roughly 4°C difference between surface and bottom values. The water column thermally mixes on day 235 and after this period, although limited thermal stratification reestablishes, there begins a linear cooling trend in the ROMS output. For salinity, the surface water experiences a freshening period from day 225-230, and again on day 235. Interestingly, during the day 235 event ROMS predicts more thermal mixing of the water column than occurs in the salinity.

The black line in Figure 15 shows bottom temperature/salinity from the CTD deployed within the ADCP. Salinity trends (blue vs. black) are similar for model and data, lying between 28-30 ppt. Generally, the data and model trends (increasing or decreasing) are in agreement, as highlighted with dark arrows (dashed arrows show where trends are not similar). Typical Willmott Skill calculations provide a record long or record average of how well time series curves match. Data-model comparisons in Figure 15 show there is significant complexity in the thermal records that would be masked by a simple skill calculation. During the period marked (I), before the day 235 mixing event, the ROMS bottom temperature is offset to cooler than the data by ~2°C, but the two records

generally follow similar trends (increases/decreases, highlighted with arrows). The magnitude of the bottom data tracks more closely with the ROMS mid-water record, located ~2m higher up in the water column. After the day 235 event, the observed bottom temperature more closely tracks with the ROMS surface record, suggesting the simulated water column is too cold.

During this period, there is also hydrographic data available from the Bullocks Reach Buoy. In Figure 16 we plot similar hydrographic records as Figure 15, but now include only surface and bottom records to bring out comparisons with both Bullocks Reach buoy surface and bottom values and ADCP/CTD bottom data values. It is reassuring that both bottom water sampling stations are in agreement. ADCP/CTD salinity and temperatures match those from the Bullocks Reach buoy. ROMS surface temperatures match very closely with observations, with the exception of a warming event days 226-229 that does not occur in the simulations. This is because there is no warming signal in the air or river temperature input files for this period. Additional data are required to add this feature to the forcing files. One last notable feature of the comparison is that surface salinity at the Bullocks Reach buoy is consistently saltier than ROMS surface values. This suggests that increasing river flows to warm the bottom water will not work, as this would serve to further freshen the water, increasing this surface data-model mismatch.

A fundamental result of these models is to highlight how potentially strong the lateral gradients are in the area of the Bullocks Reach. In channel-perpendicular cross section, the local region around the Bullocks Reach buoy transitions quickly from deep channel to shallow shoal. As outlined in Figure 5, the buoy (and ADCP/CTD) sits within a transitional region between channel and shoal. Figure 17 is similar to Figure 15, but for ROMS output from station 252, lying 270 meters to the west of the ADCP/CTD (station 253). The water is shallow here (~2m), reflected in the strongly mixed water column. Surface (red), mid-water (green) and bottom (blue) ROMS records all plot together, reflecting a vertically mixed water column. The water temperature of the shoal in Figure 17 matches very well with the bottom water at the ADCP/CTD. However, although this surface water is saltier on average than at the ADCP site, it is fresher than both surface and bottom values recorded at the Bullocks Reach buoy. Figures 18 and 20 show how lateral changes in near-bottom ROMS temperature and salinity compare with values recorded at the ADCP site. Records from station 254, in the channel, at a 7m depth equivalent to that of the ADCP depth just 270 meters to the west, show a good fit for salinity. Figure 19 shows ROMS output from stations located in the transition region where the ADCP/Bullocks Reach buoy sit, but that lie further up-estuary (station 260) or down-estuary (station 246) (see Figure 14 for locations) from the ADCP/buoy at Station 253. ROMS time series output shows consistency in absolute values and trends between these three channel-shoal transition zone stations (246, 253, 260).

The spatial patterns that exist in and around the Bullocks Reach buoy and how these might explain data-model mismatches in this location are further summarized in Figures 20-26. In Figure 20 the differences between ROMS bottom water T-S output and the ADCP/CTD T-S records over the day 210-250 interval are averaged. These differences give a measure of how far away the records at each of the surrounding stations are from

the data at the fixed site (Station 253). The dark circles represent differences along a channel-perpendicular trend passing through the ADCP/CTD site location. Stations that are up-river from this line are represented with red circles (getting smaller with distance from this trend line). Down-stream station comparisons are plotted as blue circles. The plots show a couple of key points. The data-model match for bottom water varies in a predictable pattern across the channel. Exact matches can be had between data and models with simple 250-300 m lateral shifts in properties. A perfect match for temperature could occur if water just to the west made it to the mooring spot (Figure 20b). A perfect match for bottom salinity could be had if 7-8m deep water from just to the east in the channel were shifted to the mooring location (Figure 20 c). The plot also shows that water from just up- or down-estuary is advected or mixed to the mooring site, a nearly perfect match would result (e.g., bottom temperatures up- or down-estuary from the zero or reference station in Figure 20b).

The combined data-modeling study of the Bullocks Reach region shows the shoal area just to the west of the station is complex, and can be fed with saltier water from the south or fresher water from the north and that the Bullocks Reach buoy sits just west of the distinct T-S water of the channel, where subtle lateral shifts of hydrographic gradients can result in big changes in data-model mismatches. Figures 21-26 support these points with mapview color contour plots of ROMS temperature and salinity plots for near-surface, mid-water and near-bottom depth levels. Figures 21-22 are near-surface temperature and salinity maps over intervals of 6 days. The shoal area (highlighted in red in frame b) oscillated between being fed with cooler/fresher water from the north or slivers of warmer/saltier water from the south (Figures 21b, 21g, 22b, 22g).

At both mid-water (Figures 23-24) and near-bottom (Figures 25-26) water-column depths the complex differential evolution of T-S conditions between shoal, transition region (where Bullocks Reach buoy and ADCP/CTD are located) and channel are highlighted in mapview plots. Focusing on the black square in these plots (the buoy/mooring site/station 253) shows how changes in ROMS predicted T-S at the site could be a function of delicate lateral shifts in channel versus shoal water masses. Conditions of these are in turn affected by local mixing of shoal water, channel-parallel subtidal transport flows bring water from either up-estuary or down-estuary past the site and cross-channel flows (often referred to as transverse circulation) that can carry very different shoal vs. channel water masses past the site. It is important to note that in Figures 21-26 these are contour plots of T-S conditions at similar sigma levels, which stretch in the vertical moving from the 2m shoal through the 7m transition region to the 15m channel. Values for sigma level 10 across this region are 0.7m, 2.5m and 7m depth for shoal, transition and channel, respectively. The shifting of water from one bathymetric region to another is complex and can include upwelling or downwelling and/or lateral or vertical mixing. A point of the plots is to show how sharp the lateral differences in properties can be between different depth regions that are available to alter the time series record at Bullocks Reach buoy given even small changes in turbulent mixing and lateral/vertical advection.

We next present results on circulation from the ADCP and ROMS in the Bullocks Reach area. Circulation in estuaries is often discussed in terms of instantaneous values,

reflecting oscillatory motions due the flooding and ebbing of the M2 tide, and the subtidal flows. The latter have the tidal motions filtered out and reflect more the longer term transport patterns for water and the hydrographic-biogeochemical properties of the water. Instantaneous flows are larger in amplitude in this area, from 0.2 m/s inflows to 0.3 m/s outflows (Figure 27). As has been shown in prior studies, ROMS does well at matching the observed tidal flows, shown in Figure 27 as north-south components of motion. Figure 28 shows the east-west, or transverse component of motion. An interesting feature here is that ROMS under predicts the magnitude of the tidal oscillations in the transverse direction by a factor of 2.

Transport patterns are reflected in the subtidal circulation patterns. Figures 29-30 show the near-bottom, mid-water and near-surface subtidal north-south and east-west flow rates for both ROMS (station 253) and the ADCP data. The ROMS output matches very well with the data values. At mid-level, both methods show the water moves on-average in a northwestward direction, with larger values 0.01-0.05 m/s in the northward direction than the westward direction (~0.02 m/s). The near-bottom records (Figure 29b) show a very interesting result. While the data and ROMS patterns tend to agree well, the model does under predict the magnitude of the westward component of motion past the site, which would be transporting saltier water from the channel past the mooring site (shaded region in Figure 29b). This could be one explanation for why model salinities are lower than data values. The northward component of motion of near-bottom water shows a remarkable fit between ROMS and the ADCP. They match both in magnitude and in the timing, duration and amplitude of oscillations/intrusion pulses (Figure 29b).

For near-surface levels, ROMS generally fits the trend in ADCP data for the westward component of motion and under predicts by 50% the component of net southward flow at the site (Figure 30). This is likely the result of a lateral offset of the outflow jet in this area between the model and data. The lateral variability in ROMS subtidal flows over three distinct depths is summarized in Figure 31. Here the flow velocities have been transformed into channel-parallel and channel-perpendicular components. The inner-most western shoal shows highly oscillating subtidal flow, with almost no trending transport direction. This is in both along and across channel directions (Figure 31a). The zone of maximum shallow subtidal outflow is seen to occur in the models at stations 252 and 253, located in the outer/deeper western shoal and in the transition region, at the ADCP/buoy. At station 252 outflows can reach 0.15 m/s, but these are short-lived, and offset with periods of no-motion. The most consistent southward flow is in the transition region (station 253). Here a very stable, persistent 0.05-0.1 m/s outflow of surface water occurs above the lower 2/3 of the water column. The deeper water moves inward (channel-parallel, up-estuary) at a subtidal rate of ~0.05 m/s. In the deeper channel the channel-parallel subtidal outflow is weaker, more consistent with the shallow outflow recorded at the ADCP (Figure 30). This suggests the outflow jet maximum in the model might be west of the actual feature in the estuary. Underway ADCP in this area could show if the outflow jet is stronger in the channel, east of our moored ADCP. Channel-perpendicular records in ROMS show/predict a consistent pattern of transverse circulation, with near-surface water moving from the channel towards the shoal and deeper water moving from shoal to channel.

The final velocity plots for this reference case using actual 2016 forcing data are shown in Figure 32. Here channel-parallel and channel-perpendicular flows are compared for three stations aligned along the transition region between shoal and channel. These are stations 253 (site of the buoy and ADCP), 246 (southeast of the ADCP) and 260 (northwest of the ADCP). ROMS predicts that subtidal flow patterns, both for inflow/outflow and transverse flow, are strongly consistent within this transition region between shoal and channel. All show surface outflow underlain by slightly weaker inflow throughout the lower 2/3 of the water column. The transverse pattern of surface from and bottom towards the channel is also consistent between these stations.

4.2 Parameter Study Results

While no single numerical model can be expected to perfectly match the natural system, models provide a number of valuable benefits for understanding essential processes. Results so far have shown that data-model comparisons are particularly tricky in the area of Bullocks Reach. This is because the area has such strong bathymetric gradients that help to generate strongly varying hydrographic and hydrodynamic gradients over very small spatial scales. Models can be producing nearly perfect conditions in the area, but show a data-model mismatch simply because modeled features are slightly displaced east or west of the data moorings. As summarized in Figures 29-31, the ADCP seems to be measuring outside of the peak surface outflow, which is presumably situated east of the mooring location, in slightly deeper water. ROMS predicts the peak subtidal outflow is at the mooring site. Even if hydrographic fields were perfectly matched, this difference in the peak inflow/outflow location along with the under representation of transverse tidal mixing energy by 50% in ROMS, is enough to generate the observed mismatches in salinity and temperature for the Bullocks Reach buoy. It is also likely that hydrographic input parameters, such as river temperature, river salinity, evaporation effects in shallow retention area, surface thermal fluxes, and groundwater input along the edges of the estuary that is presently unaccounted for in the models, could explain a portion of the remaining data-model mismatch in the very complex Bullocks Reach area.

A strength of models like SNB-ROMS is the ability to test the role of numerous input and forcing parameters on the solutions and the data-model comparisons. A second part of this study involves testing the sensitivity of solutions to alterations in winds, runoff and internal mixing characteristics. Figure 33 summarizes schematically the range in cases for rivers and wind forcing. A series of runs were performed where the strength of the closest large river, the Pawtuxet River, is modified. The river volume flux was multiplied by reduction/enhancement factors of 0.7, 1.5, 2 and 3. A single case was done (BP1.5), where both the Pawtuxet and Blackstone River volume fluxes were multiplied by 1.5. Modifications to winds were also attempted. One factor roughly takes into account local geometries that could alter the wind vector values obtained from distant NOAA-PORT stations and applied uniformly to the water surface (Figure 34). This is the so called fetch effect. The orientation of the long-axis of the Providence River is in the northwest-southeast direction. This should mean that the eastward direction has less fetch (length that wind blows unhindered by land, across water). A number of runs

were conducted where only the east-component of wind was modified, either reduced by a factor of 0.25, 0.5 or 0.75, or increased by a factor of 1.5. Two runs simulated an enhancement of southward blowing wind components (by factors of 1.5 or 2.5) to test if these conditions led to stronger intrusions to the Providence River of cold, high salinity water. The final parameters to be tested were the background values for vertical and horizontal mixing coefficients. The latter produced no effect and is not reported on here. Vertical mixing involves a turbulent closure scheme, where mixing magnitude varies nonlinearly with changes in vertical water column shear and stratification levels. Outside of the nonlinear regime, vertical mixing reduces to a background, or constant reference value. Runs were done with K_v=0.2 and K_v=5 m^2/s.

Figures 35-38 summarize the relative impacts on circulation of a number of these parameter sensitivity cases. Reducing the Pawtuxet River to 70% of its original volume flux has no discernable effect on either the larger channel-parallel subtidal flows or weaker channel-perpendicular flows (Figure 35). Increasing the flow by a factor of three produces only a minor change in the near-surface channel-parallel outflow record at station 253, but does produce a noticeable stalling-rebound event in the transverse that mimics data (Figure 35a-bottom, day 227). Results for cases with enhanced southward winds are shown in Figure 36. These are able to enhance the size of the deeper return flow up estuary as seen in events on days 211, 220, 227, 230 and 235 (Figures 36b-top, 36c-top). The case with southwards winds increased by 2.5 times produces an instability during the day 235 event that killed the run. Very little effect on subtidal flows is evident in cases that alter the eastward component of wind (Figure 37).

It is interesting that the parameter that produces the biggest effect on subtidal velocities at the ADCP location (station 253) is also the most poorly understood coastal physics parameter, the vertical turbulent eddy mixing term. Figure 38 summarizes the effect on ROMS currents of reducing or increasing the background value for this parameter, K_v from a reference value of 1 m^2/s. Decreasing K_v decreases the size of the subtidal surface outflow recorded at the ADCP location. Alternately, increasing K_v greatly increases the size of this outflow, both increasing the magnitude of the flow and decreasing the oscillations in this outflow, in effect making it more of a steady state feature (Figure 38a-top). The larger K_v also generates stronger deep channel-parallel inflows and, while they are generally smaller in magnitude, also produces enhanced near-bottom flow of water from the mooring location towards the channel (e.g., more water moving from the shoal to the ADCP). The impact of K_v on bottom water is highlighted in more detail in Figure 39. Here the enhanced subtidal velocities are more clearly seen for higher K_v. Interestingly, the impact on temperature-salt transport appears to be dominated by transverse flow. Values recorded at the ADCP/Bullocks Reach buoy location show a warming to produce an improved match with data, but also a freshening, that worsens the match with observed salinity. Further studies should continue to test the combinations of parameters that allow ROMS data at the Bullocks Reach buoy site to warm and increase salinity at the same time. While the salinity remains difficult to match even in the channel, the higher K_v leads to much stronger bottom temperature matches at stations from shoal to channel (Figure 40).

As summarized at the end of the results section 4.1 for the reference ROMS case of actual environmental forcing conditions, the Bullocks Reach region is one with very complex bathymetry and related hydrodynamic and hydrographic spatial-temporal patterns. Figures 41-44 use mapview color contour plots to represent how the strong lateral gradients in temperature and salinity coincide closely with the location of the Bullocks Reach buoy and ADCP/CTD mooring (circled in plots). Comparing the top row (reference cases at various times) with bottom rows (cases with higher K_v=5 m^2/s) in Figures 41-42 reveals how warming occurs at the mooring site in simulations with a higher vertical mixing term. Figure 43 shows how freshening occurs in bottom water at the mooring site for this parameter case. While the flow data did not show a large difference in values for cases with modified eastward wind magnitudes, Figure 44 illustrates in mapview how reductions in eastward wind, which is consistent with reduced fetch along this direction, can result in higher salinity water recorded at the mooring/buoy site.

5.0 Discussion

5.1 Bullocks Reach

Results of SNB-ROMS simulations and analysis of moored ADCP and CTD data in the Bullocks Reach area reveal the extreme levels of complexity involved with transport and mixing processes between shallow shoal, deep channel and the intermediate transition region where the instrument moorings reside. This study was motivated by a detailed sensitivity analysis of ROMS versus all fixed site buoys that showed Bullocks Reach had the largest, most consistent mismatch between modeled and observed temperature-salinity. Results of this work suggest this is not unexpected given the complexity of the channel-parallel flows, transverse flows and local hydrographic gradients. These are summarized schematically in Figure 45, along with changes in bathymetry. Very stable flow features are the subtidal inflow of deep channel water that carries cold/salty water northward into the estuary. A shallow outflow jet running parallel to the trend of the channel, that carries fresher water is also a well-documented feature (also shown schematically). Without more data on currents, it is unclear as to how far east of the mooring the core of this outflow resides. The ADCP mooring deployed for this project shows only weak surface outflow. What is surprising is that most of the channel-parallel water flow past the ADCP mooring and the Bullocks Reach fixed-site buoy is from the south, not the north. Given that there is a relatively weak, but persistent component of northward and eastward flow of deep water past the ADCP site suggests that much of the transition zone water between shoal and channel where the Bullocks Reach buoy resides is supplied from the broad shallow shoal region lying to the southwest of the data collection site. Just as the Edgewood Shoals in the north is a complex system, with its own stable circulation and hydrographic system, the Bullocks Shoal is also likely to provide a home for a complex mixing/retention zone which could be supplied with water that is warm but could be either high or low salinity (as depicted in the Figure 45 schematic). In order to further determine the source of the data-model mismatch at the Bullocks Reach buoy, additional observational work is needed on the shoal.

The fact that ROMS significantly under represents transverse tidal mixing energy (Figure 28) could mean the models miss lateral/upslope mixing of deep channel water to the buoy

site. This could lead to increased salinity (improved data-model match) required at both surface and bottom locations (Figure 16). The problem is this should lead to cooler temperatures at the buoy where the comparisons require warmer water in ROMS. It could be that enhanced mixing with warmer waters towards the shoal could produce mooring site values that are warm enough. What is clear is that enhanced river flows do not help the salinity deficit in ROMS in this region relative to data. More likely is that subtidal intrusions of salty water up the channel and intruding up onto Bullocks Reach Shoal is under predicted in ROMS. This is consistent with findings at the mouth of Narragansett Bay (Pfeiffer-Herbert, 2014).

5.2 Phillipsdale Fixed Site Station

All model results produce output in the Seekonk River, which is a relatively new feature of the Narragansett Bay ROMS model. Station output was recorded for each simulation near the location of the Phillipsdale environmental fixed site station in the upper Seekonk River. Figure 46 shows comparisons of buoy data time series records for surface and bottom salinity and temperature. These are compared with ROMS values for this same time period. The system is fairly well mixed thermally, and data and model temperatures are generally closely matched. Data from this fixed-site buoy show surface values record a larger amplitude tidal oscillation, suggesting tidal velocities are higher in this section of the river and/or lateral thermal gradients are higher than ROMS is predicting. This record also shows the large warming event starting near day 225 that is present in the Bullocks Reach buoy data. A question remains if this is driven by surface heating or river input temperatures which could be factored into the model. The model could test whether this thermal pulse also explains the relatively warmer temperatures in the data than in the model following the day 225-229 warming event. More notably however, the ROMS salinity values are significantly lower than those recorded at the Phillipsdale fixed site station. It would be important to better understand if ROMS is accurately representing the subtidal inflow of water and salt near India Point, at the mouth of the Seekonk River. Figure 47 summarizes impacts on Seekonk River hydrography and how it compares with data for cases in which eastward and southward wind magnitudes are enhanced and when the Blackstone and Pawtuxet River outflows are increased by 50%. These parameters tend to have larger impacts on the Bullocks region, but do not appear to significantly improve the comparison between ROMS output and data from the Phillipsdale fixed site station. The changes in wind that might occur due to fetch do not significantly increase the model salinity to match observations or eliminate the model cooling that occurs starting around day 239. Moreover, the increased runoff case (Figure 47c) that attempts to represent what effect adding back in ungauged sections of the Blackstone and Pawtuxet Rivers might have, worsens the issue that ROMS salinities are too low in this region.

6.0 Conclusions

A series of 40 day SNB-ROMS simulations have been combined with ADCP and CTD data for the Bullocks Reach region of the estuary. The work was motivated by a desire to better understand the mismatches that tend to occur between ROMS models and time series data from the Bullocks Reach buoy and the Phillipsdale fixed site station. Results

clearly highlight the extreme spatial and temporal complexity of the Bullocks Reach buoy location, which typically exhibits the worst data-model comparisons. Our results suggest the buoy location, which is in a relatively narrow hydrodynamic-hydrographic transition region between the deep (dredged) shipping channel and a broad shallow shoal region, is a primary contributing factor to the data-model mismatches. Key findings include:

SNB-ROMS does very well at reproducing both channel-parallel and channel-perpendicular subtidal flows recorded by an ADCP at the Bullocks Reach buoy site.

Data-model comparisons at the buoy site show subtidal flows include shallow (upper 1/3 of water column) outflow and a broad, persistent subtidal inflow of water over the lower 2/3 of the water column.

A well-defined subtidal transverse circulation is defined, where deeper water moves weakly past the Bullocks Reach buoy location from a shallow shoal towards the channel.

Model bottom temperatures are too cold and salinities are too fresh at the Bullocks Reach buoy location.

Strong lateral gradients in temperature/salinity with subtle shifts in currents or local turbulent mixing, will significantly impact hydrographic trends recorded at Bullocks Reach buoy.

SNB-ROMS model salinities are much fresher than values recorded at the Phillipsdale fixed site station.

Altering parameters such as wind enhancements do to fetch effects or runoff increases to reflect ungauged inputs do not improve the data-model mismatch at Phillipsdale.

Additional work is needed to better understand northward fluxes of salt and temperature though the Seekonk River mouth and on the shoal that supplies water to the Bullocks Reach buoy.

The combination of SNB-ROMS flow and hydrography (temperature-salinity) reveal just how complex the Bullocks Reach buoy location appears. Subtidal circulation information suggests that Bullocks Reach buoy is primarily supplied with water from the south, or the transitional shoal south of the instrument, that lies between deeper channel and a shallow shoal along the western side of the estuary. Little is known about conditions in the shallow western shoal. Is there a recirculation gyre or is this region dominated by saltier water from the south or fresher water from the north and west? The ADCP also suggests significant channel-perpendicular transverse tidal mixing of deeper channel water to the Bullocks Reach buoy site could be occurring. This could produce the higher salinity recorded at the Bullocks Reach buoy, but has trouble explaining the warmer temperatures recorded in the data versus in ROMS.

Despite the fact that SNB-ROMS temperatures are generally too cool in bottom waters and both surface and bottom waters are too fresh, excellent matches can be found between models and data by looking only 300 m in any direction from the Bullocks Reach buoy site. This result suggests a large portion of the mismatch comes from local complexity, where very slight changes in mixing/flow processes could erase such differences in temperature and salinity. This is likely not the explanation for the poor salinity match between ROMS and data from the Phillipsdale fixed site station. Here it is

unlikely that such large spatial gradients exist, and more likely that the model is under representing the flux of salt in through the mouth of the Seekonk River.

7.0 Future Work

The Seekonk River is one of the regions of Rhode Island's coastal waters that has chronic water quality issues. This work represents the first fully 3-D, time varying model simulations capable of representing conditions within the Seekonk River at high grid resolution, where circulation and transport is dynamically coupled to the lower estuary. As is often the case, data-model comparisons reveal areas where the model needs improvement. These results on comparing model output to times series data on salinity and temperature at the Phillipsdale fixed site station show the SNB-ROMS model significantly underestimates the observed salinity. Runs conducted here suggest none of the model parameters tested could be used to improve the fit with data in the Seekonk. Additional observational measurements are needed, most crucially along the interface between the Providence and Seekonk Rivers to better understand the northward flux of water and salt, and to determine how the model is doing at representing these properties. The mouth of the Seekonk River, near India Point Park, is the boundary that requires additional observations of currents, temperature and, most critically, salt.

References:

Balt, C, 2014. Subestuarine circulation and dispersion in Narragansett Bay, PhD dissertation, University of Rhode Island, 184 pages.

Bergondo, D., 2004. Examining the processes controlling water column variability in Narragansett Bay: Time series data and numerical modeling," Ph.D. dissertation, University of Rhode Island.

Bergondo, D., and C. Kincaid, 2007. Development and calibration of a model for tracking dispersion of waters from Narragansett Bay Commission facilities within the Providence River, Narragansett Bay Commission Final Report, 46 pages.

Brush, M.J. 2002. Development of a numerical model for shallow marine ecosystems with application to Greenwich Bay, RI. Ph.D. dissertation, University of Rhode Island, Graduate School of Oceanography

Codiga, D., H. Stoffel, C. Deacutis, S. Kiernan, C. Oviatt. 2009. Narragansett Bay hypoxic event characteristics: Inter-annual variability, geographic distribution, intermittency, and spatial synchronicity. Estuaries and Coasts. 32(4):621-641.

Deacutis, C., D. Murray, W. Prell, E. Saarman, and L. Korhun, 2006. Natural and anthropogenic influences on the Mount Hope Bay ecosystem, Northeastern Naturalist 13(Special Issue 4):173–198.

Deacutis, C., 2008. Evidence of ecological impacts from excess nutrients in upper Narragansett Bay," in Science for Ecosystem-Based Management: Narragansett Bay in the 21st Century, Desbonnet, A. and Costa-Pierce, B., Eds. Springer, pp. 349-381.

Del Barrio, P., N. Ganju, A. Aretxabaleta, M. Hayn, A. Garcia and R. Howarth, Modeling future scenarios of light attenuation and potential seagrass success in eutrophic estuary, Est. Coastal Shelf Sci, 149, 13-23, 2014.

Edwards, A., Adding detritus to a nutrient-phytoplankton-zooplankton model: a dynamical systems approach, J. Plankton Res., Vol. 23, No4, 389-413, 2001

Franks, P.J.S., Wroblewski, J.S., Flierl, G.R., 1986. Behavior of a simple plankton model with food-level acclimation by herbivores. Marine Biology 91, 121–129

Franks, P.J.S., 2002. NPZ models of plankton dynamics: their construction, coupling to physics, and application. Journal of Oceanography 58 (379–387).

Greenwich Bay Special Area Management Plan, Coastal Resources Management Council by the Coastal Resources Center/Sea Grant, University of Rhode Island, 498 pages, May, 2005

Janeković, I., Powell, B., 2012. Analysis of Imposing Tidal Dynamics to Nested Numerical Models. Continental Shelf Research, 34, 30-40.

Kincaid, C., The exchange of water through multiple entrances to the Mt. Hope Bay Estuary, Northeast Naturalist, 13(Special Issue 4): 117-144, 2006.

Kincaid, C., R. Pockalny, and L. Huzzey, 2003. Spatial and temporal variability in flow at the mouth of Narragansett Bay, Journal Geophysical Research, doi:10/1029/2002JC001395.

Kincaid C., and D. Bergondo, 2005, Development and Calibration of a Model for Tracking Dispersion of Waters from Narragansett Bay Commission Facilities within the Providence River & Narragansett Bay, Report submitted to the Narragansett Bay Commission, Prov., R.I., 27 pp.

Kincaid, C., D. Bergondo, and K. Rosenburger, 2008. Water exchange between

Narragansett Bay and Rhode Island Sound, in Science for Ecosystem-based Management, edited by A. Desbonnet and B. A. Costa-Pierce, chap. 10, Springer, 2008.

Kincaid, C., 2001a. Results of Hydrographic Surveys on the Providence and Seekonk Rivers: Summer Period, Report submitted to the Narragansett Bay Commission, Prov., R.I., 45 pp.

Kincaid, C., 2001b. Results of Hydrographic Surveys on the Providence and Seekonk Rivers: Fall Period, Report submitted to the Narragansett Bay Commission, Prov., R.I., 35 pp.

Kincaid, C., 2001c. Results of Hydrographic Surveys on the Providence and Seekonk Rivers: Winter Period, Report submitted to the Narragansett Bay Commission, Prov., R.I., 27 pp.

Kincaid, C., 2012a. Results of tilt current meter time series measurements in the Bristol Harbor estuarine system during August, 2011, Report submitted to Save Bristol Harbor, Bristol (RI), 46 pages.

Kincaid, C., 2012b, Development of the Full Bay ROMS Hydrodynamic-Dye Transport Model for the Providence River: Comparisons with data from Spring 2010 tilt current meter network. Final Report Prepared for the Narragansett Bay Commission (Project 08A-114-01-00).

Kincaid, C. 2018, A Seekonk-Narragansett Bay (SNB) ROMS Model applied to coupled circulation-ecosystem processes: A 2010 Seasonal Study, Final Report Prepared for the Narragansett Bay Commission (Project 08A-114-01-00).

Kremer, J.N., J. Vaudrey, D. Ullman, D. Bergondo, N. LaSota, C. Kincaid, D. Codiga, and M.J. Brush. 2010. Simulating property exchange in estuarine ecosystem models at ecologically appropriate scales. *Ecological Modelling* 221:1080-1088.

Mendahlson, D., 2007. Review of the University of Rhode Island ROMS Hydrodynamic Model application to Narragansett Bay. Report prepared for the Narragansett Bay Commission by Applied Technology Management Inc., 5 pp.

Mukai, A., Westerink, J., Luettich, R., and Mark, D., 2002. East coast 2001, a tidal constituent database for western North Atlantic, Gulf of Mexico, and Caribbean Sea, Report ERDC/CHL TR-02-24, Coastal Inlets Research Program, U.S. Army Corps of Engineers., Tech. Rep.

Oviatt, C.A. 2008. Impacts of nutrients on Narragansett Bay productivity: A gradient approach. In: Desbonnet, A. and B.A. Costa-Pierce (eds.) Science for Ecosystem-based Management. Springer, N.Y. p. 519-539.

Patterson, M, 2007. Evaluation of nutrients along the Blackstone River, Master of Science Thesis, Univ. of Massachusetts at Amherst, 2007.

Pfeiffer-Herbert, A. S., 2012. Larval transport in an estuarine-shelf system: Interaction of circulation patterns and larval behavior, Ph.D. Thesis, Graduate School of Rhode Island, University of Rhode Island, 227pp.

Pfeiffer-Herbert, A. S., C. Kincaid, D. Bergondo and R. Pockalny. Dynamics of wind-driven estuarine-shelf exchange in the Narragansett Bay estuary, *Continental Shelf Research*, vol 105, pp42-59, 2015.

Rogers, J., 2008. Circulation and transport in upper Narragansett Bay, University of Rhode Island, Master Thesis, Kingston, RI, 107 pages

Rosenberger, K., 2001. Circulation patterns in Rhode Island Sound: Constraints from a bottom mounted acoustic Doppler current profiler, M.S. Thesis in Oceanography, University of Rhode Island, Narragansett, RI, 226pp.

Saarman, E., Prell, W., Murray, D., and Deacutis, C., 2008. Summer bottom water dissolved oxygen in upper Narragansett Bay, in Science for Ecosystem-Based Management: Narragansett Bay in the 21st Century, Desbonnet, A. and Costa-Pierce, B., Eds. Springer, pp. 325-348.

Shchepetkin, A.F. and J.C. McWilliams, 2003: A Method for Computing Horizontal Pressure-Gradient Force in an Oceanic Model with a Non-Aligned Vertical Coordinate, *Journal of Geophysical Research,* 108, 1-34.

Shchepetkin, A. and McWilliams, J., 2005. The regional oceanic modeling system (ROMS): a split-explicit, free-surface, topography-following-coordinate oceanic model, Ocean Modelling, vol. 9, pp. 347-404.

Smayda, T.J. & Borkman, D.G. 2008. Nutrient and Plankton Dynamics in Narragansett Bay. In: Desbonnet, A., B.A. Costa-Pierce [Ed.] Science for Ecosystem-based Management. Springer, New York, pp. 431-484.

Warner, J., Geyer, W., and Lerczak, 2005. J., Numerical modeling of an estuary: a comprehensive skill assessment," Journal of Geophysical Research, vol. 110, p. C05001.

Willmott, C. J., 1981. On the validation of models, *Phys. Geogr.*, 2, 184 – 194.

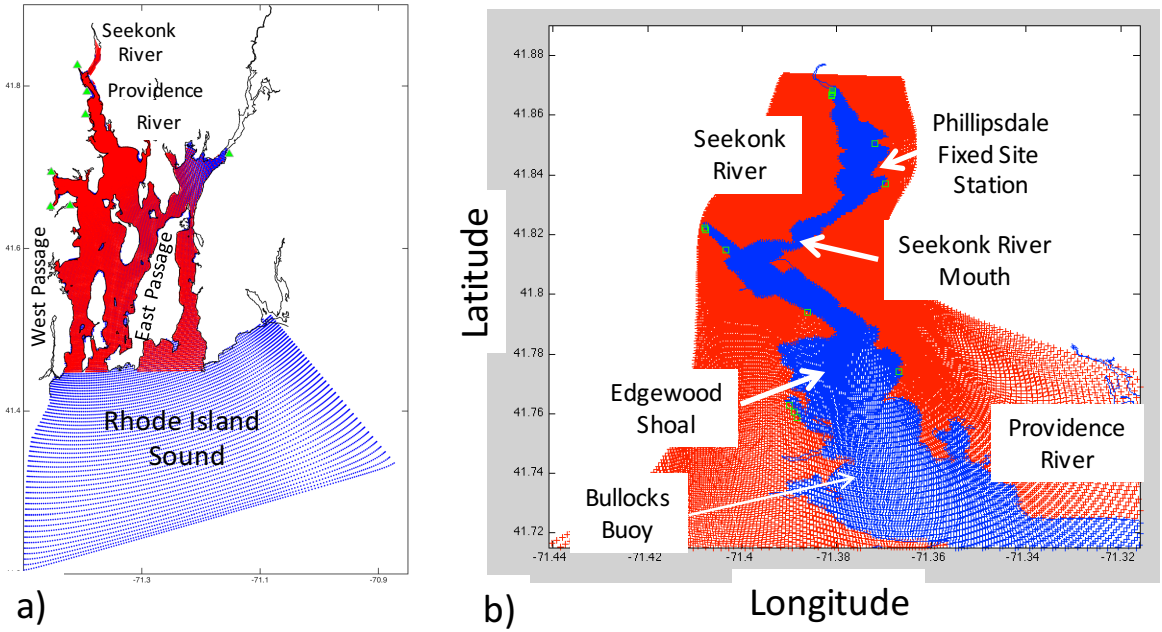

Figure 1. a) A progression of Narragansett Bay ROMS model grids have evolved to improve the models scientific capabilities and utility as a research and management tool. Shown here is the high resolution grid used for this study (red markers show grid node locations/densities). The strategy is to force the finer grid model (red nodes) at the ocean boundary with a coarser regional model (blue nodes). Green markers show locations of freshwater inputs for rivers and WWTFs. b) A close-up of the finer grid model (e.g. red nodes in (a)) used in this work that shows details of the Providence and Seekonk River sections of the grid. In frame (b) the blue markers represent the water nodes and the red nodes represent the land nodes.

Table 1: List of acronyms used in the report.

ADCP: Acoustic Doppler Current Profiler
BR: Bullock Reach
CECs: Chemicals of Emerging Concern
CTD: Conductivity-Temperature-Depth sensor
NB: Narragansett Bay
NBC: Narragansett Bay Commission
NOAA: National Oceanic and Atmospheric Administration
NPZD: Nitrogen Phytoplankton Zooplankton Detritus model
PORTS: Physical Oceanographic Real-Time System
RIS: Rhode Island Sound
ROMS: Regional Ocean Modeling System
SNB-ROMS: Seekonk-Narragansett Bay ROMS model
TCM: Tilt Current Meter
T-S: Temperature Salinity data
URI-GSO: University of Rhode Island Graduate School of Oceanography
WWTF: Wastewater Treatment Facility

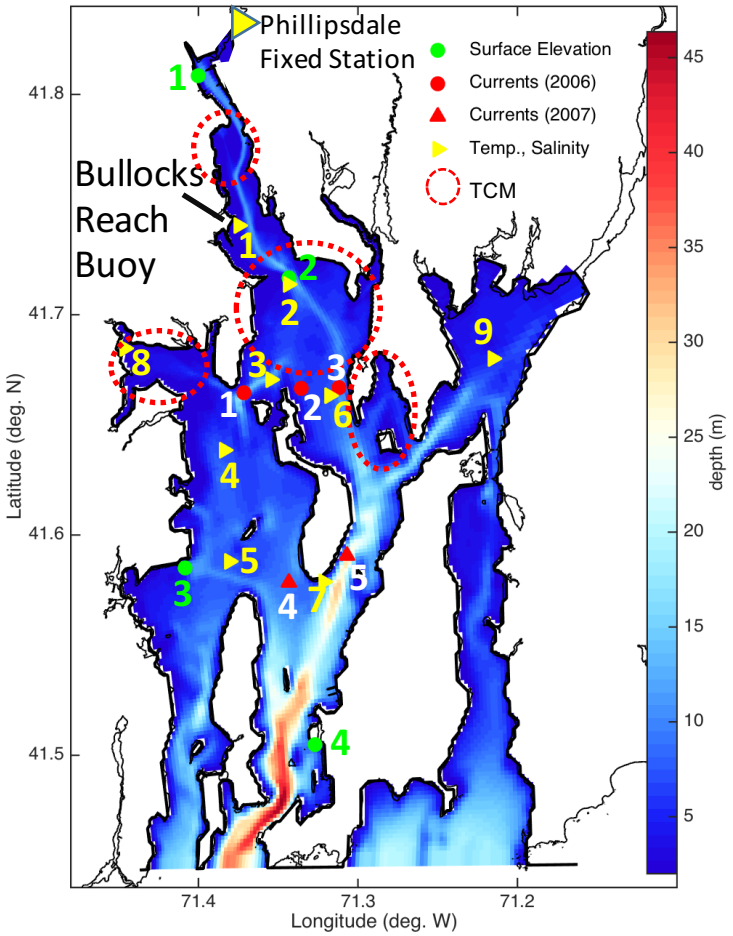

Figure 2. The accuracy of NB-ROMS at representing physical parameters of the Bay has been assessed through data-models comparisons made with tilt current meters (TCM) on Edgewood Shoals and other areas (shown as red dashed circles) and other moored ADCP current meter deployments (shown by red markers). Other data-model comparison points are surface elevations at NOAA tide gauges (green circles) and temperature/salinity at the fixed-site buoy network for Narragansett Bay (yellow markers). Focuses of this study are the Bullocks Reach buoy and Phillipsdale fixed station, which are labelled on the map.

Model Skill: Sea Level 2006-07

Site		Raw	Subtidal	Tidal
Providence	1	0.955	0.851	0.967
Conimicut	2	0.957	0.844	0.970
Quonset	3	0.960	0.818	0.978
Newport	4	0.963	0.841	0.980

Table 2. Model skills (determined using the widely published Willmott Skill) for surface elevations or water levels through time are shown for each NOAA tide gauge compared with ROMS model runs covering years 2006-2007. Willmott Skills of >0.7 are considered acceptable. Values here for raw data, data filtered for tides and for sub-tidal patterns show extremely good skill levels. (calculated by D. Ullman, URI-GSO, 2016). Numbers in the site column refer to numbered green circles in Figure 2.

Model Skill: Depth-Averaged Major Axis Currents 2006-07

Site	year	Site ID	Raw	Subtidal	Tidal
West Passage Channel 1	2006	WP	0.812	0.724	0.812
East Passage Channel 3	2006	EPc	0.894	0.846	0.906
East Passage Shoal 2	2006	EPs	0.832	0.512	0.876
East Passage Channel 5	2007	EP07	0.865	0.737	0.869
Between Prudence and Conanicut Islands 4	2007	MD07E	0.932	0.617	0.938

Table 3. Model (Willmott) skills for depth averaged, axis-parallel currents for ROMS vs. moored ADCP records during 2006-2007 are shown. Station location information is given in the first two columns. Tidal records show high skill values. Subtidal skills, more challenging for models, are also very good for all stations except the East Passage shoals and the ADCP just west of the southern tip of Prudence Island (MD07E). This is likely due to eddy features that would need better spatial resolution, such as with tilt current meter data, to more fully understand the poor fit. It could also be due to poor representation of wind fields into the model. Numbers correspond to red triangle numbers in Figure 2.

Model Skill: Hydrography 2006-07

Site		Tsurf	Tbott	Ssurf	Sbott
Bullock	1	0.99	0.97	0.95	0.68
Conimicut	2	0.98	0.98	0.95	0.81
North Prudence	3	0.99	0.99	0.93	0.87
Mount View	4	0.99	0.98	0.96	0.89
Quonset	5	0.98	0.98	0.90	0.91
Popasquash	6	0.99	0.98	0.93	0.88
T-Wharf	7	0.99	0.99	0.93	0.83
Greenwich Bay	8	0.99	0.99	0.88	0.77
Mount Hope Bay	9	0.98	0.98	0.97	0.91

Table 4. Model skills for hydrography, or salinity and temperature of near-surface and near-bottom water from fixed-site buoy network compared with NB-ROMS output at the buoy locations. Skills are generally exceedingly high for all stations. The exception is the Bullocks Reach buoy (see Figure 2). At this location the bottom salinity is off between data and models, whereas models do very well at reproducing surface salinity and both surface and bottom temperature. Numbers in site column refer to numbered yellow triangles in Figure 2.

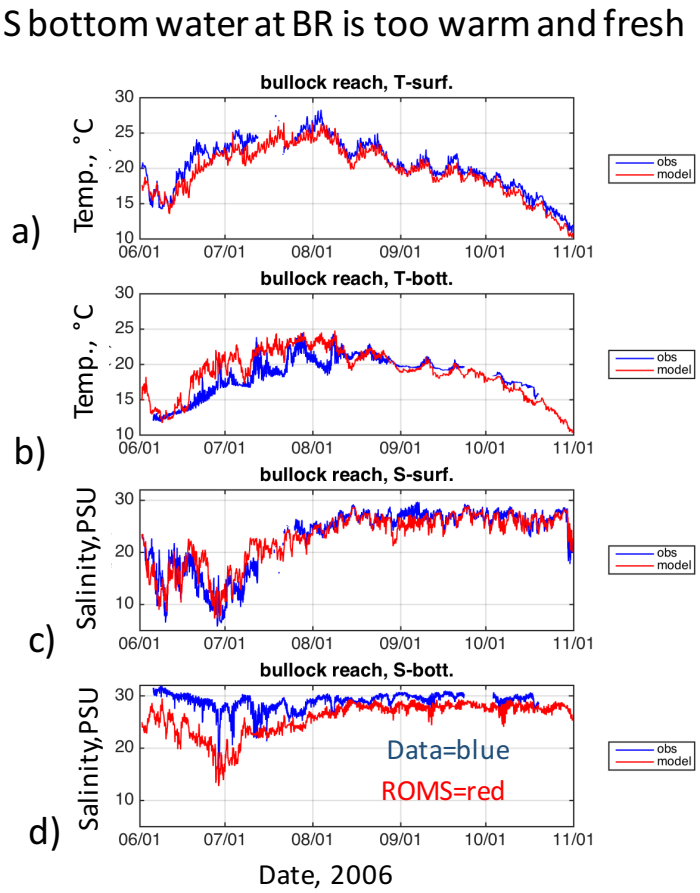

Figure 3. Bullocks Reach buoy site time series data (blue) and model (red) plots of (a) surface temperature and (b) bottom temperature, (c) surface salinity and (d) bottom salinity reveal details for 2006 data versus model skill values. ROMS surface and bottom temperatures are slightly cool (-0.9°C) and slightly warm (+0.5°C) respectively. ROMS surface salinity is very close to data, or very slightly fresher on average (-0.2 PSU). The largest discrepancy is in bottom salinity, where ROMS sits roughly 2.5 PSU fresher than data. The largest mismatch occurs during summer months, whereas data-model values align during the fall period. Willmott skills for surface and bottom temperature are 0.99 and 0.97 out of 1.0, respectively. For surface and bottom salinity skills are 0.95 and 0.68, respectively.

a)

b)

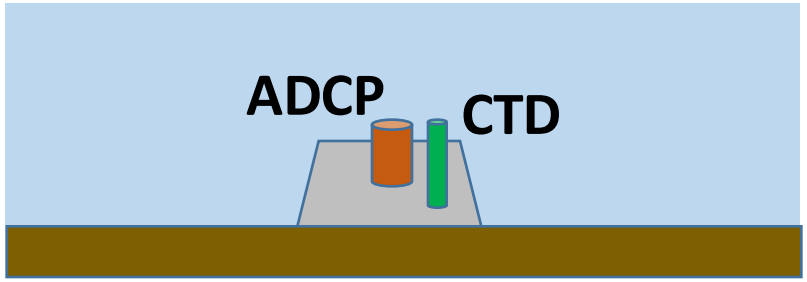

Figure 4. A bottom mounted ADCP was deployed in summer-fall of 2016 at the Bullocks Reach buoy location along with a CTD to provide water column time series data on currents and near-bottom time series data on salinity and temperature. (a) The ADCP transducer head is shown being prepared with anti-fouling gel to keep acoustic transducers (red circles) free of growth. (b) Schematic ADCP and CTD in a trawl-resistant bottom mooring.

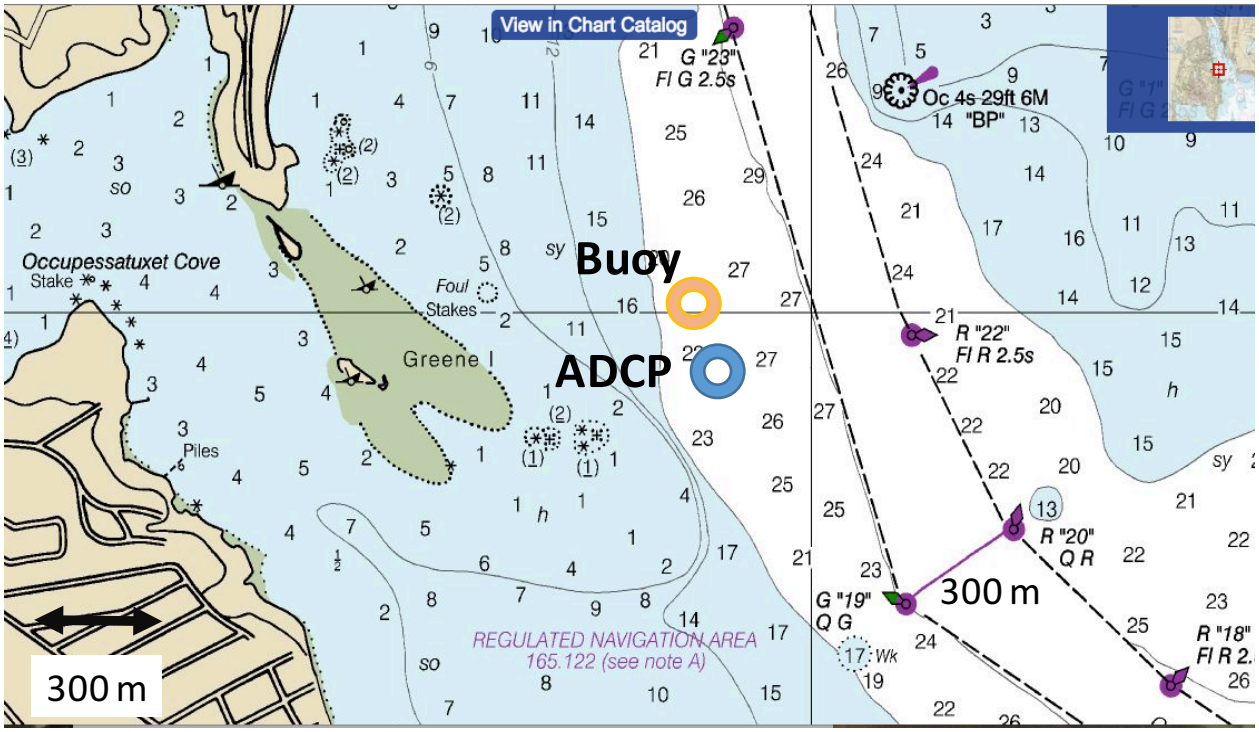

Figure 5. Close-up map of fixed-site buoy location at Bullocks Reach section of lower Providence River. The ADCP mooring was placed just to the southeast of this site. The map shows local details of bathymetry. Both moorings lie just west (~250 m) of the dredged shipping channel (~15 m deep) on a relatively shallow shoal of 6-8 m water depth. Just to the west of the moorings, water shoals again to <1m depth. The Bullocks Reach buoy lies in a region of the estuary with extreme east-west or channel-perpendicular changes in bathymetry/water depths. Depth values shown on the chart are in feet.

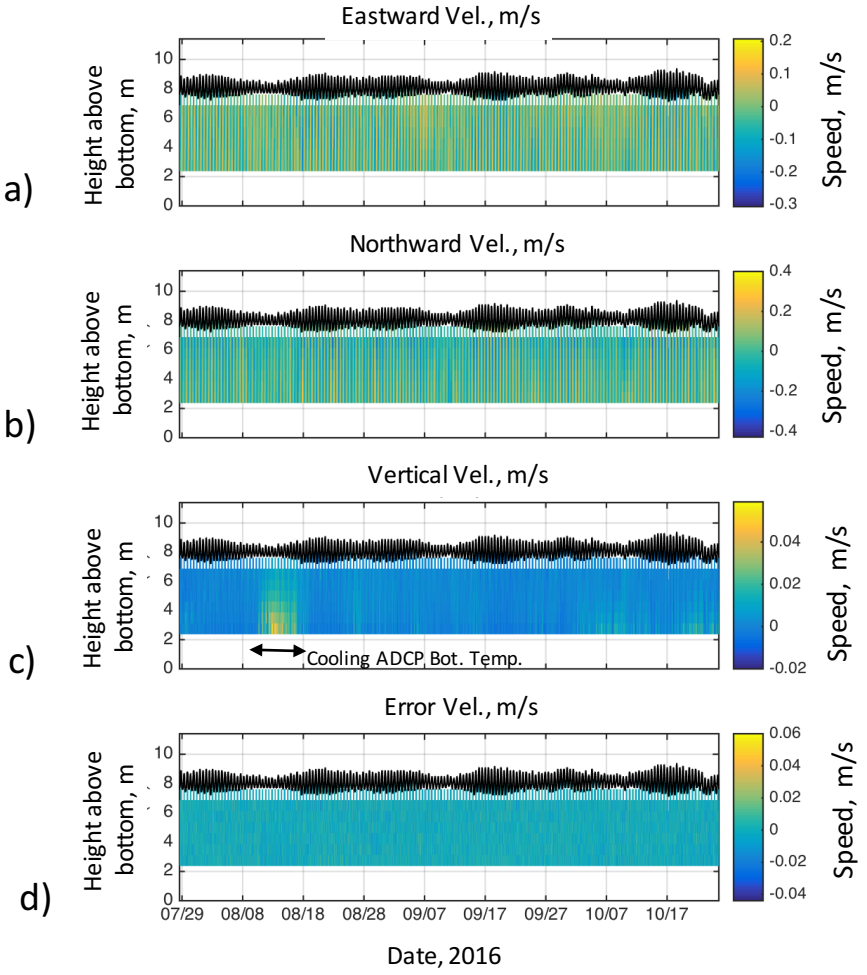

Figure 6. Time series plots of ADCP velocity versus depth for 2016 Bullocks Reach deployment. The largest values are for (a) Eastward and (b) Northward velocity components of water flow. (c) Vertical velocity is a factor of 10 smaller. Also shown is estimated error in horizontal velocity values (d).

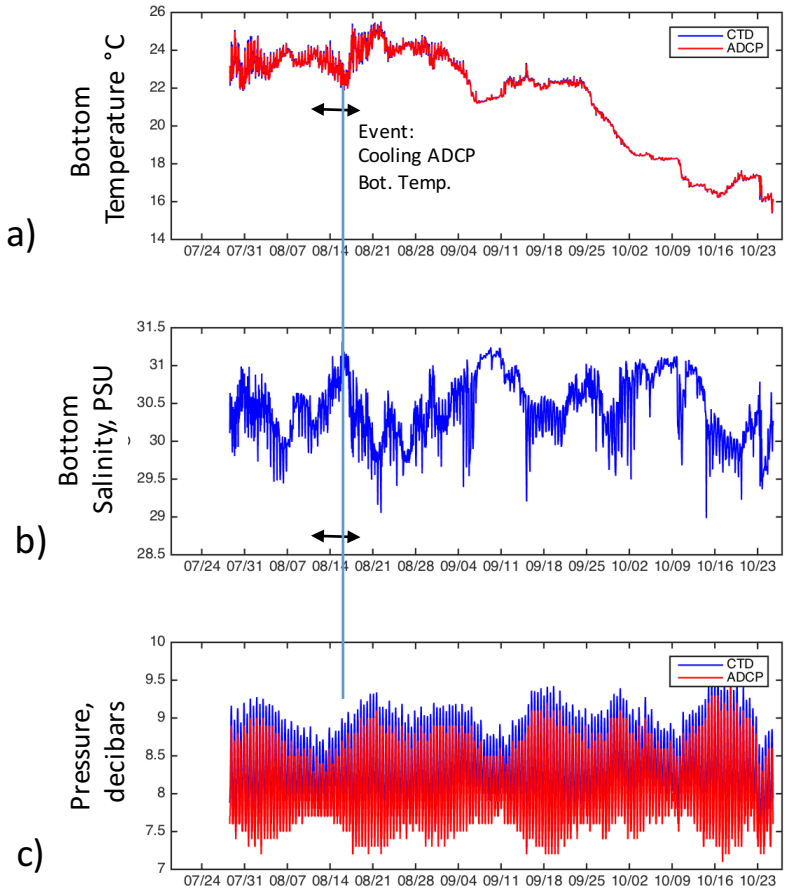

Figure 7. Time series plots of (a) bottom temperature, (b) bottom salinity and (c) bottom pressure recorded at mooring during 2016 deployment window. Both the ADCP and CTD had temperature and pressure sensors. ADCP values are shown in red and CTD values are shown in blue.

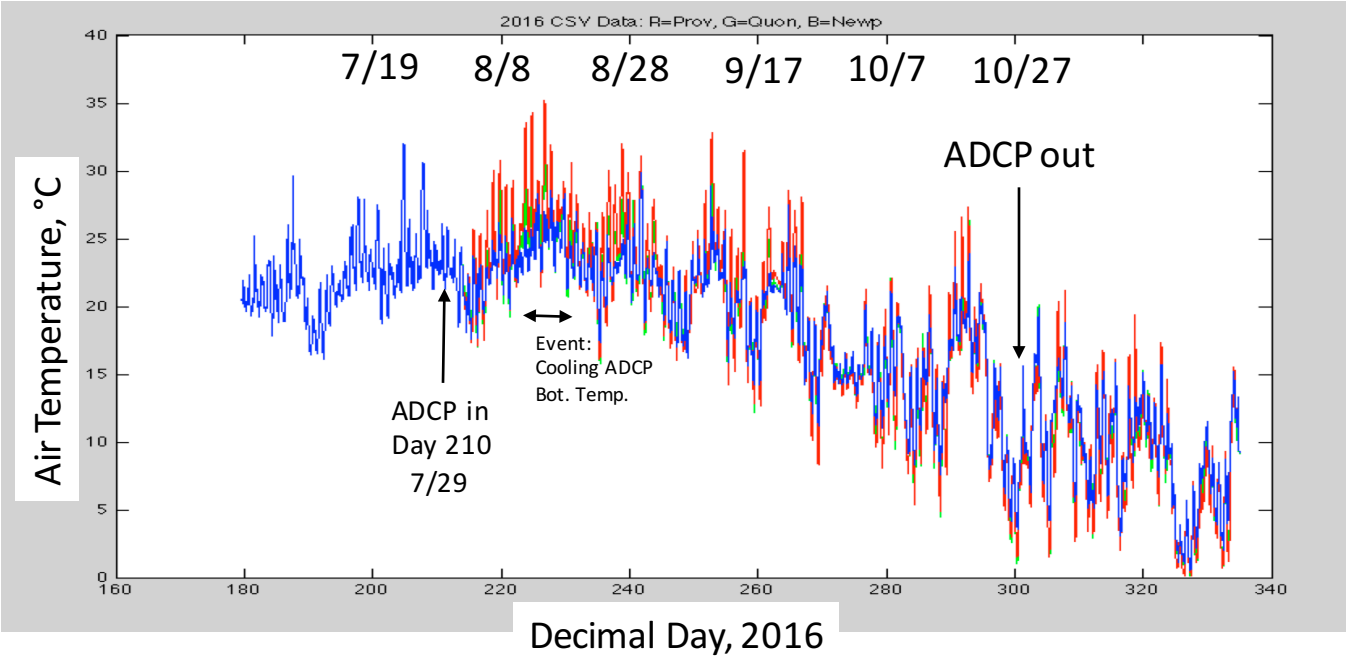

Figure 8. Time series plots of air temperature measured at Providence, RI during the deployment period, running from day 210 (7/29/16) to day 300 (10/27/16). Air temperatures are relatively high 20-35 °C during the summer period through early September. Temperatures decline over the end of the deployment, from days 260-300 (or 9/17/16 – 10/27/16). Data are from fixed network stations: Red=Providence buoy; Green=Quonset buoy; Blue=Newport buoy.

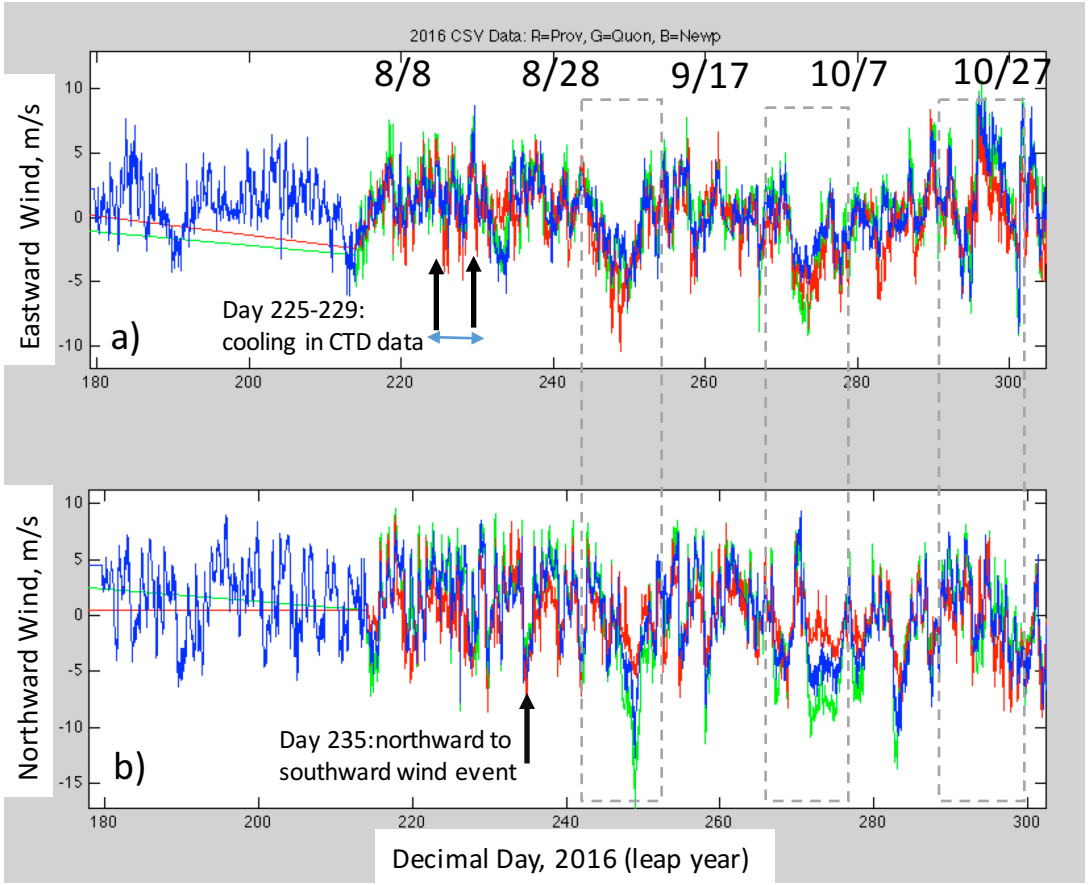

Figure 9. Plots of (a) eastward and (b) northward components of the wind field for 2016. Data are averaged from stations at Providence (red), Quonset (green) and Newport (blue) to eliminate periods of data drop out at each station. Data show that larger events (such as those in dashed box regions) are felt differently throughout Bay. In particular, southwestward winds, such as the shaded period around day 250, are felt more strongly at Quonset. A rapid wind change on day 235 is marked. There are also changing winds days 225-229, when bottom water at the ADCP cools (Figure 15).

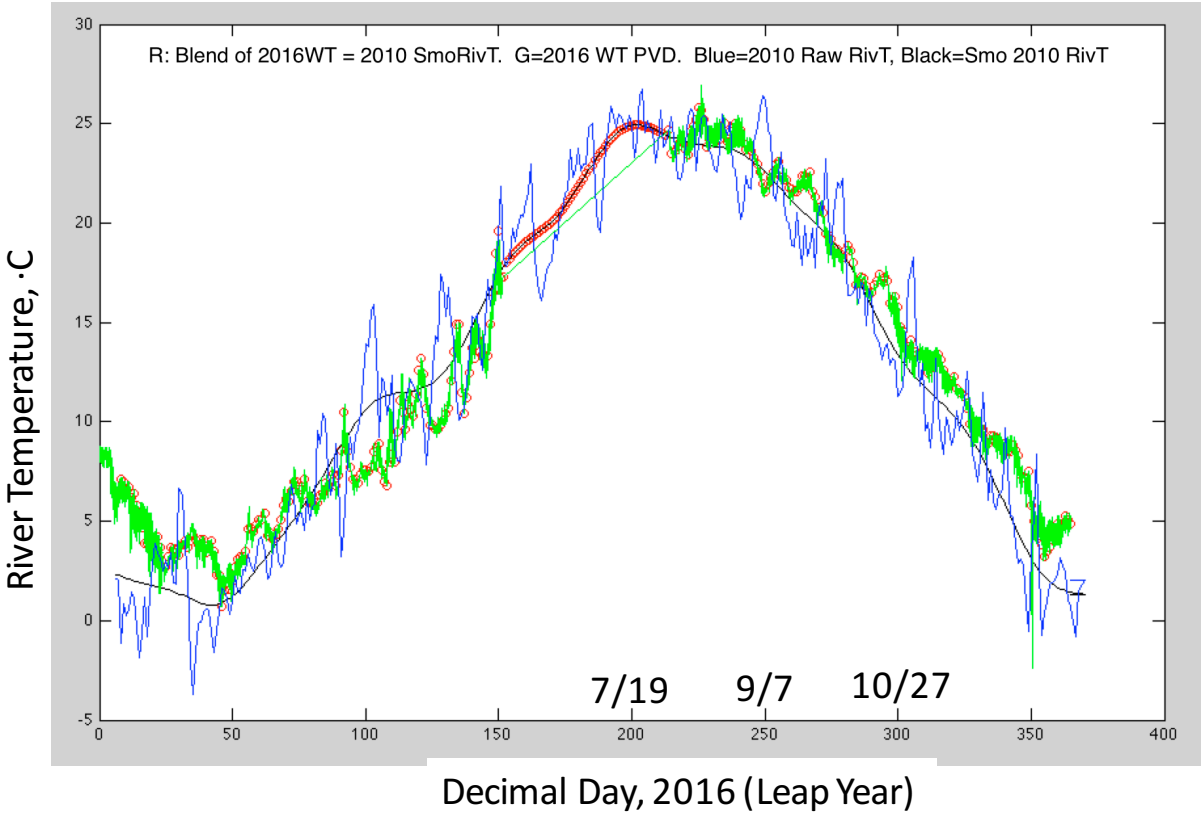

Figure 10. Plot of river temperature applied to all rivers in the ROMS 2016 simulations during the period of the Bullocks Reach ADCP deployment (7/19-10/27). Data are used for the Providence station surface water temperature (green). A data gap occurred at the start of the sampling period. An interpolated 2016 river temperature record (red) was developed that combined information from 2016 and 2010 (blue=raw data, black=smoothed 2010 data) to make sure values fell within acceptable bounds. The straight green line is what the record would look like with if a simple linear interpolation was used to fill the missing 2016 data window.

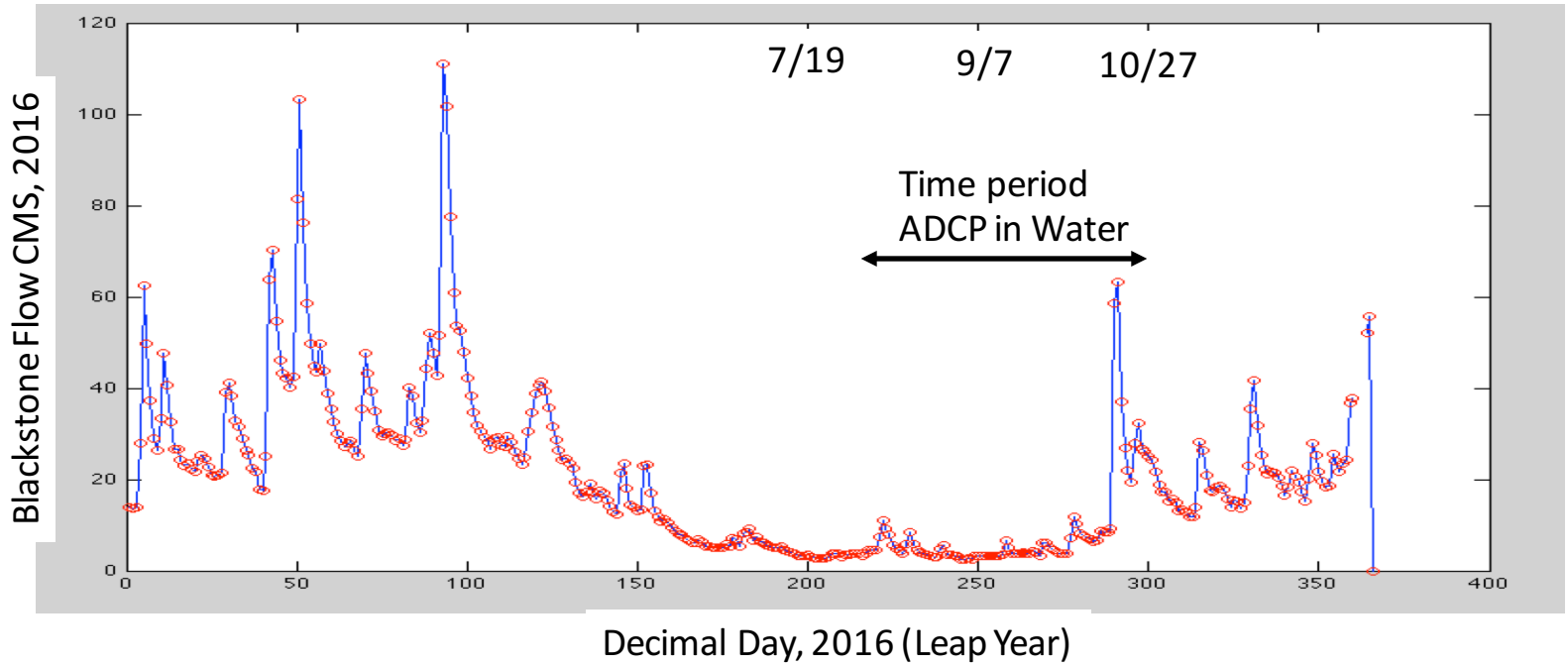

Figure 11. Plot of river runoff in cubic meters per second for the Blackstone River. Data from USGS gauging station.

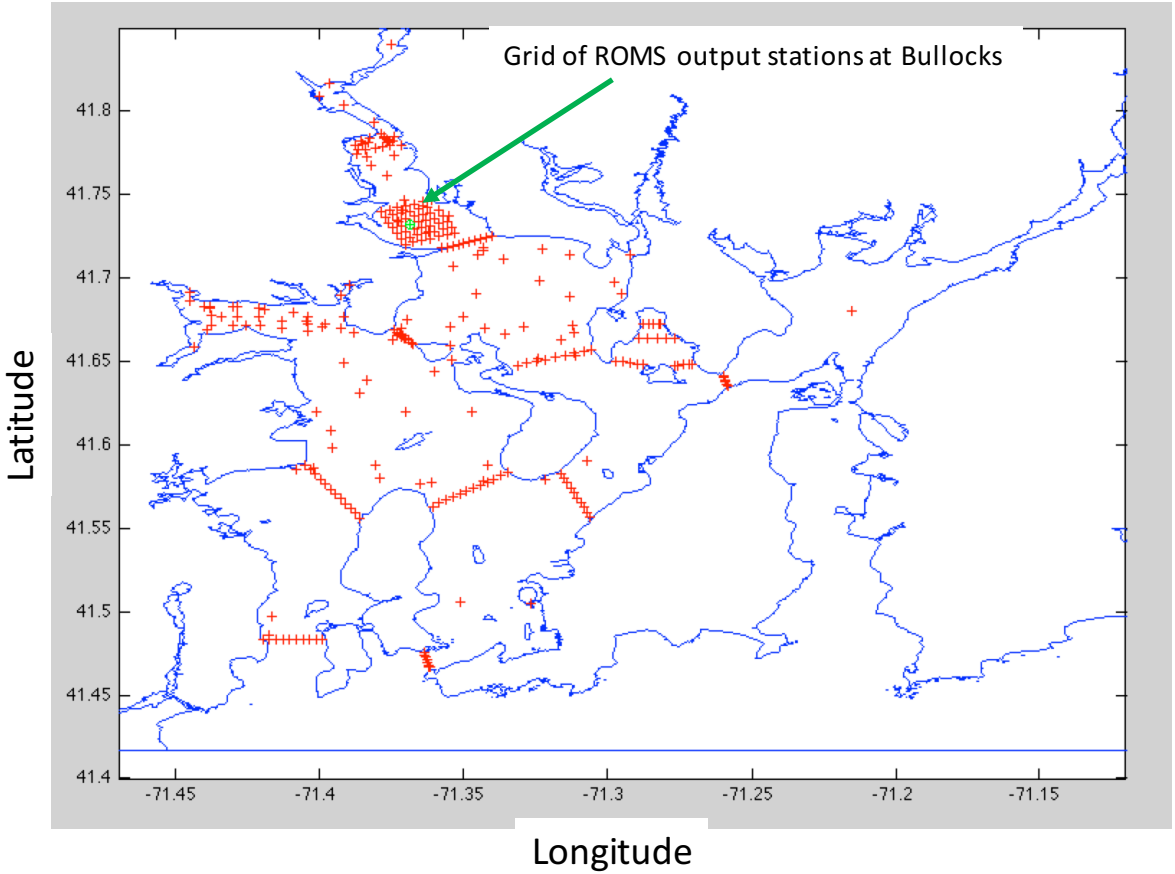

Figure 12. Map plot of station locations where time series information on currents and hydrographic parameters from ROMS 2016 models is output at 6 minute intervals. A change from prior NBC-ROMS simulations is a denser grid of stations located in the Providence River near the Bullocks Reach buoy. This denser grid allows for better characterizations of spatial variations in model output relative to the fixed-site buoy at this location and the 2016 ADCP.

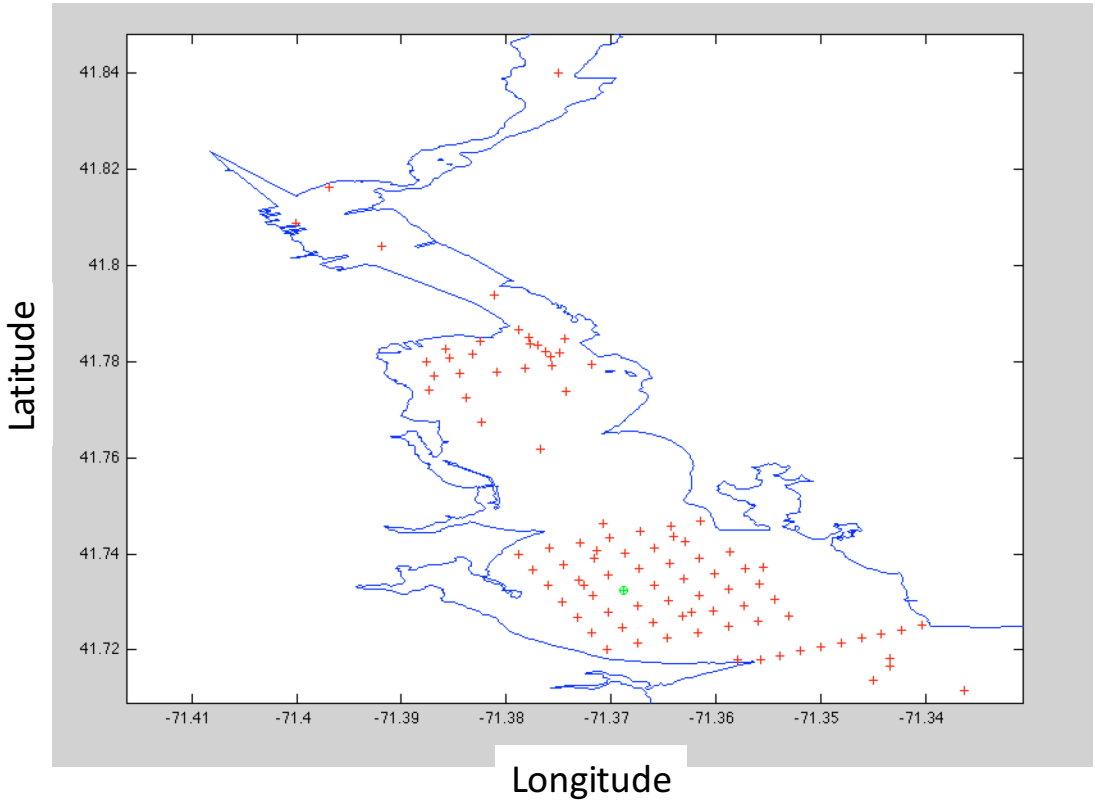

Figure 13. Close up map plot of station locations in the Providence River near the Bullocks Reach buoy described in Figure 12. The green marker represents the latitude/longitude of the 2016 moored ADCP.

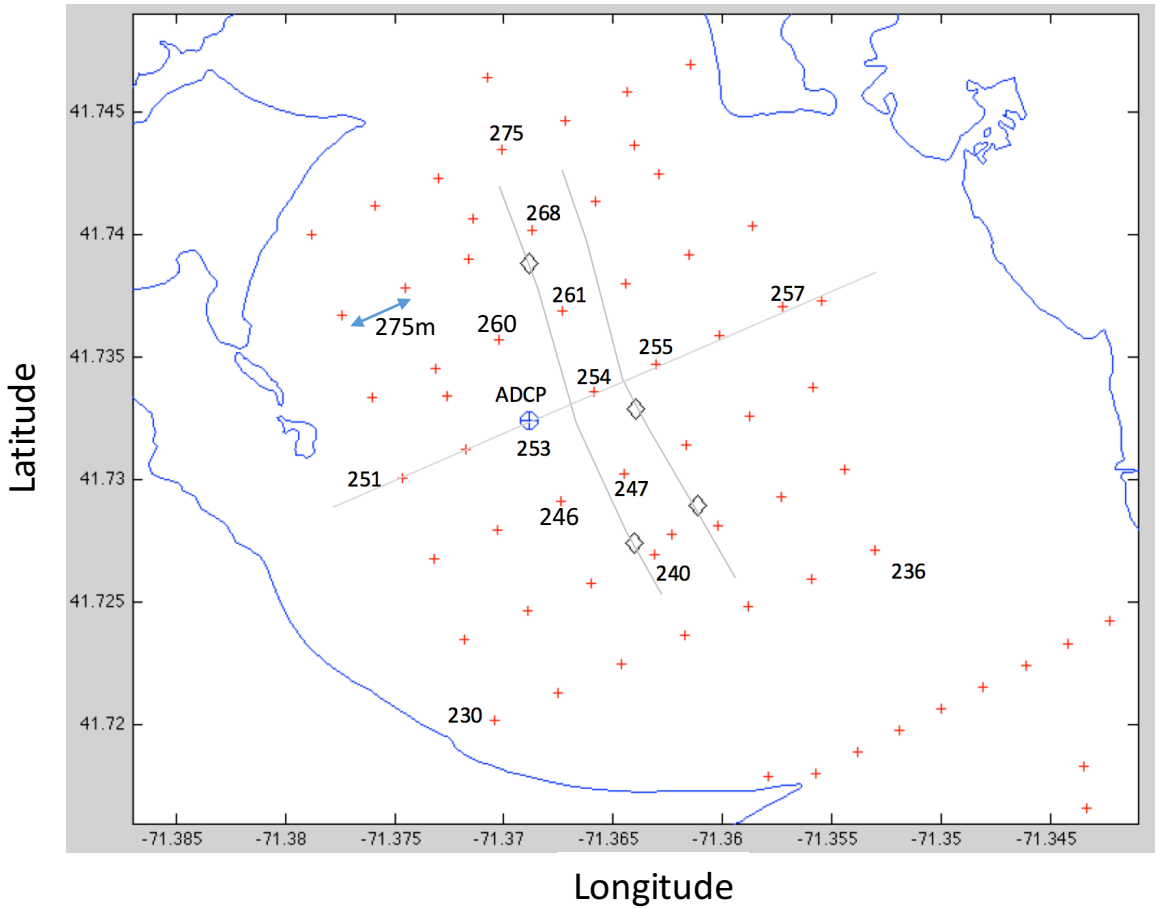

Figure 14. Close up map plot of stations (red markers, some with select ROMS identification numbers) in the immediate vicinity of the moored ADCP / Bullocks Reach buoy (blue marker). The black diamonds are locations of navigation aids, also marking the local boundaries of the dredged shipping channel. Stations are spaced approximately 275 meters apart. Results from stations 246 and 260 are shown below, for conditions in the transitional zone (between shoal and channel) up- and down-estuary from ADCP location (253).

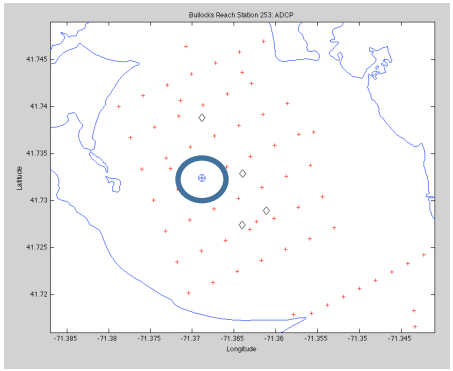

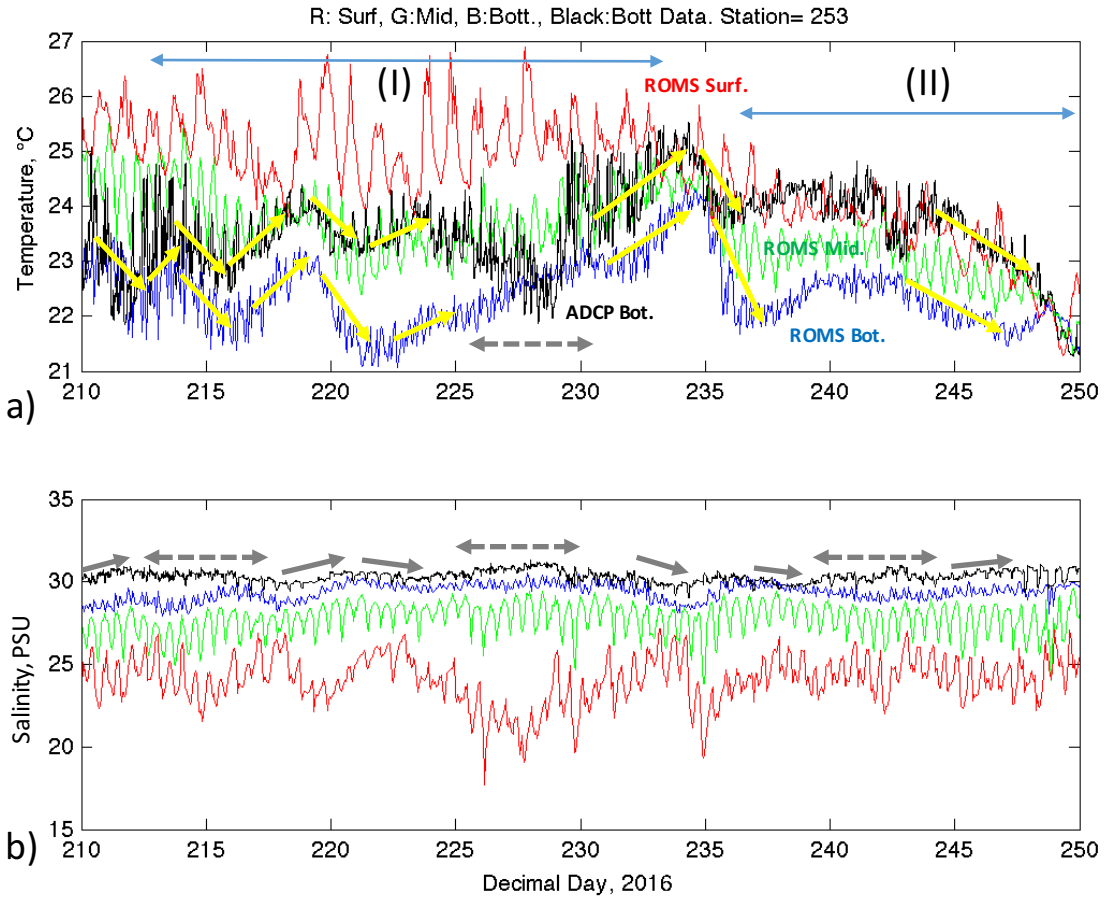

Figure 15. Time series plots of temperature (a) and salinity (b) for the 40 day ROMS-data comparison period (7/19/16:Day 210 to 9/7/15:Day 250). Measured data (black lines) for near-bottom water at the ADCP location. Near-surface (red), mid-water (green) and near-bottom (blue) values show ROMS output at the ADCP location (Station 253 shown in inset). Data and model bottom salinities are close. Model bottom temperature is 1-3°C colder than data values (blue vs. black in (a)). Period I: ROMS mid-water temperature (green in (a)) is closest to observed bottom temperature (black in (a)) during much of record. (II) ROMS surface water temperature is closest to ADCP bottom temperature after the day 235 wind shift (Figure 9). Yellow and grey arrows highlight regions where trends in ROMS/DATA match. Dashed grey arrows highlight periods where trend slopes do not match. For temperature, ROMS captures most of the trends but is offset by fixed amount (a).

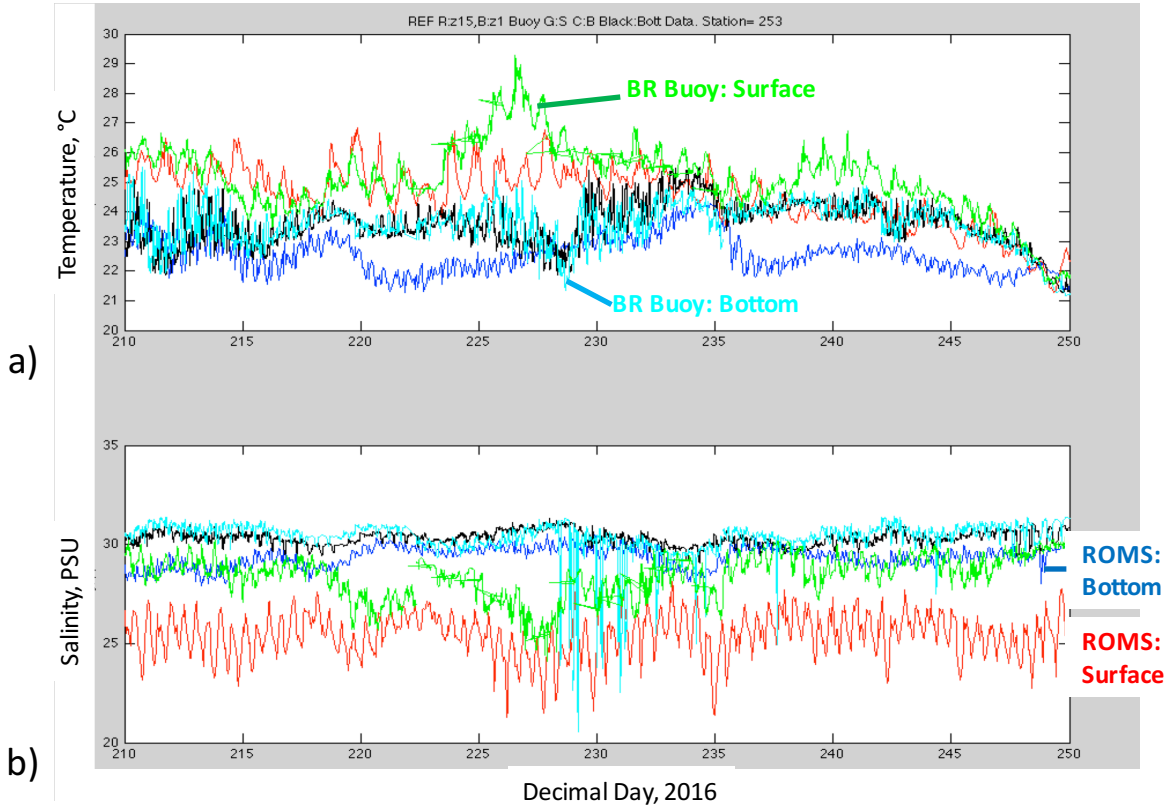

Figure 16. Data-model comparison time series plots of salinity and temperature at ROMS station 253, site of the ADCP that includes data from the nearby Bullocks Reach buoy. Colors for surface/bottom trends of data and models are labeled. Values shown for the reference case, using actual ROMS forcing conditions from this period of 2016. For a data-data comparison, bottom (a) temperature and b) salinity measurements from the ADCP/CTD (black) and the buoy (cyan) are very close in magnitude and patterns. For temperature data-model comparisons (a), ROMS bottom water at this site is cooler in some periods (a: days 218-225; 236-247) and close during others (days 210-215; 227-235). Surface temperature is well-matched for much of the record, except the warm period around day 226. The salinity comparison shows bottom salinity matches within 1-2 PSU, but that ROMS surface waters are fresher than the buoy data values.

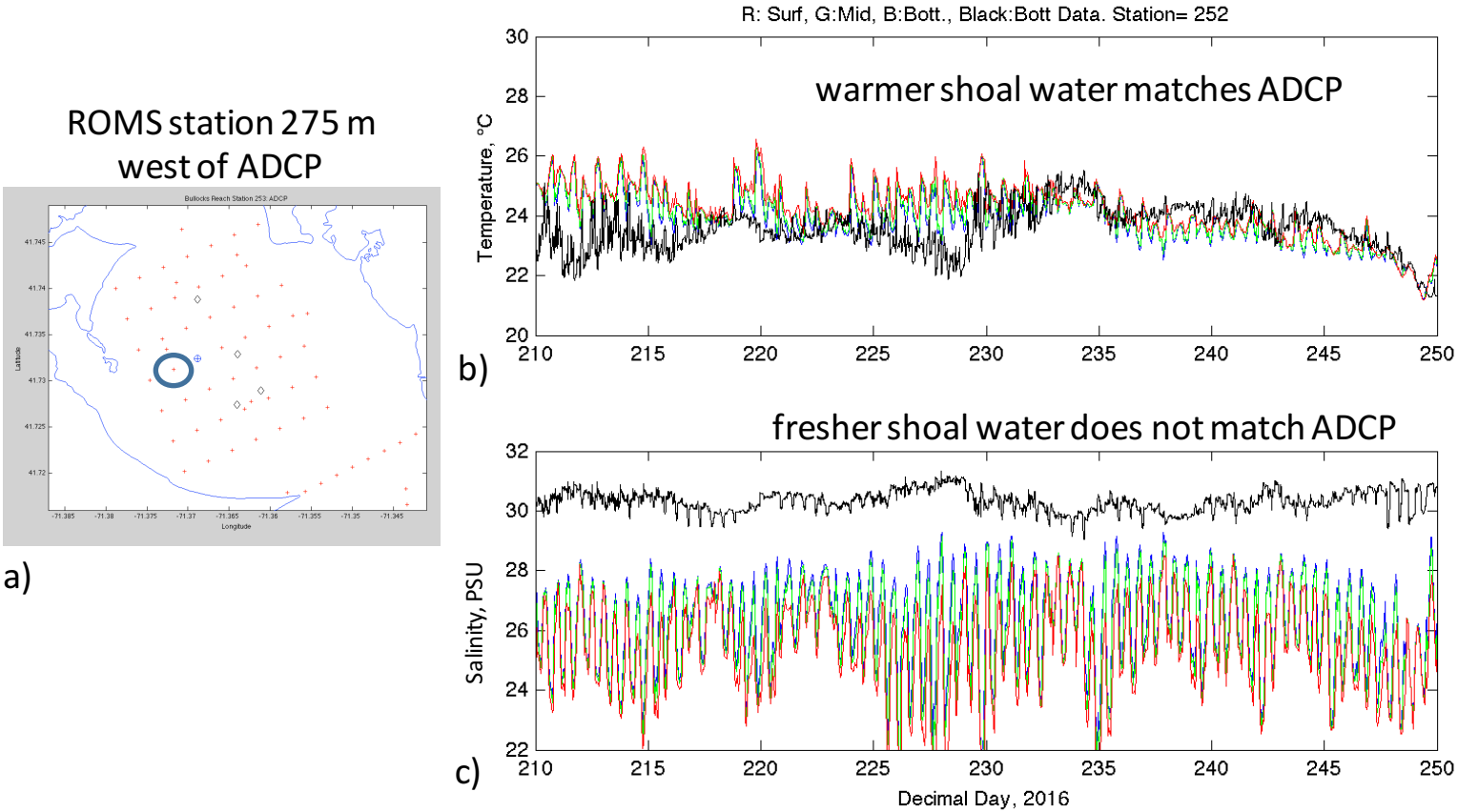

Figure 17. Similar time series plots of temperature (b) and salinity (c) that show data-model comparison for ROMS output from station 252, or 1 station (~275 m) to the west-southwest of the ADCP location, compared to data (black lines) from the ADCP station. Near-surface, mid-water and near-bottom values for ROMS output at Station 252 (shown in (a) map inset) are shown in red, green and blue, respectively. Interestingly, the bottom temperature at station 252 is a closer match with bottom temperatures ~275m away at the ADCP site. However, ROMS bottom salinity which matched at the ADCP site is now too fresh by 2 PSU. Results highlight the extreme lateral gradients that exist for both temperature and salinity in this region.

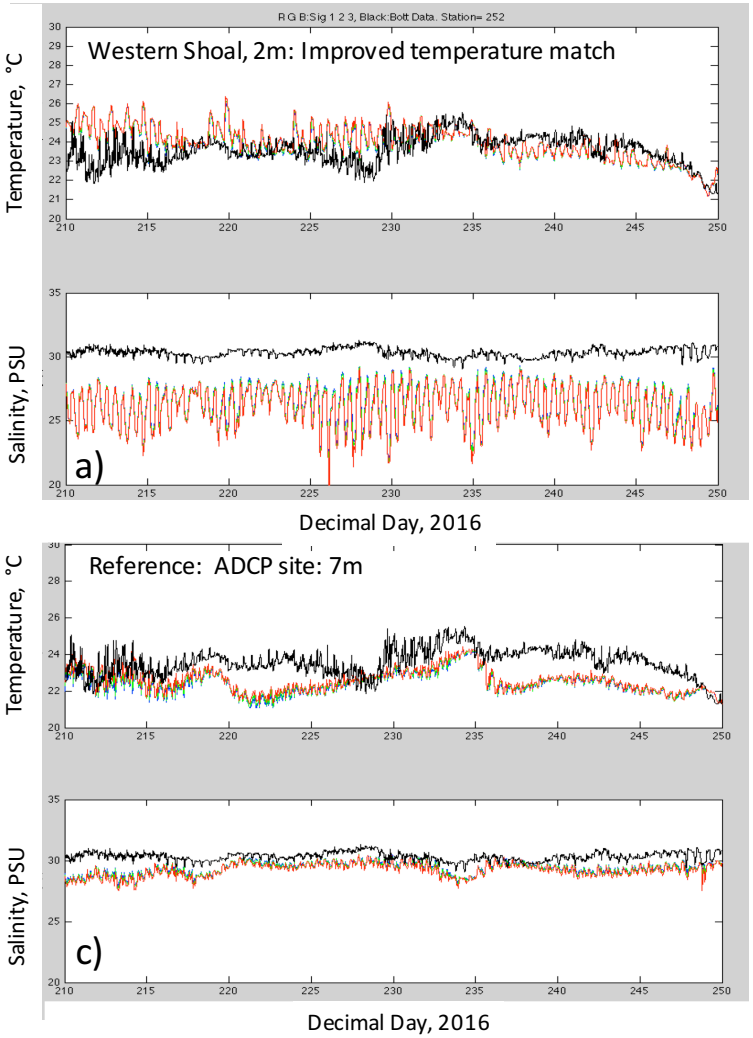

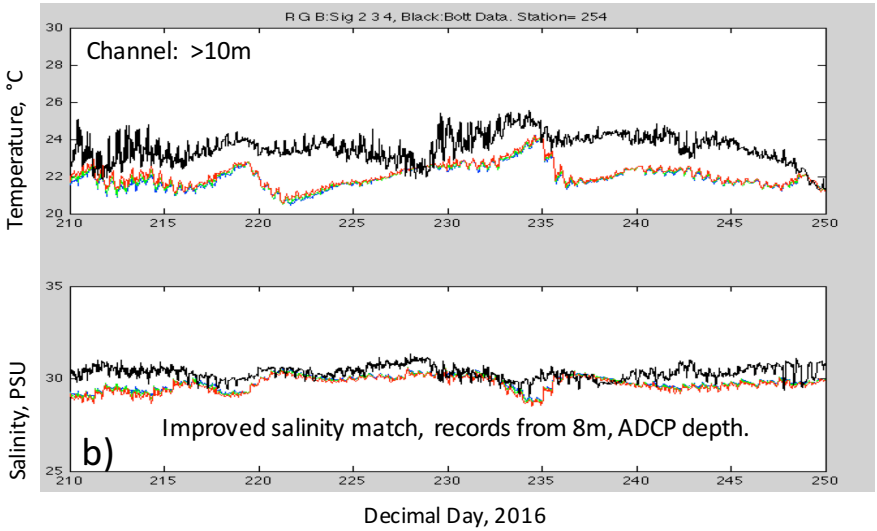

Figure 18. Sequence of temperature (top) and salinity (bottom) time series plots in a grid surrounding the ADCP/CTD mooring and Bullocks Reach buoy where ROMS output is focused on a tight range of near-bottom grid points (R: sigma1, G: sigma2, B:sigma3). Plots reveal how lateral cross channel changes of ~270m can produce improved or worsening matches between ROMS near-bottom values and bottom data values (black). a) Station 252, on shallow western shoal, 2m depth. b) Station 254 in shipping channel, >10m depth. Plots are from the depth of ~7-8m depth of the ADCP. c) Reference site, at the ADCP, in 7m of water. Across this restricted region close temperature and salinity matches can be achieved individually, but not for both at the same station. This suggests local flow/mixing processes require further study.

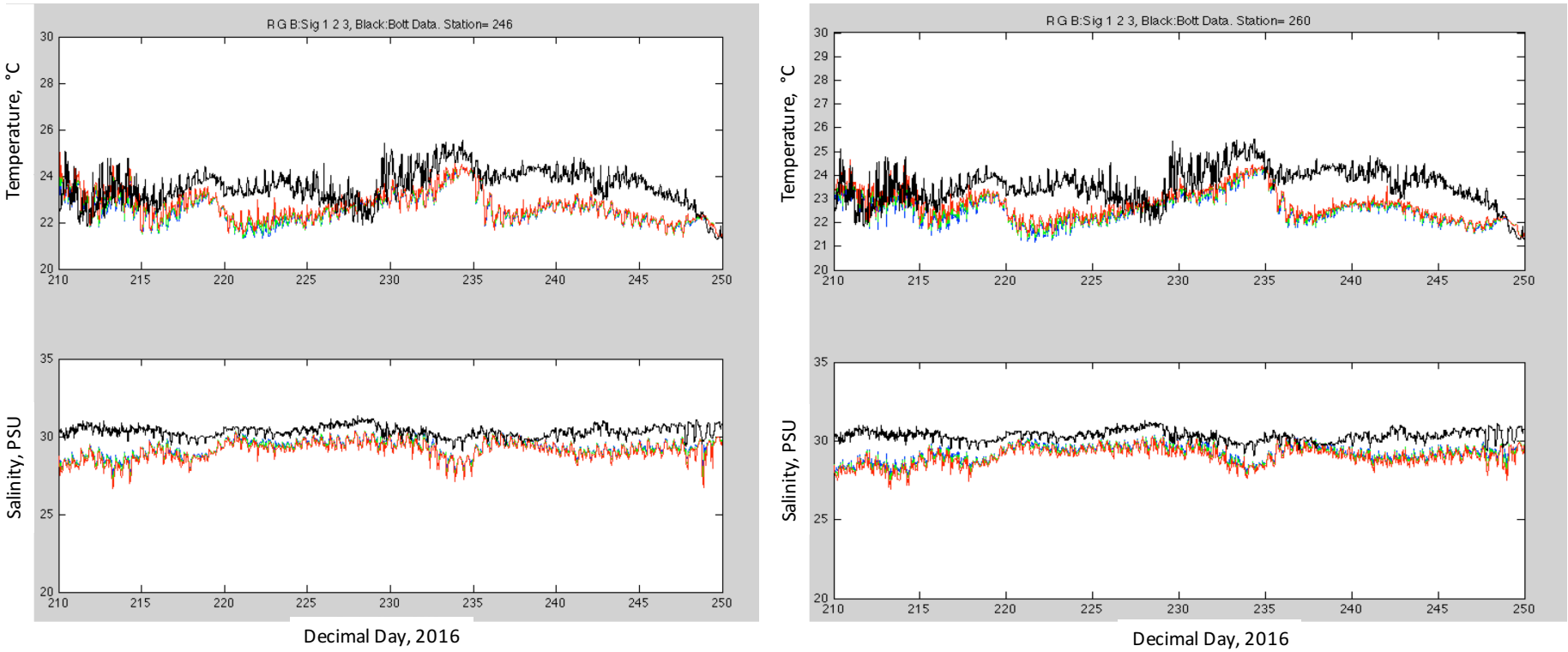

Figure 19. Sequence of temperature (top) and salinity (bottom) time series plots for ROMS output stations in the transitional shoal, south (a, station 246) and north (b, station 260) of the ADCP/CTD mooring and Bullocks Reach buoy. Plots reveal how changes along this bathymetric level can produce improved or worsening matches between ROMS near-bottom values (R: sigma1, G: sigma2, B:sigma3) and bottom data values (black). Stations 246, 253 and 260 are all in the transition zone (7m of water) between the shallow western shoal and the deeper channel.

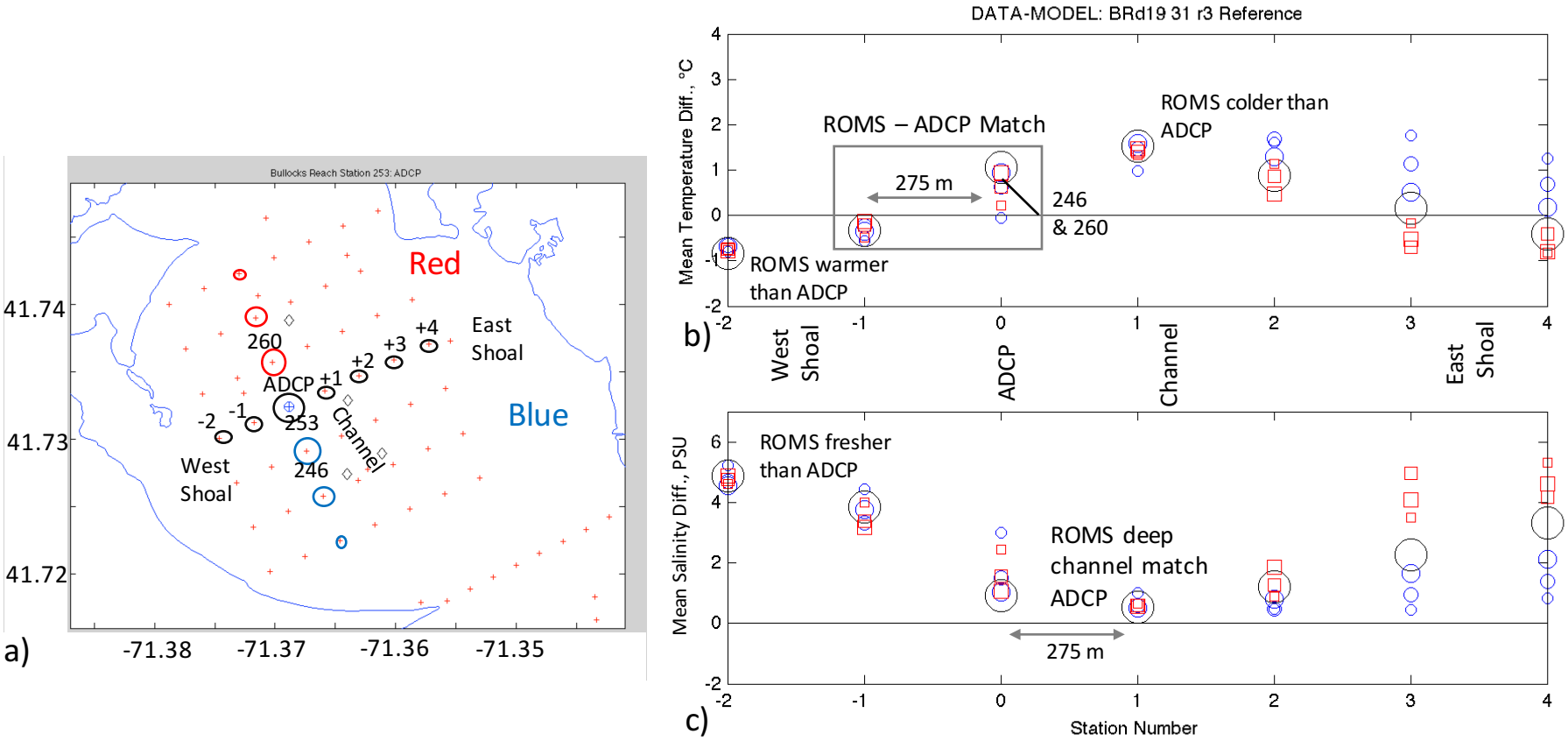

Figure 20. a) Map showing the Bullocks region. Red dots are ROMS station output locations. Blue-cross circle is ADCP location. Diamonds are navigational buoys. Channel location labeled. Average difference values (b. temperature, c. salinity) for near bottom hydrographic parameters are shown (recorded data minus ROMS data). These plots represent the spatial complexity of the region. Dark circles show cross-estuary change in mismatch from ADCP locations. Red/blue circles show how this mismatch changes in the channel-parallel direction northwest of (red) and southeast of (blue) the ADCP. Size of the circle shows distance from the black circle, across-estuary reference line (shown in (a)). ROMS stations are approximately 275 meters apart. ROMS is too cold at ADCP. Mixing with shoal water would improve match. ROMS salinity is slightly too fresh at ADCP. Very limited mixing with channel water will improve match. Stations 246, 253 and 260 are labeled. Relative station numbers to 253 (channel-normal transect) from plots (b,c) are labeled in (a).

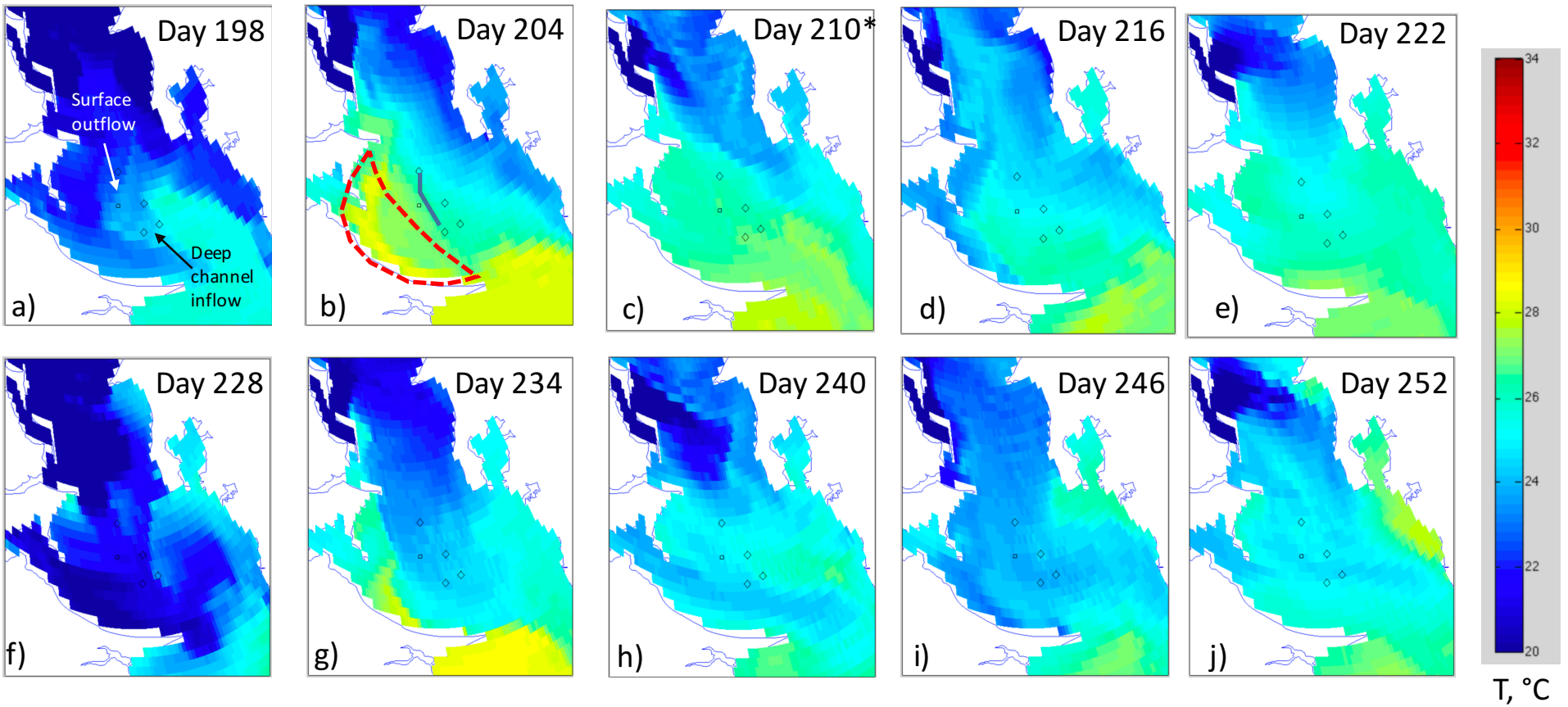

Figure 21. Mapview contour plots surface temperature in Bullocks Reach area of Providence River before and during the 2016 ADCP deployment (beginning day 210). Day numbers are marked on each frame. Diamonds show navigational buoys. Square shows ADCP location. Solid line connecting diamonds in (b) highlights how closely the ADCP sits to channel edge. Bullocks Reach shoal (red dashed in b) alternates between periods of warmer (b) and cooler (h) than channel water. Bullocks Reach buoy and ADCP reside between hydrographic regimes of the shoal and the channel.

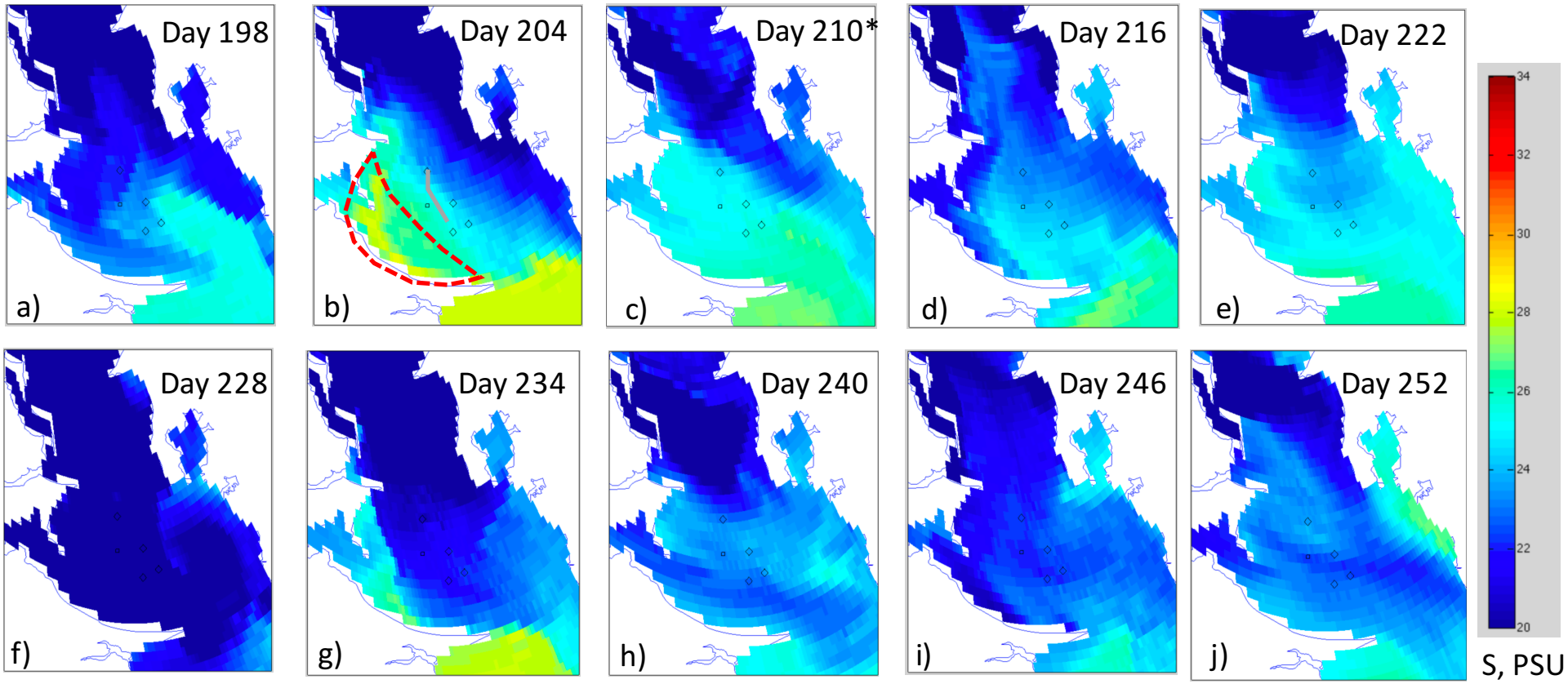

Figure 22. Mapview contour plots surface salinity (S, in PSU, see color bar) in Bullocks Reach area of Providence River before and during the 2016 ADCP deployment (beginning day 2010). Diamonds show navigational buoys. Square shows ADCP location. Bullocks Reach shoal (red dashed in b) alternates between periods of being saltier (b,g) than surface channel water and similar salinity as surface channel water. Often this is because fresh outflows follow the channel (frame g), isolating remnant saltier surface water on shoal. Grey line in (b) highlights western channel edge.

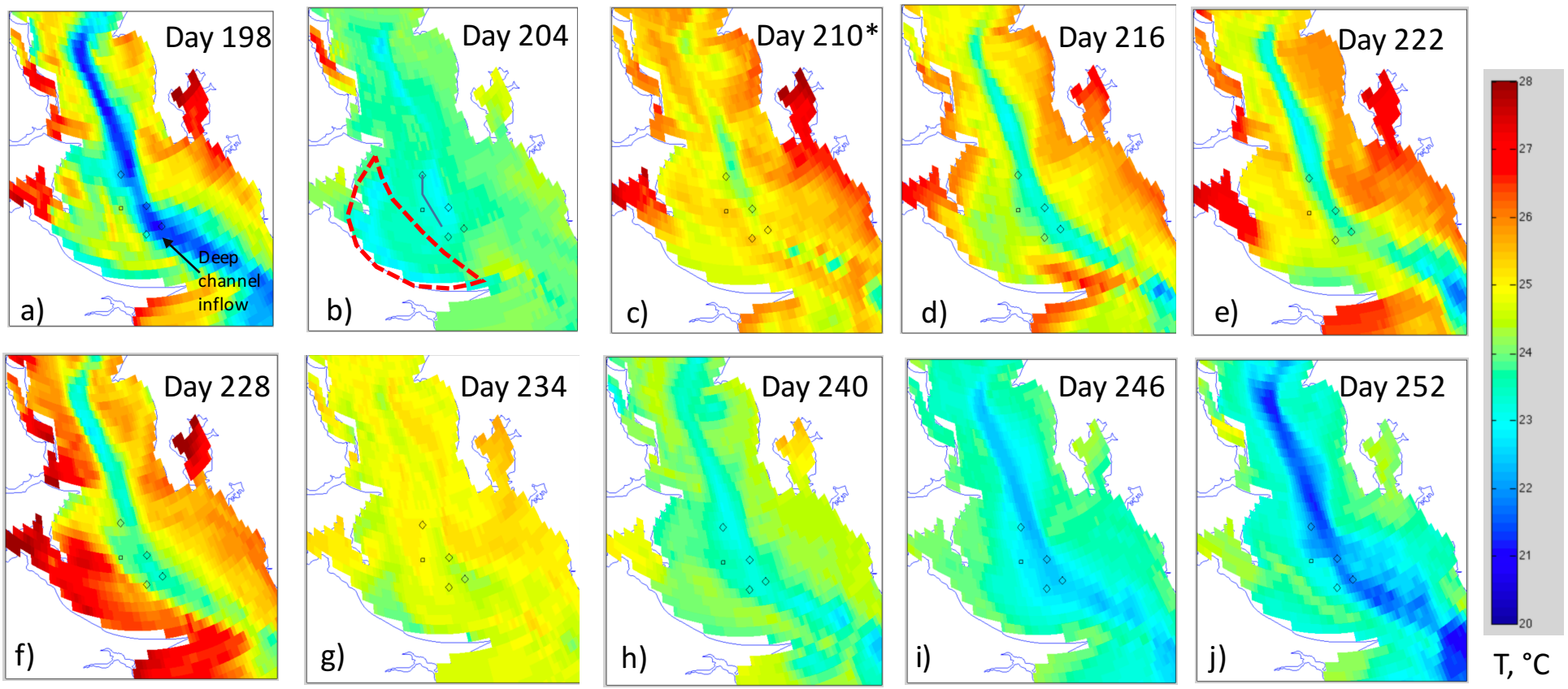

Figure 23. Mapview contour plots of temperature at MID-water column depth (sigma layer 10, 1=bottom, 15-surface) near Bullocks Reach, 2016. Decimal day numbers are marked on each frame. Diamonds show navigational buoys. Square shows ADCP location. Bullocks Reach shoal (red dashed in g), and all of the shallower shoals, experience extensive periods of warmer water conditions than central, mid-depth channel water. Frames a, c, e, h and i show the ADCP location sits along an extreme lateral (east-west) gradient in temperature. Frame f (day 228) is a period of extreme 3°C lateral gradient in mid-water temperature. Even small changes in how ROMS simulates the east-west location of this gradient will result in appreciable changes in the time series values at this output station (253). Grey line in (b) highlights western channel edge.

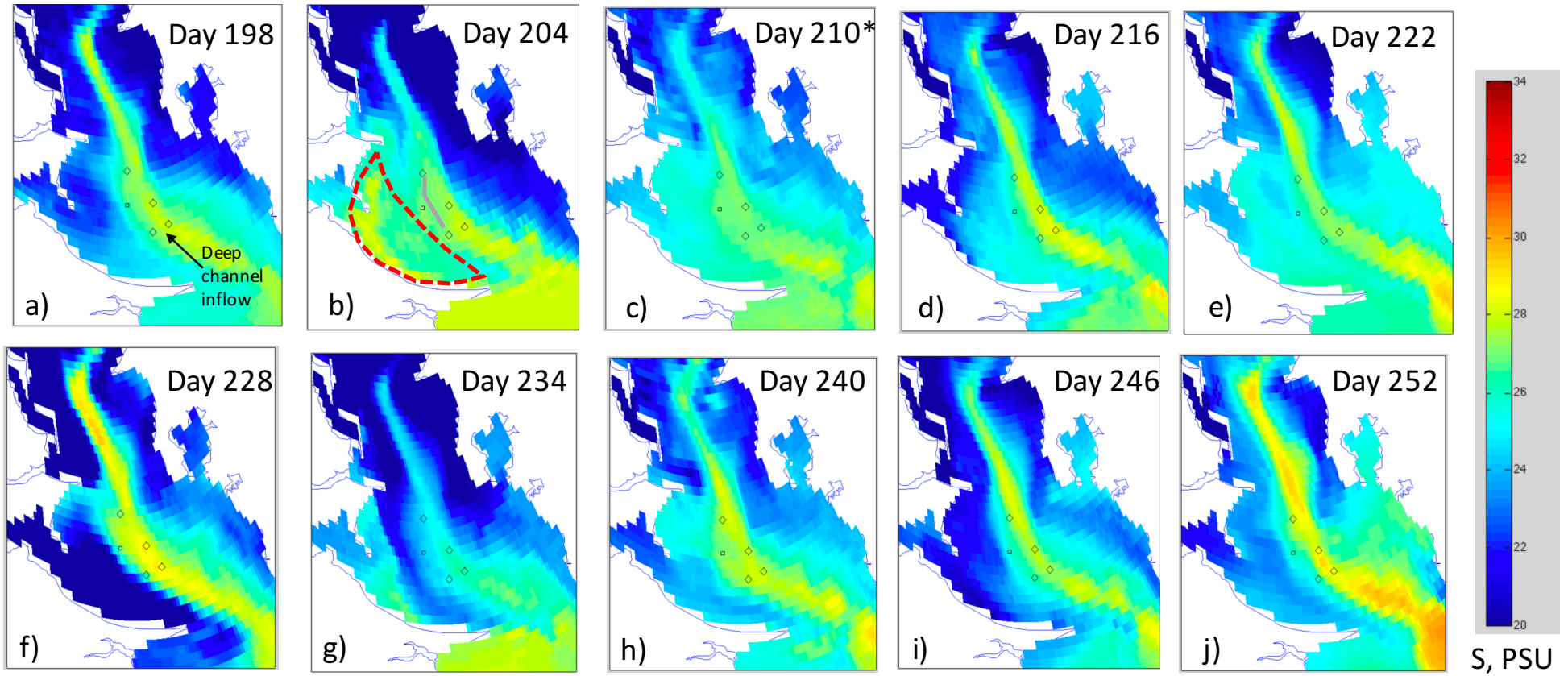

Figure 24. Mapview contour plots of salinity at MID-water column depth (sigma layer 10, 1=bottom, 15-surface) near Bullocks Reach, 2016. and during the 2016 ADCP deployment (beginning day 210). Diamonds show navigational buoys. Square shows ADCP location. Bullocks Reach shoal (red dashed region in b) is consistently fresher than channel water at mid-depth, or roughly 4 meters depth in the channel. Salty intrusions, as shown in frame j are often isolated from the shoal. During these periods the ADCP and Bullocks Reach buoy lie in the complex lateral mixing zone between hydrographic end points. Grey line in (b) highlights western channel edge.

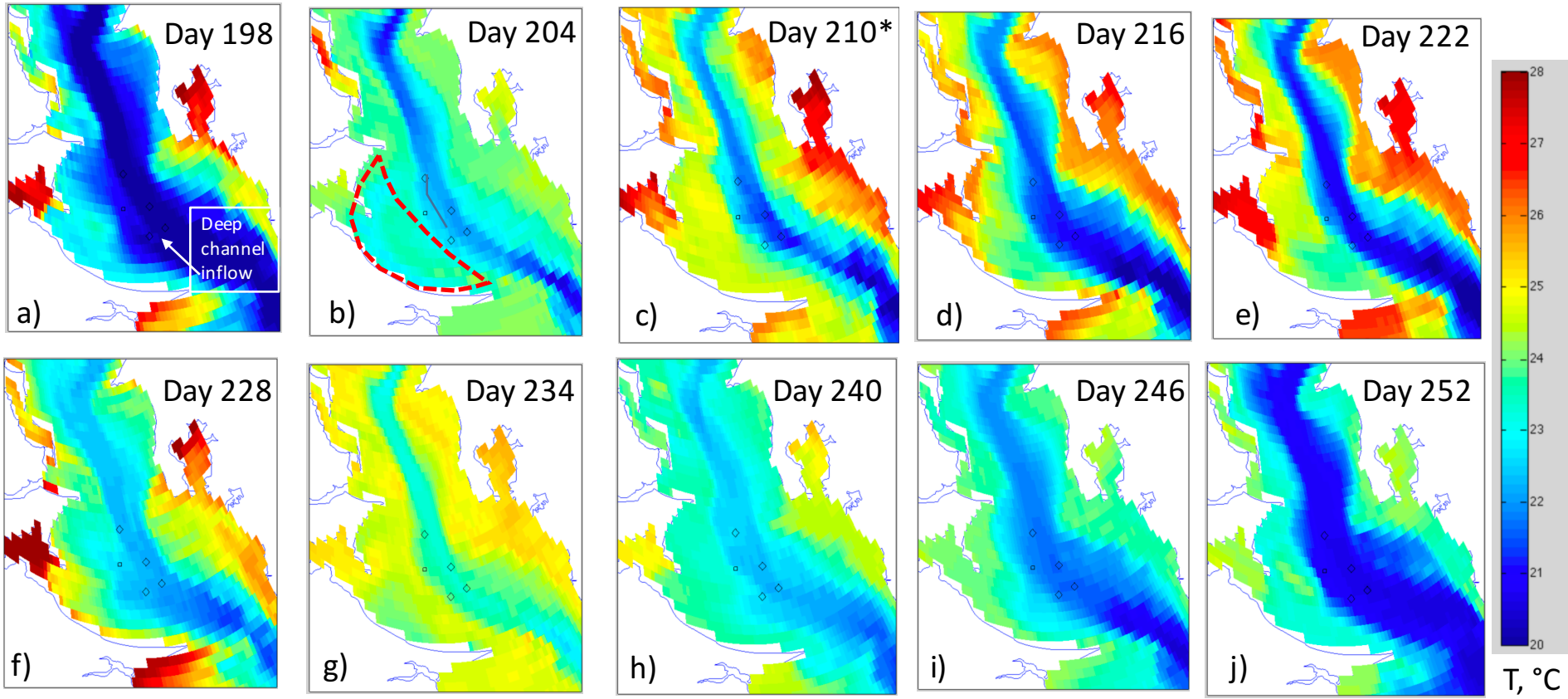

Figure 25. Mapview contour plots of temperature at near bottom depths (sigma layer 2, 1=bottom, 15-surface) near Bullocks Reach, 2016. Day numbers are marked on each frame. Diamonds show navigational buoys. Square shows ADCP location. Solid line in (b) shows west edge of channel, and close proximity of this to ADCP. Shoals are consistently warm relative to deep channel. The Bullocks Reach buoy and ADCP lie in lateral mixing zone between these temperature endmembers, often reaching 7°C in temperature difference (frames c, d, e). Grey line in (b) highlights western channel edge. Bullocks Reach shoal is highlighted by red dashed region in (b).

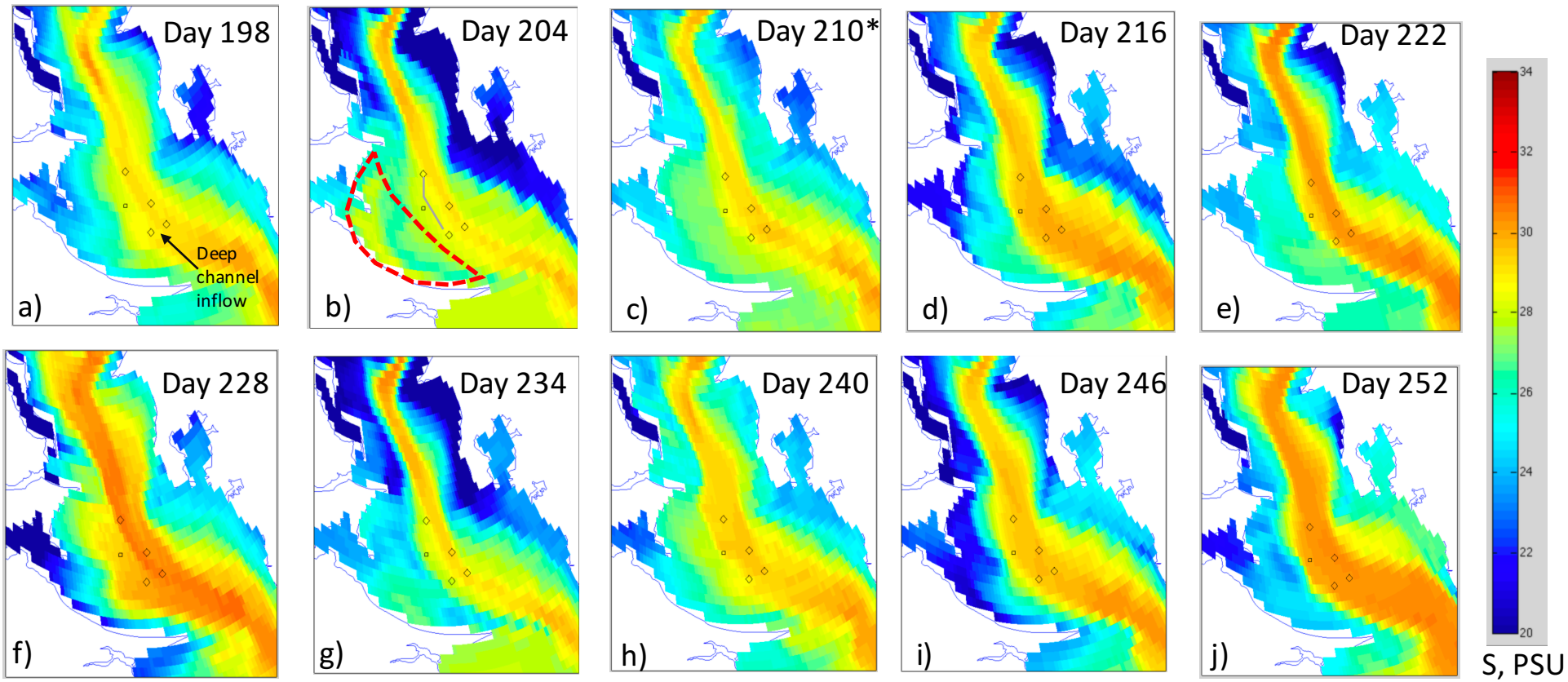

Figure 26. Mapview contour plots of salinity at near-bottom depth (sigma layer 2, 1=bottom, 15-surface) near Bullocks Reach, 2016. and during the 2016 ADCP deployment (beginning day 210). Diamonds show navigational buoys. Square shows ADCP location. Bottom shoal water is consistently fresher than deep channel water. Slight changes in how ROMS shifts these lateral fronts in an east-west direction, or in lateral mixing processes or in upslope advection will lead to large swings in hydrographic properties at the ADCP/Bullocks Reach Buoy. Grey line in (b) highlights western channel edge. Bullocks Reach shoal is highlighted by red dashed region in (b).

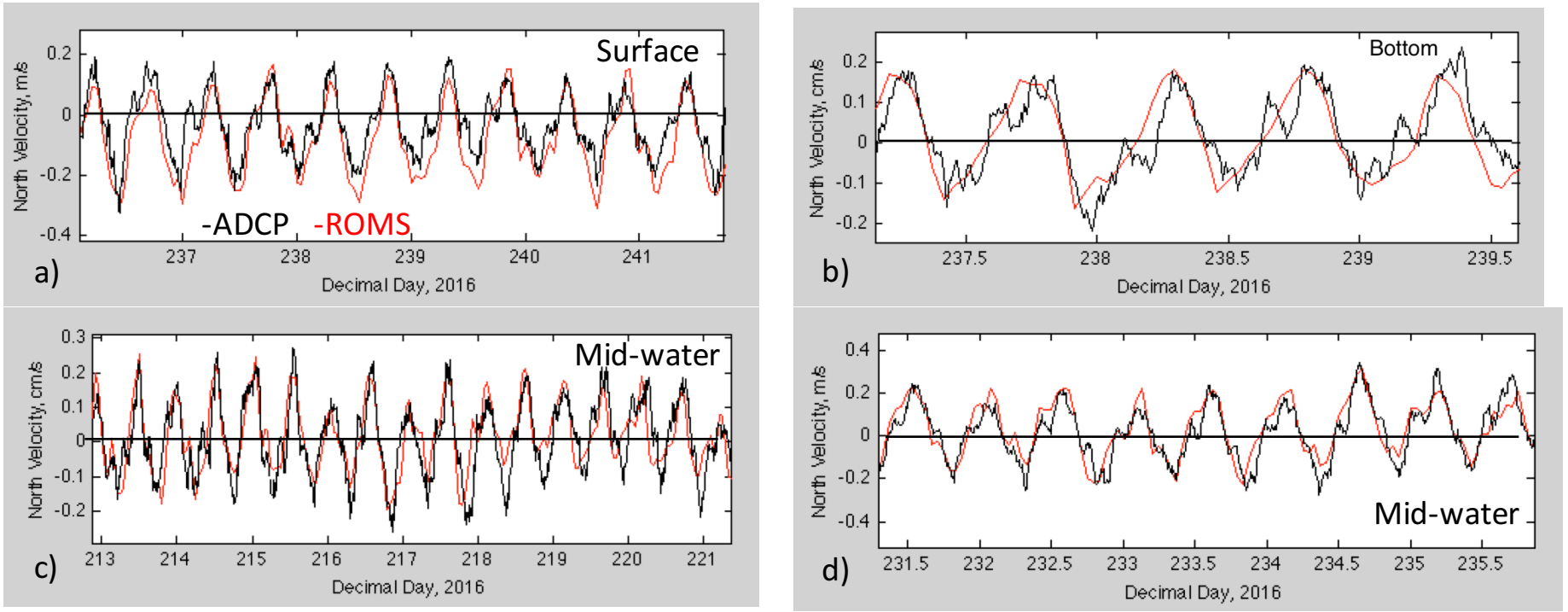

Figure 27. Time series plots of ROMS (RED) versus ADCP (BLACK) northward velocity component for various depths and time periods of the deployment window. Velocities are unfiltered, and therefore include the large magnitude inflow/outflow swings of the flood and ebb tides. a) The agreement of ROMS and ADCP for near surface tidal velocity is very high, ranging from ~0.2 m/s during flood and between -0.25 to -0.3 m/s during ebb. b) The close agreement between ROMS and the ADCP for near-bottom velocity is shown for a shorter time window. Frames c, d show similar close ROMS-ADCP velocity agreement for mid-water column over different time windows.

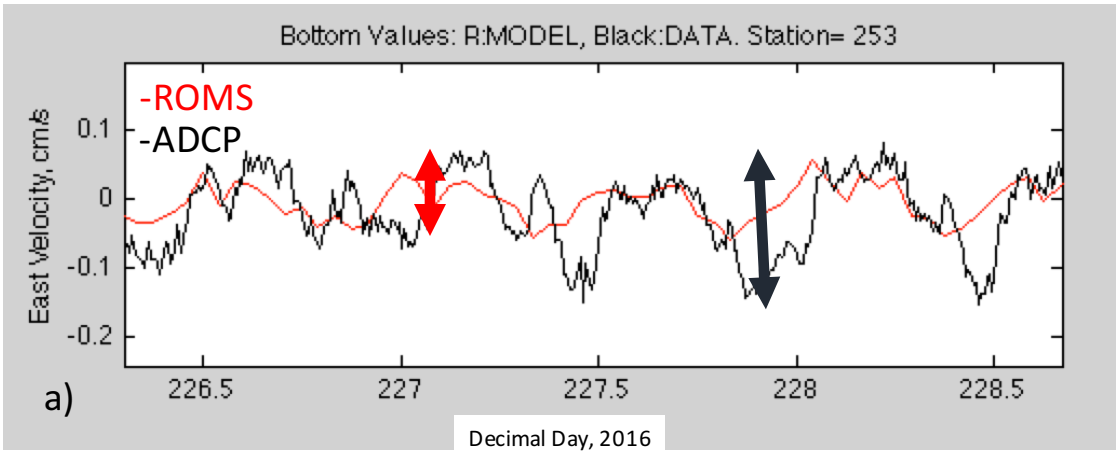

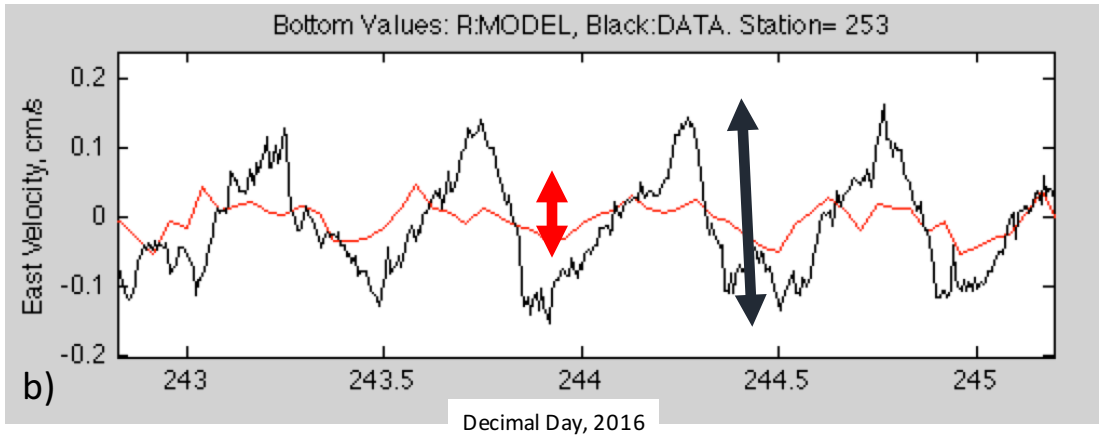

Figure 28. Time series plots of ROMS (RED) versus ADCP (BLACK) eastward near-bottom velocity components. Velocities are unfiltered, and therefore include the large magnitude oscillations due to tidal flows. a) For the period of days 226-229, ROMS under-predicts across-estuary flow (+0.03 to -0.05 m/s) relative to ADCP values (+0.1 to -0.15 m/s). ROMS transverse energy is 25-50% of the ADCP recorded energy.

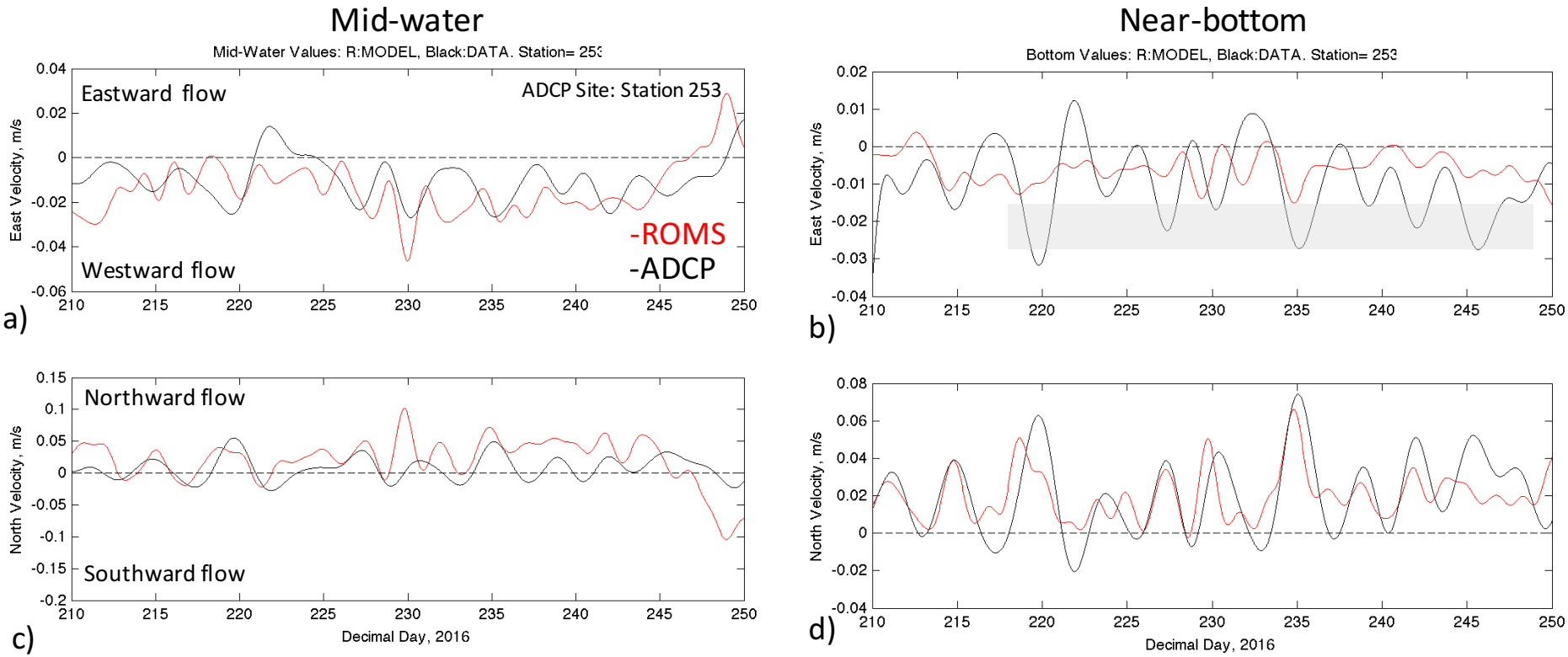

Figure 29. Time series plots of ROMS versus ADCP sub-tidal velocity components, where tidal oscillations have been filtered out using the MATLAB filtfilt command. Frames (a, b) are eastward flow for mid-water (a) and near-bottom (b) depths. Frames c and d are northward flows for mid-water (c) and near-bottom (d) depths. Sub-tidal model velocities, often hard to match with data, are very close to data in both a mean sense and in oscillations. a) Mid-level water moves northward and westward in both ROMS and data, roughly parallel to the local trend of the channel. b) Bottom water moves similarly in both model and data, though ROMS under predicts the magnitude of this flow (shaded region). This could explain why salinities tend to be under predicted in ROMS at Bullocks Reach. ROMS does an exceptional job of representing ADCP residual northward flow at (c) mid-level and (d) near-bottom depths.

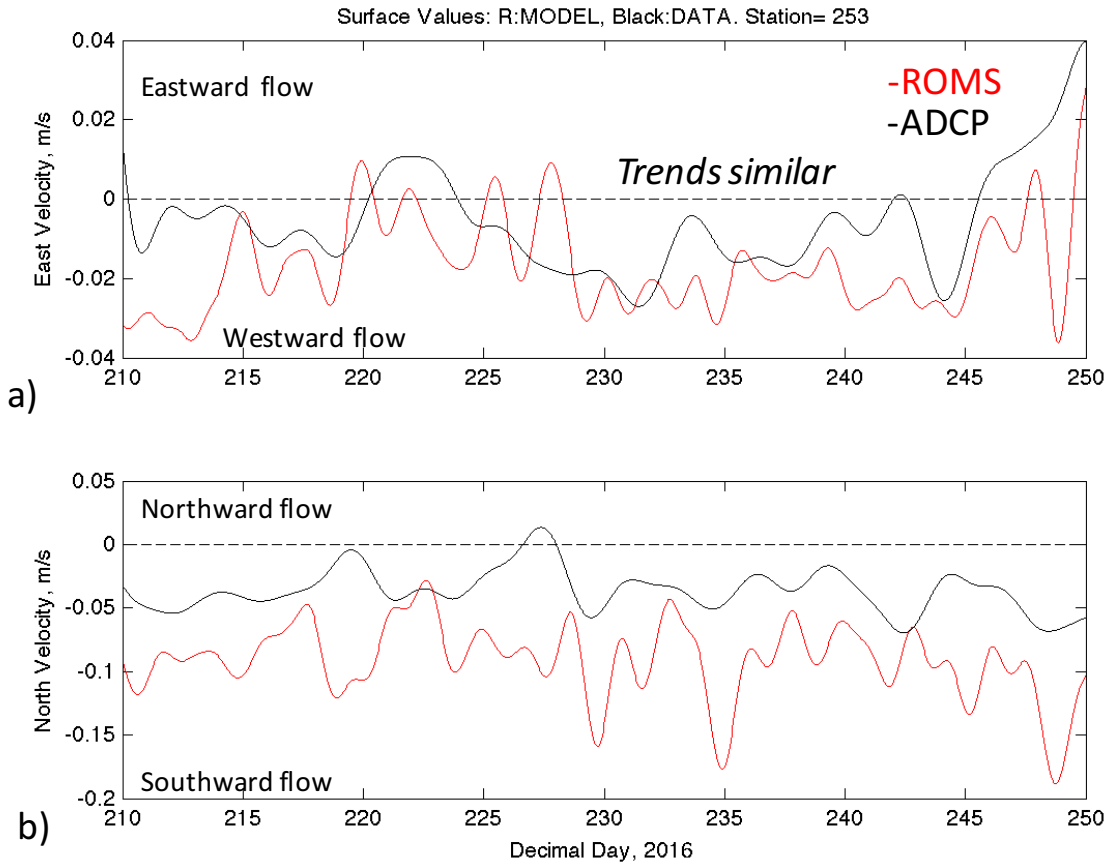

Figure 30. Similar time series plots of ROMS versus ADCP sub-tidal velocity components, as **Figure 29** but for near-surface values. Both ROMS and ADCP show prevailing southwestward subtidal flow of surface water. Plots show a weaker correlation between ROMS values (red) and ADCP data values (black). This is not unexpected as the information available to drive surface winds, which strongly control surface water velocity is very poorly known. Values are used from PORTS stations that are removed from this area, and which do not include the influence of fetch (e.g. local wind variations due to wind interacting with land).

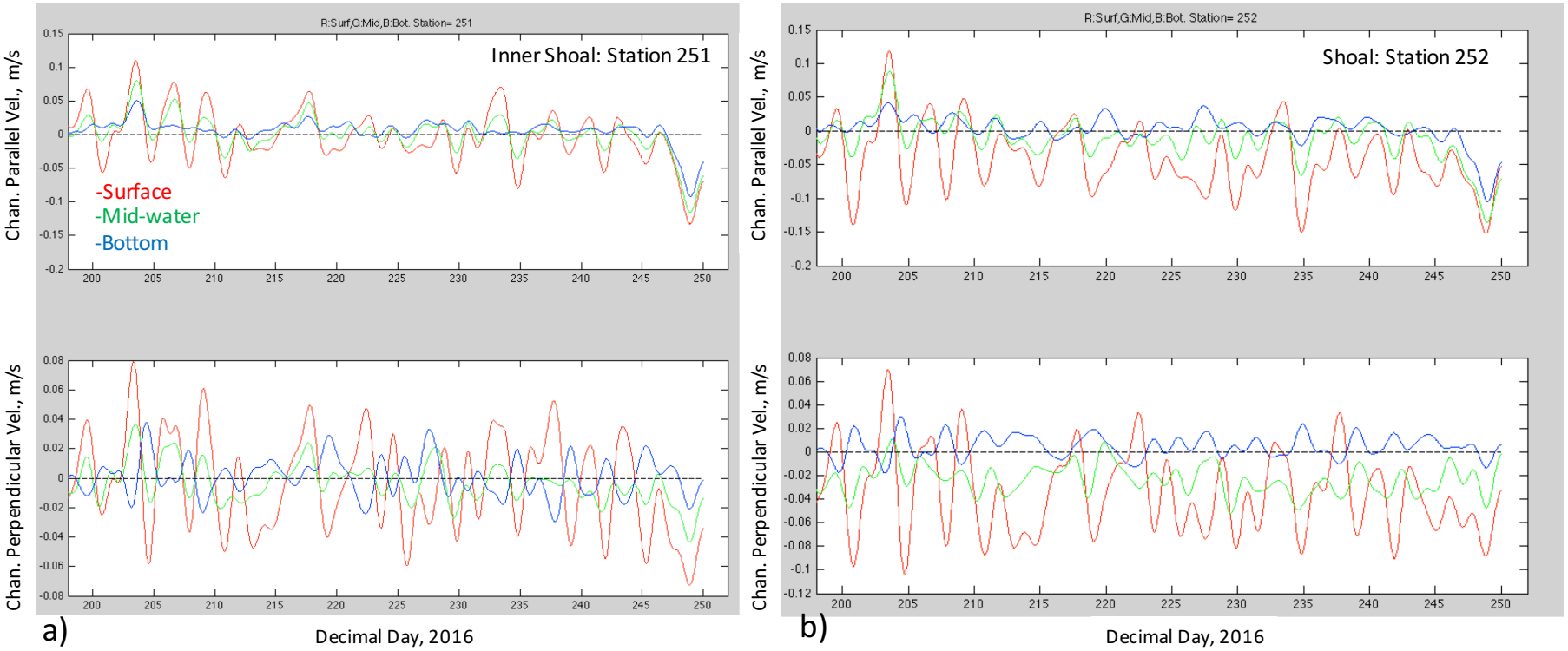

Figure 31. Time series plots of channel parallel and channel-perpendicular subtidal (residual) flow from the reference ROMS 2016 run. Average velocity at surface (red), mid-water (green) and bottom (blue) levels are shown. The sequence shows lateral (channel-perpendicular) changes in flow from a) the westernmost shoal (station 251, 2m depth), b) western shoal (station 252, 2m depth), c) the transitional zone between shoal and channel (station 253, location of ADCP/CTD mooring, 7m depth) and d) the shipping channel (station 254, >10m depth). a) The westernmost shoal has weak channel-parallel flow, oscillatory at the surface and stagnant (oscillatory, <0.03 m/s) at depth. There is a weak (<0.04 m/s) and oscillatory channel-perpendicular flow. b) At station 252, ~270m west of the ADCP, there is clear net southwestward outflow (0.1-0.15 m/s) and more stagnant sub-surface flow. Bottom flow does exhibits very weak estuarine flow, or opposite surface motion, which is toward the channel (b bottom). Figure 31 (c,d) continued below.

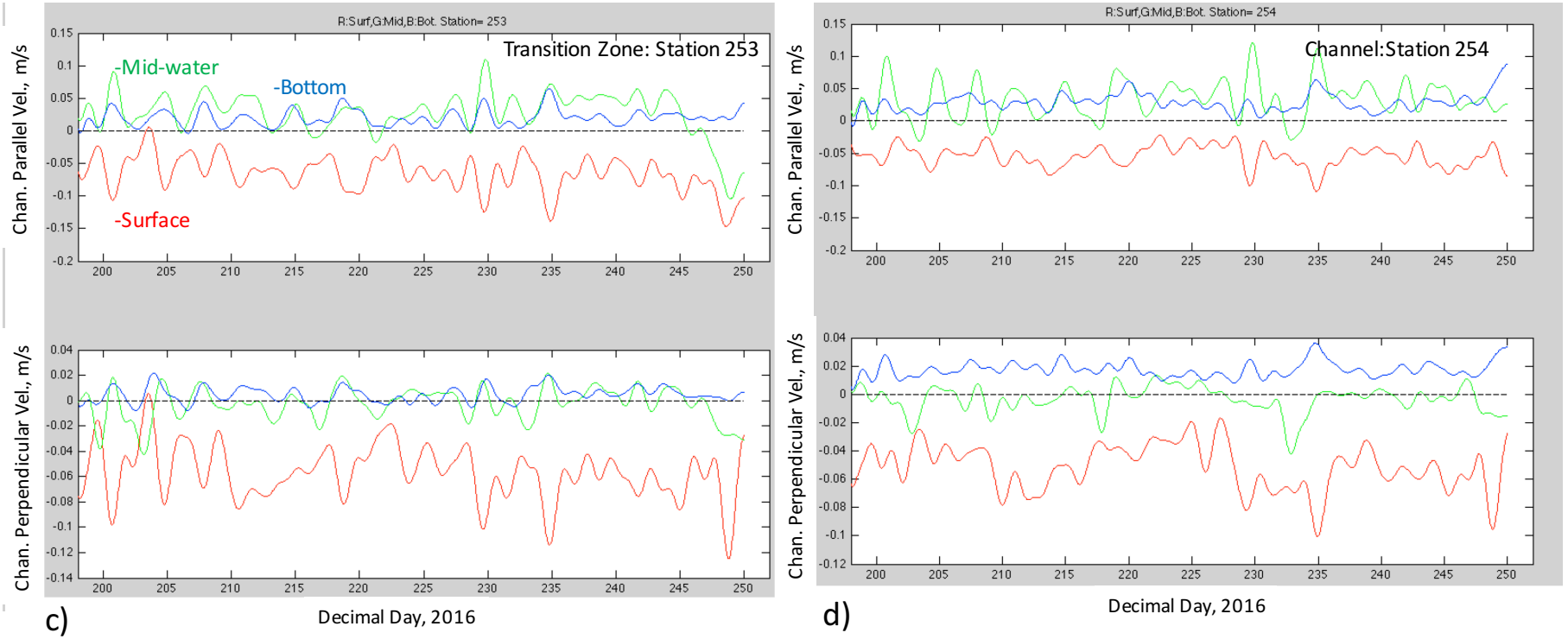

Figure 31 continued. Time series plots of channel parallel and channel-perpendicular subtidal (residual) flow: c) At the ADCP location (station 253) estuarine flow is better developed, surface outflow (0.1-0.15 m/s) with consistent inflow through mid-bottom sections (c top: 0.02-0.08 m/s). Data show important transverse (channel-perpendicular) flow, with surface (deeper) water moving shoal-ward (channel-ward), respectively. d) Similarly, 2-layer estuarine subflow is recorded (station 254) in the western side of the shipping channel, where surface water is weakly towards the western shoal and from the shoal at depth.

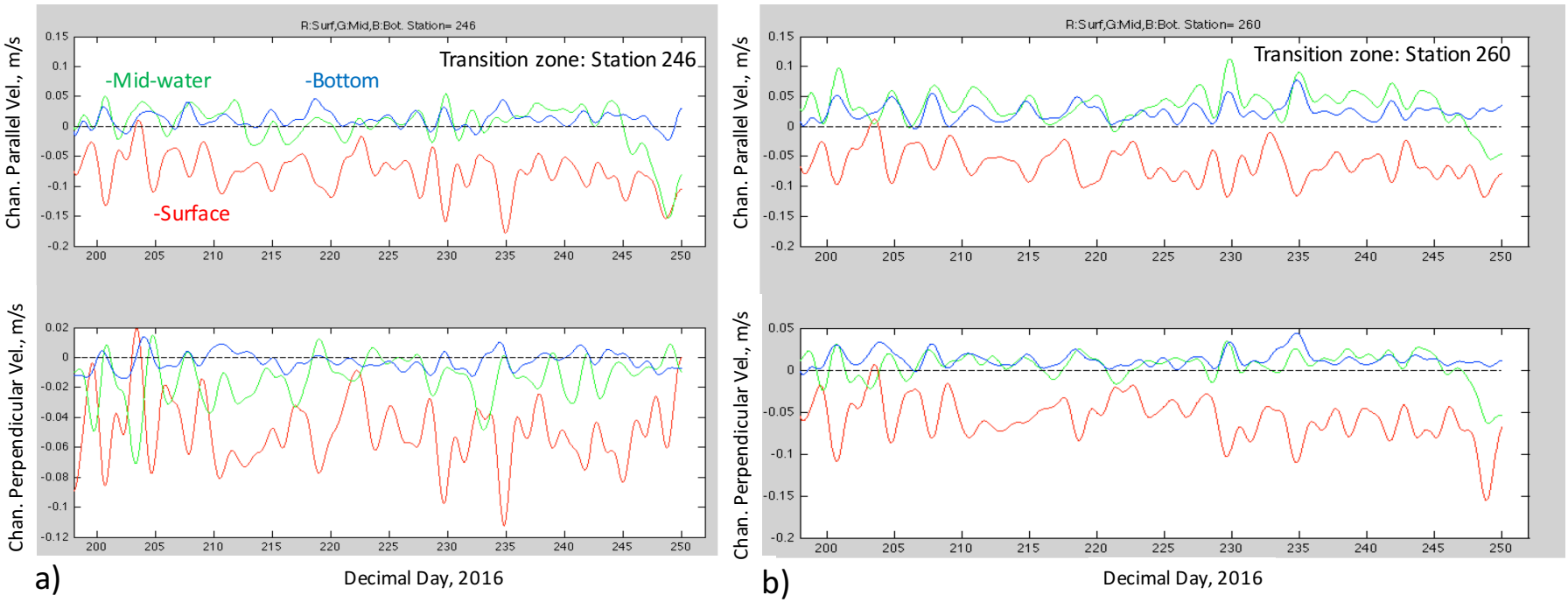

Figure 32. Plots of channel perpendicular and channel parallel flow for ROMS 2016 reference simulation. Lateral comparison of flow near ADCP and Bullocks Reach buoy. Here a progression in flow is shown from ROMS output moving along the transitional zone, west of the shipping channel from a) station 246, south of the ADCP ((c)station 253) and b) station 260, north of the ADCP site shown in (c). The model predicts this to be a region of consistent subtidal flow, with similar layered estuarine patterns (surface out, deeper in) at all three sites.

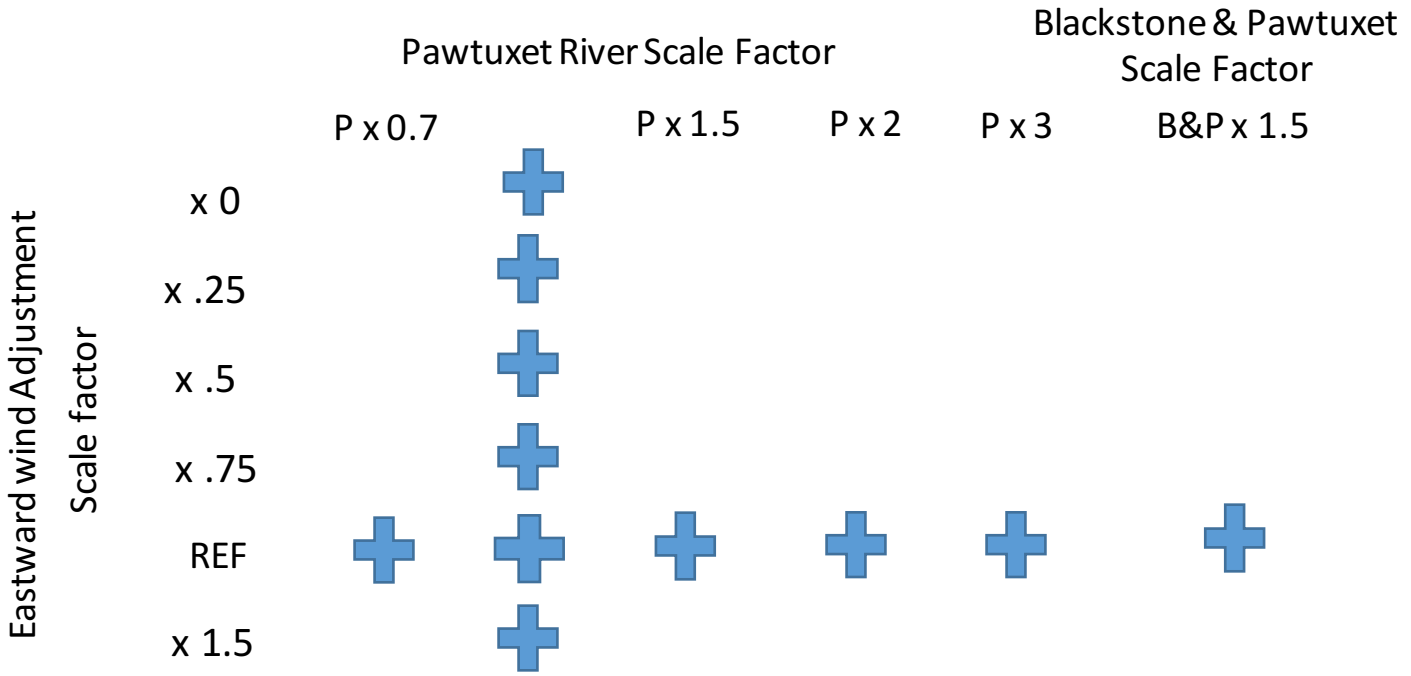

Figure 33. Schematic representing range in forcing parameters investigated for impact on circulation and temperature-salinity distributions in the Bullocks Reach area. Along the x-axis is the range in scale factors used to decrease or increase the Pawtuxet River outflow. One case had both Pawtuxet and Blackstone scaled up by a factor of 1.5. Along the y-axis are scale factors used to enhance or decrease the eastward component of wind to roughly simulate the effect of fetch acting on winds. Two cases were also run with enhanced southwestward blowing winds.

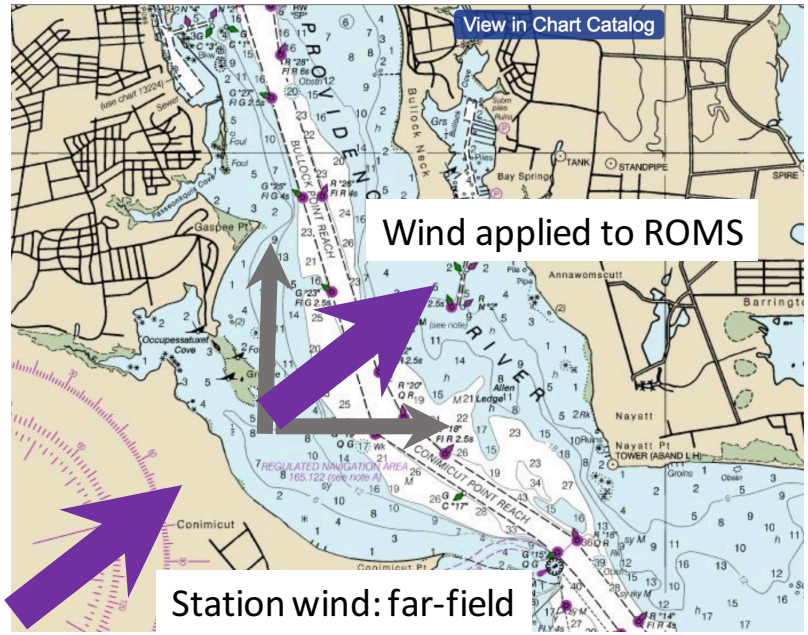

a)

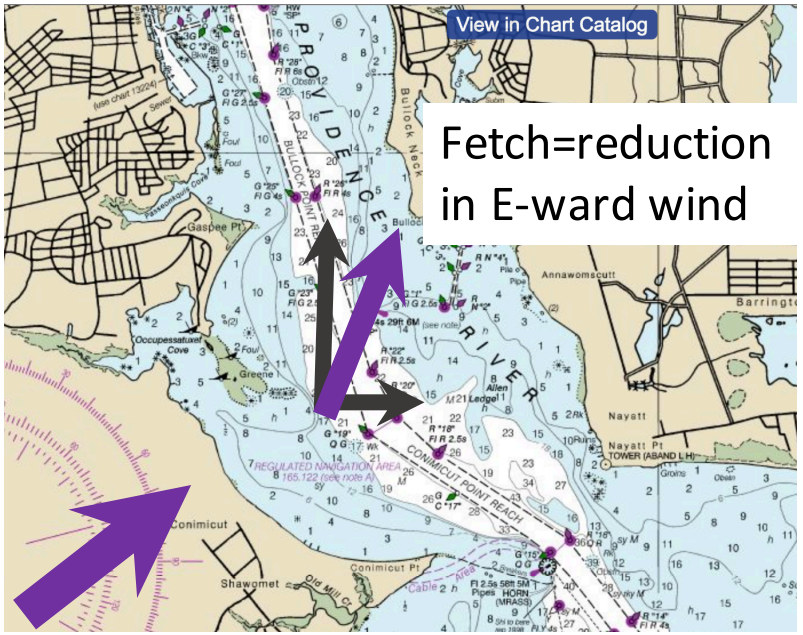

b)

Figure 34. The application of environmental forcing to ROMS is simplified. a) Wind data from distance NOAA-PORTS stations are applied uniformly to the water surface. b) Local effects of land can produce a change in wind components in particular directions, known as fetch. A few model runs were done to quantify the role of fetch effects on ROMS flow/hydrography at Bullocks Reach.

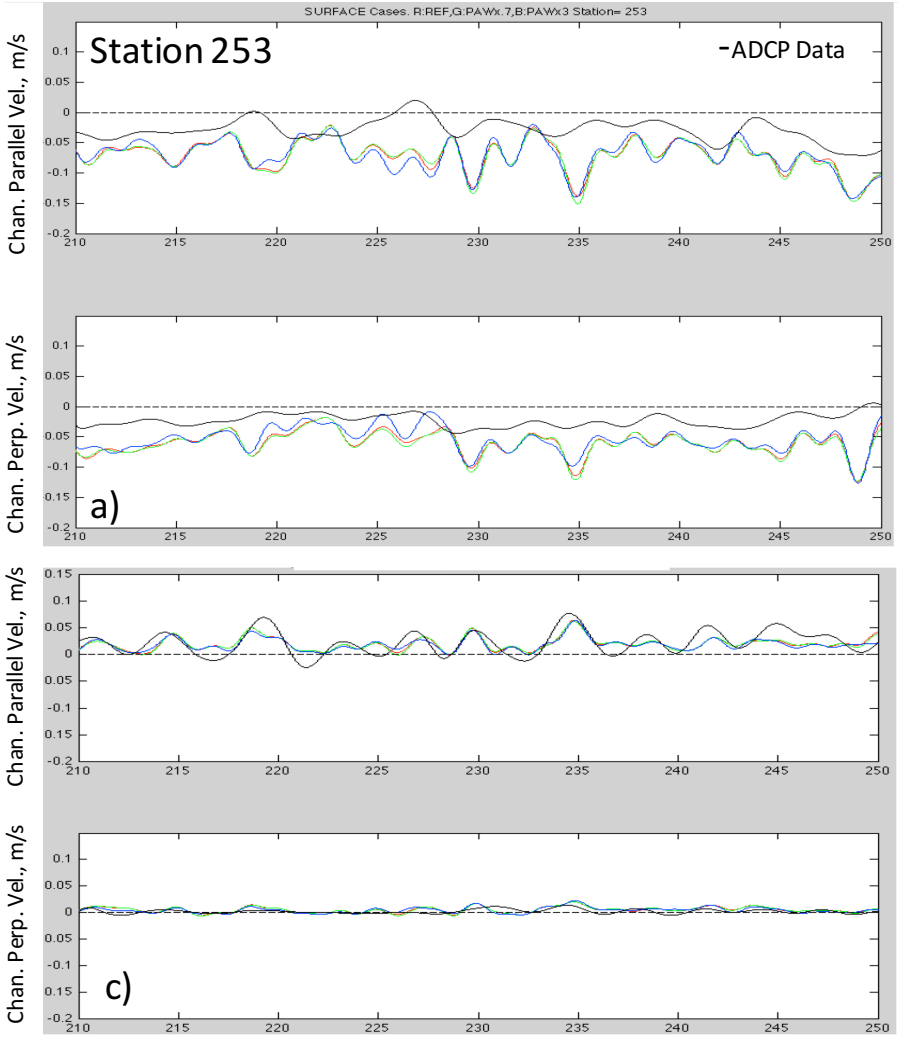

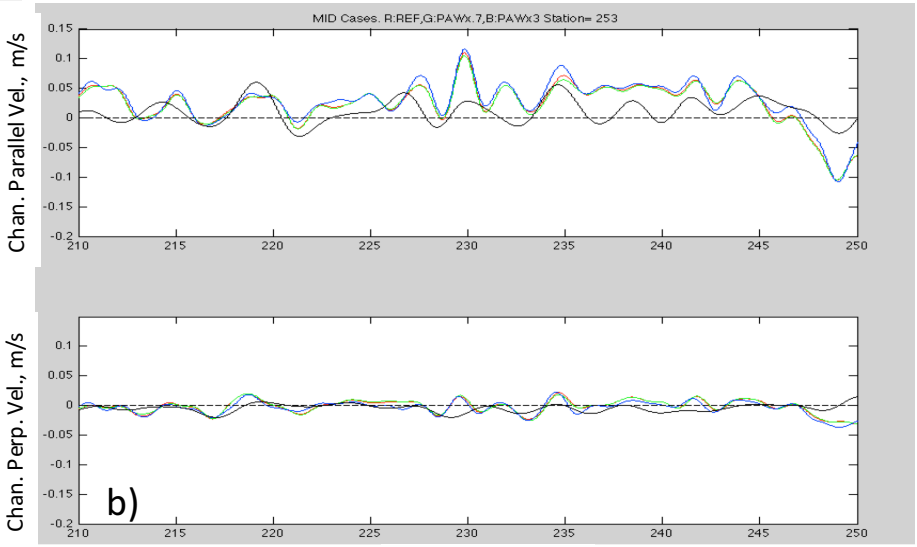

Figure 35. Data-ROMS velocity comparison plots for reference run (red) versus **changing Pawtuxet River strength** (green=reduced to 70%; blue= 3 times larger flow) at station 253, co-located with BR buoy and ADCP/CTD. The enhanced runoff case (blue) ends early due to instability. ADCP data are shown in black lines. All records (data and ROMS) are filtered to produce subtidal flows. a) Near-surface comparison. b) Mid-water comparison. c) Near-bottom. Velocities are rotated into channel parallel (top frame) and channel-perpendicular (bottom frame) components. Variations in Pawtuxet River flow does not significantly alter water flow at the station location (red-green-blue overlay). Generally, ADCP and ROMS sub-tidal flows show strong agreement. Key patterns are: a) Stronger outflow at the surface, with equal along and cross channel values. b) Net inflow of mid-level water and very weak cross channel flow at this depth. c) Bottom flow similar to mid-level, stronger inflow and very weak cross-channel flow.

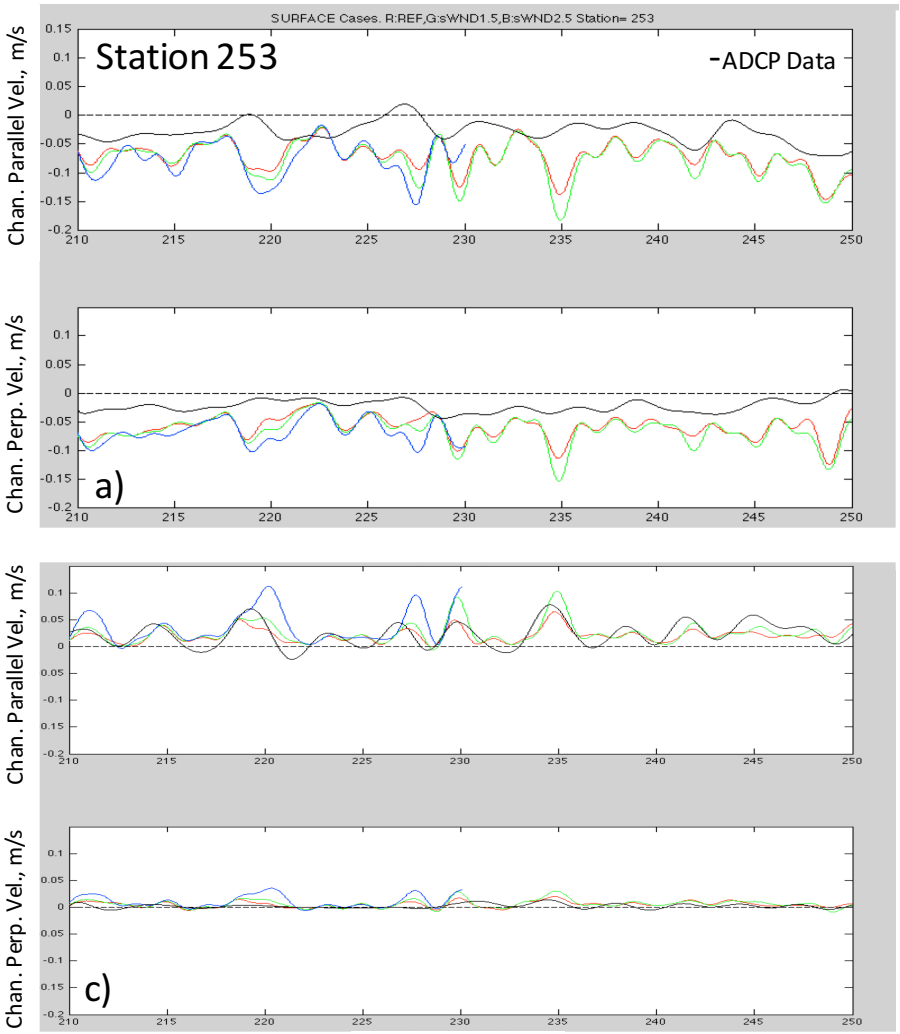

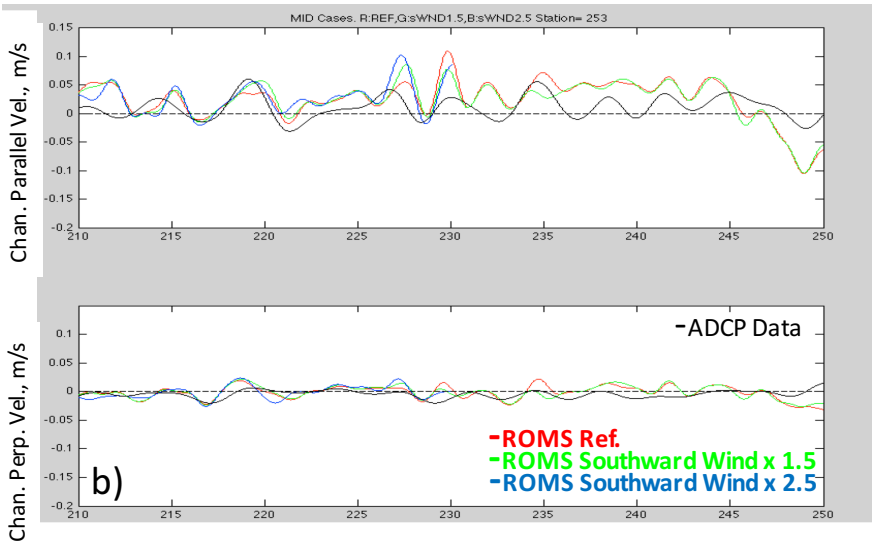

Figure 36. Data-ROMS velocity comparison plots for reference run (red) versus cases where only **southward winds are enhanced** (green=increased by 1.5; blue= increased by 2.5) at station 253, co-located with BR buoy and ADCP/CTD. ADCP data are shown in black lines. All records (data and ROMS) are filtered to produce subtidal flows. a) Near-surface comparison. b) Mid-water comparison. c) Near-bottom. Velocities are rotated into channel parallel (top frame) and channel-perpendicular (bottom frame) components.

a) Surface outflows increase from ~0.1 m/s to as high as 0.15-0.2 m/s. Enhancing southward winds make the fit with ADCP worse. b-c) Interestingly, southward wind increases result in stronger subtidal intrusions (>0.1 m/s). The strongly enhanced wind case (blue) ends early by numerical instability.

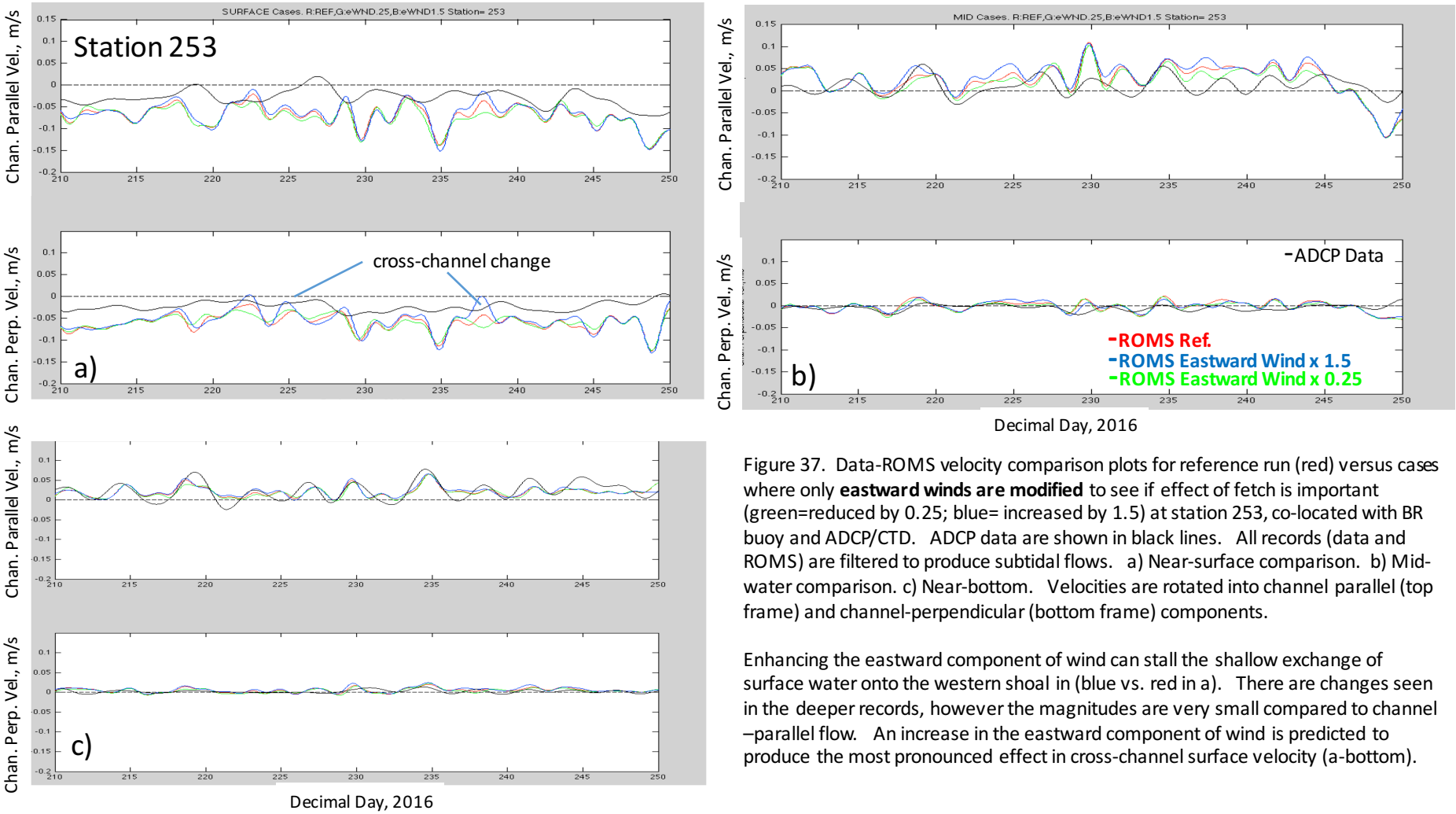

Figure 37. Data-ROMS velocity comparison plots for reference run (red) versus cases where only **eastward winds are modified** to see if effect of fetch is important (green=reduced by 0.25; blue= increased by 1.5) at station 253, co-located with BR buoy and ADCP/CTD. ADCP data are shown in black lines. All records (data and ROMS) are filtered to produce subtidal flows. a) Near-surface comparison. b) Mid-water comparison. c) Near-bottom. Velocities are rotated into channel parallel (top frame) and channel-perpendicular (bottom frame) components.

Enhancing the eastward component of wind can stall the shallow exchange of surface water onto the western shoal in (blue vs. red in a). There are changes seen in the deeper records, however the magnitudes are very small compared to channel –parallel flow. An increase in the eastward component of wind is predicted to produce the most pronounced effect in cross-channel surface velocity (a-bottom).

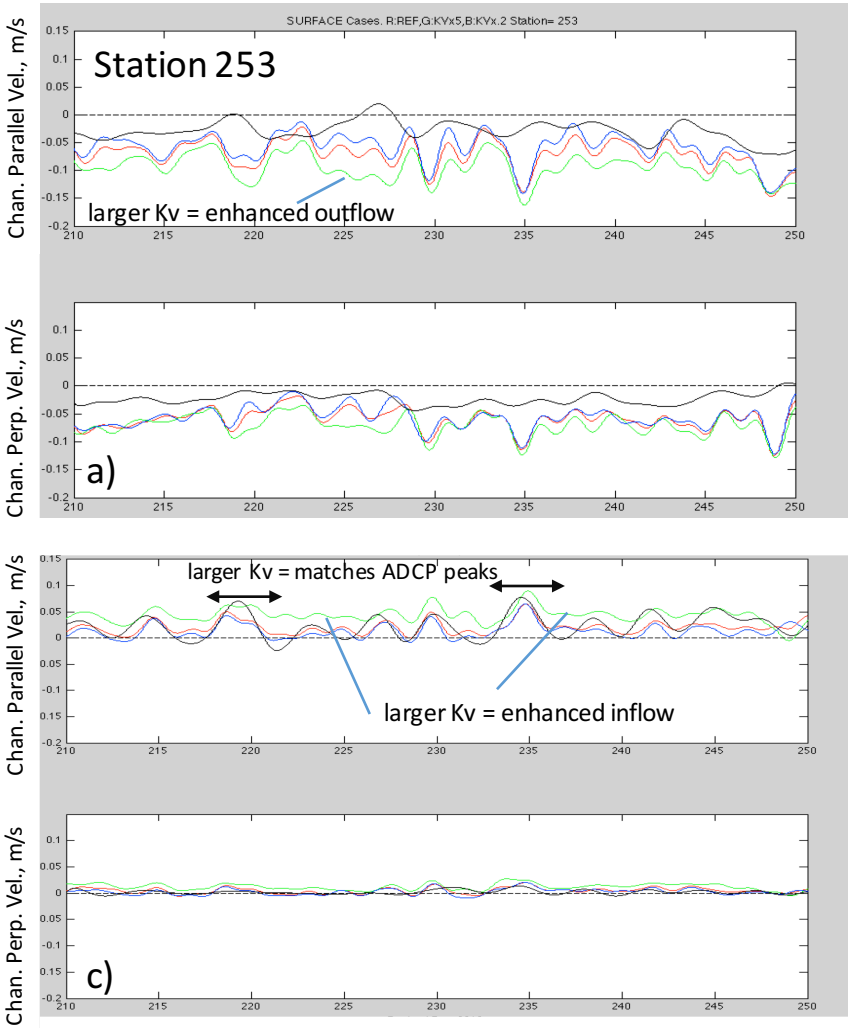

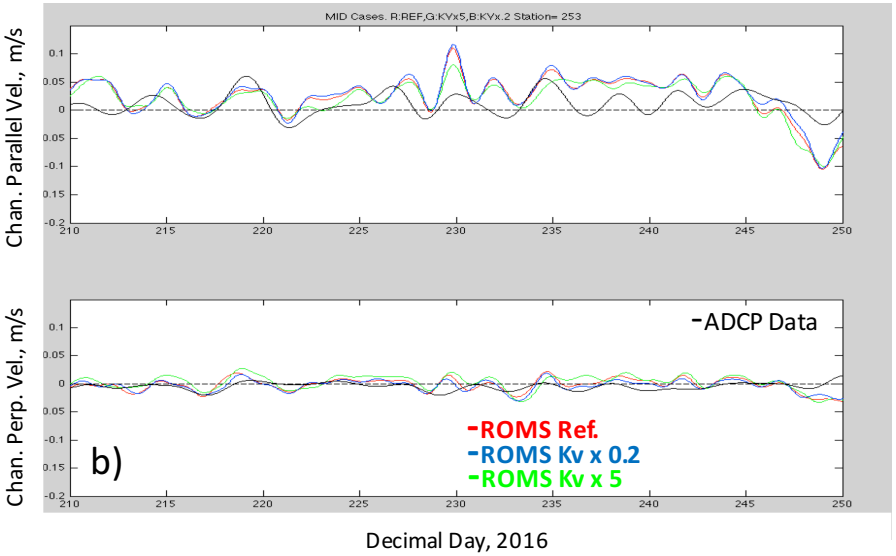

Figure 38. Data-ROMS velocity comparison plots for reference run (red) versus cases where **vertical mixing coefficient (Kv) is modified** (green=increased by 5; blue= decreased by 0.2) at station 253, co-located with BR buoy and ADCP/CTD. ADCP data are shown in black lines. All records (data and ROMS) are filtered to produce subtidal flows. a) Near-surface comparison. b) Mid-water comparison. c) Near-bottom. Velocities are rotated into channel parallel (top frame) and channel-perpendicular (bottom frame) components.

The largest sensitivity or differences in flows are recorded for this parameter change. Increasing Kv leads to stronger shallow outflow (green in a), weaker inflow at mid-level (green in b) and stronger deep inflow, meeting the peaks recorded in ADCP data (green vs. black in c). As with other parameter changes, there is an impact on deeper cross-estuary flow, but the question remains as whether the lower magnitudes of these changes can have a significant longer term impact on hydrography in the area.

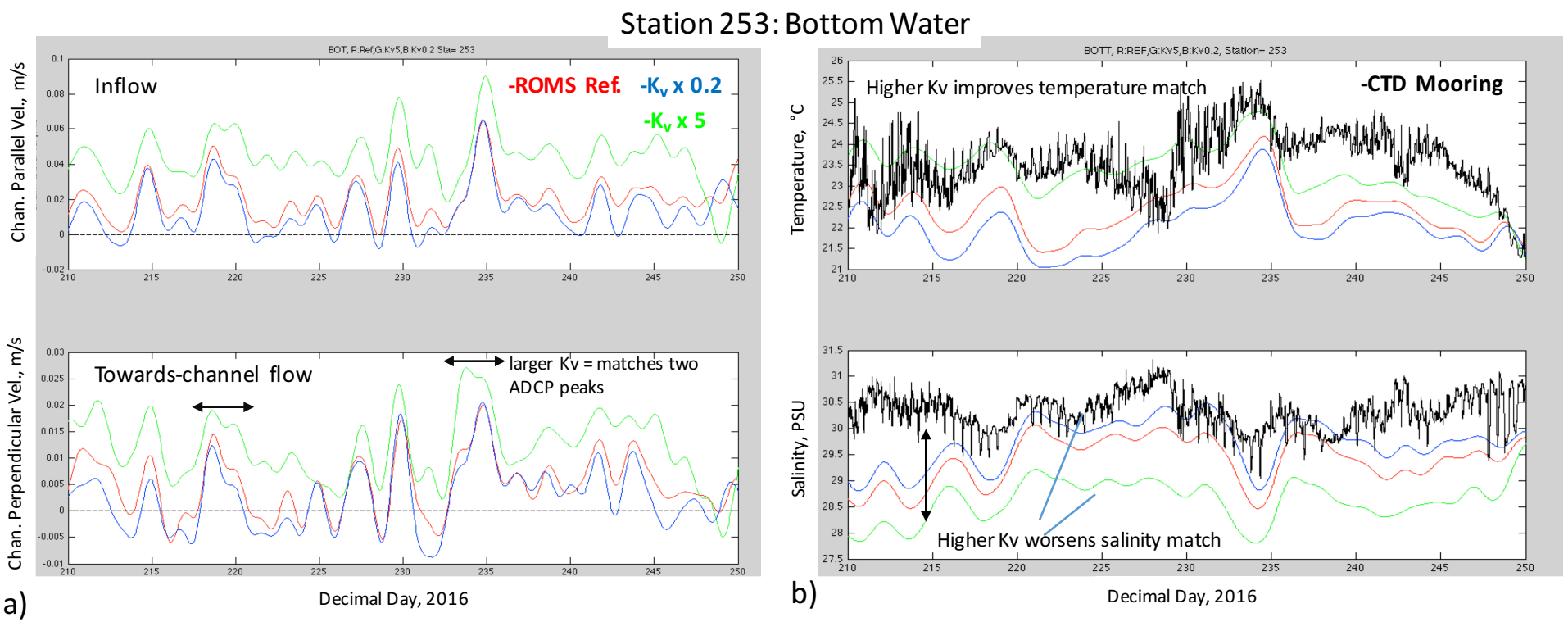

Figure 39. The process of testing ROMS parameters for their sensitivity in influencing solutions and changing the match with data is complex. Here the influence of altering the vertical mixing parameter (K_v) is looked at in more detail for near-bottom water. Frames are a-top) channel-parallel flow, a-bottom) channel-perpendicular flow, b-top) temperature and b-bottom) salinity. Colors are: red=reference case, green=Kv increased by 5, blue=K_v decreased by 0.2. The black line is data from the ADCP/CTD mooring. Reducing K_v (red vs. blue) has little effect on flow (a) and a small effect on T-S (b). Increasing K_v, or enhanced vertical mixing (green lines) leads to stronger deep inflow (a-top) and flow from the shoal to the channel (a-bottom). It also leads to a better fit with observed bottom temperature (b-top). However, it also results in freshening of the bottom water (green line in b-bottom) and therefore a much poorer match with bottom salinity.

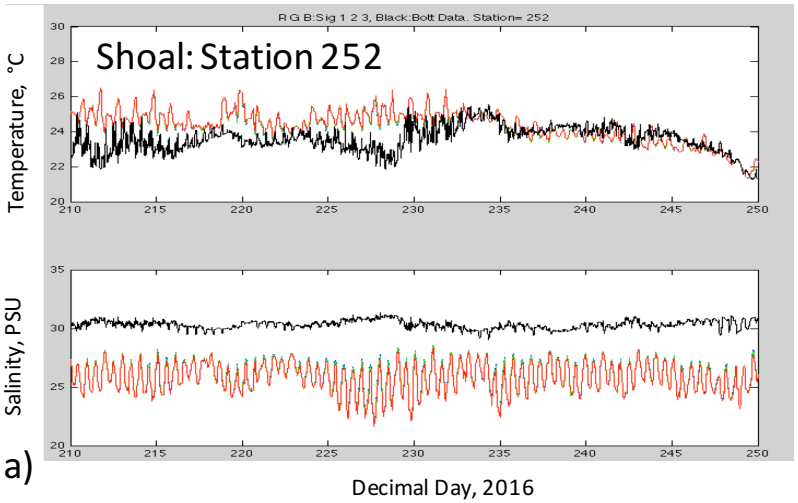

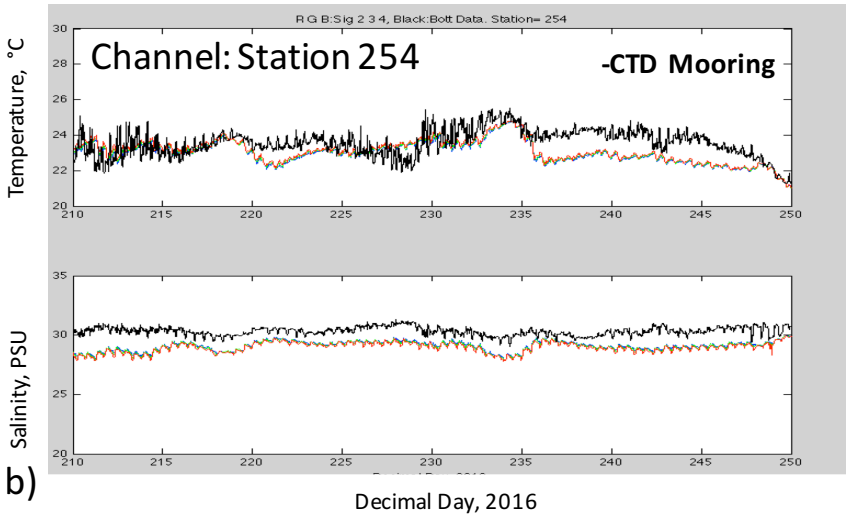

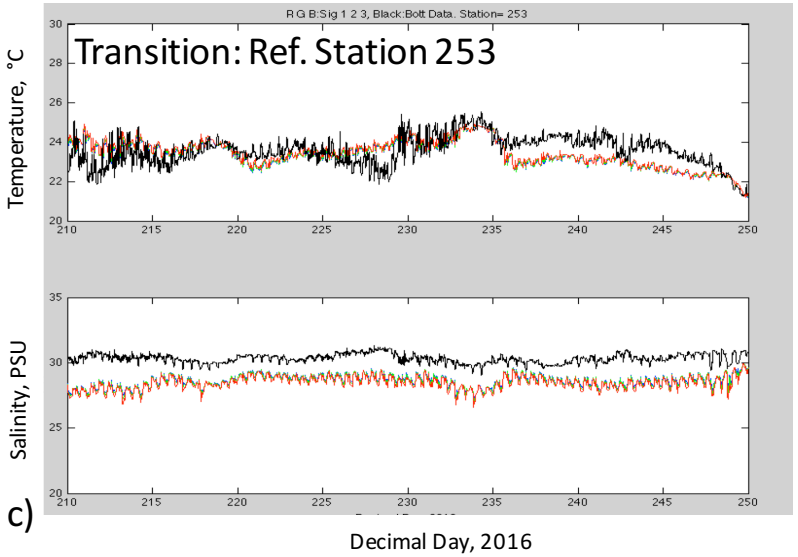

Figure 40. Sequence of temperature (top) and salinity (bottom) time series plots in a grid surrounding the ADCP/CTD mooring and BR buoy for ROMS run with increased vertical mixing (K_v, five times larger). ROMS near-bottom temperature-salinity values vary little for sigma values of 1 (red), 2 (green) and 3 (blue). Bottom data values are shown in black. a) Station 252, on shallow western shoal, 2m depth. b) Station 254 in shipping channel, >10m depth. Plots are from the depth of ~7-8m depth of the ADCP. c) Reference site, at the ADCP, in 7m of water. Enhanced vertical mixing improves the temperature data-model match at all locations, including the ADCP site, station 253 (c). The salinity data-model match remains weak on the shoal (a), marginal at the ADCP (b) and good in the channel, at the depth of the ADCP (c).

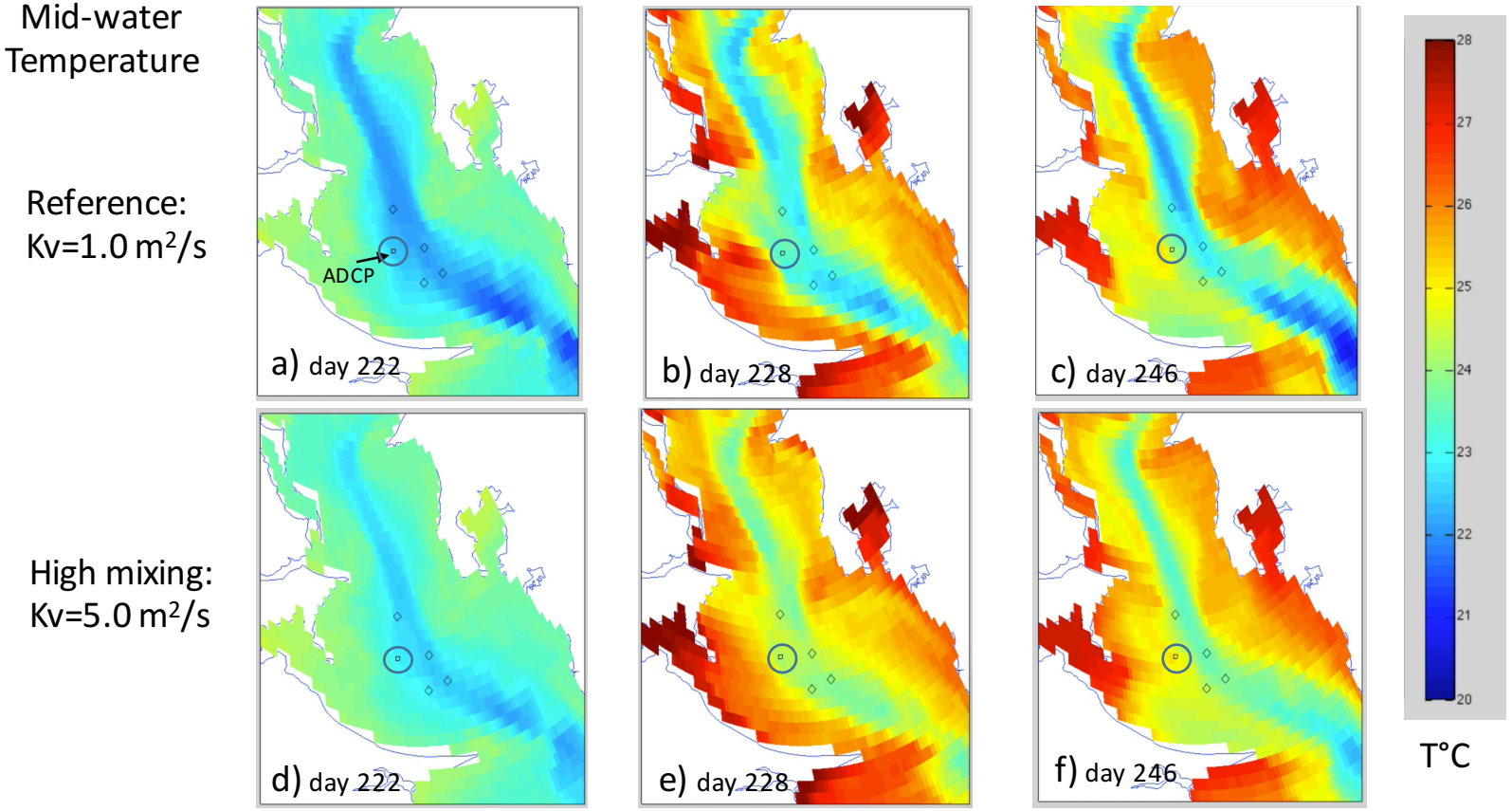

Figure 41. Mapview plots of temperature at a mid-water column depth, comparing reference run (Kv=1.0 m^2/s) (top row) to the higher vertical mixing case (Kv=5 m^2/s) (bottom row). Plots are for different days and highlight how differential mixing within neighboring sections of the estuary can drift past the sampling station, creating non-local signals in the time series data. In each of the high mixing cases, the ADCP sits along a hydrographic boundary such that subtle changes in lateral/vertical mixing and advection of fronts can influence time series records at the mooring location.

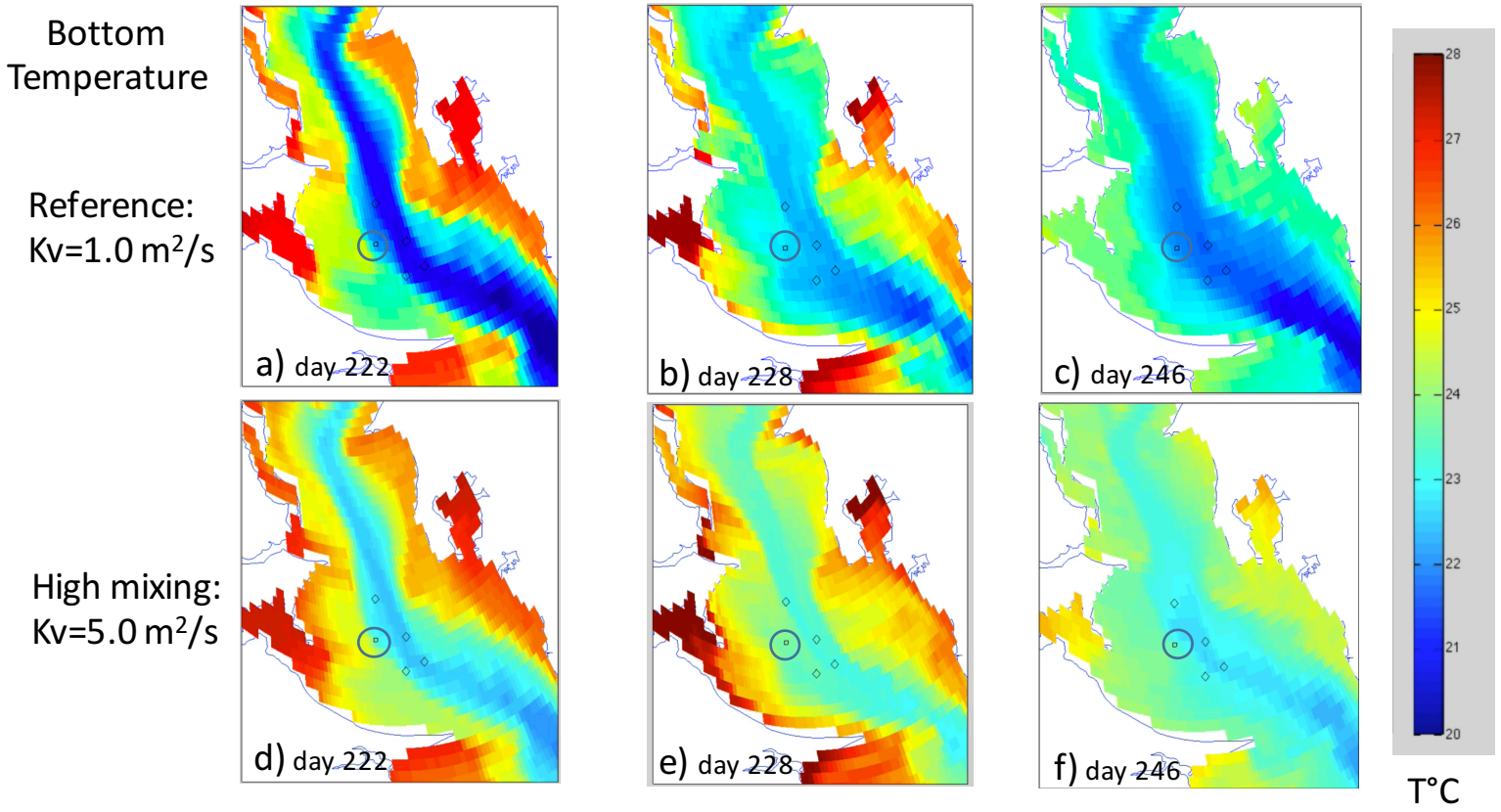

Figure 42. Mapview plots showing temperature of near-bottom water, for the reference case (a-c) and with higher vertical mixing (Kv=5 m^2/s) (d-f). Plots are for different days as labeled. As in Figure 41, enhanced vertical mixing can shift the locations of strong lateral hydrographic gradients/boundaries. For this case, enhanced mixing warms shoal bottom water that moves past the ADCP location, making a better fit with observed values.

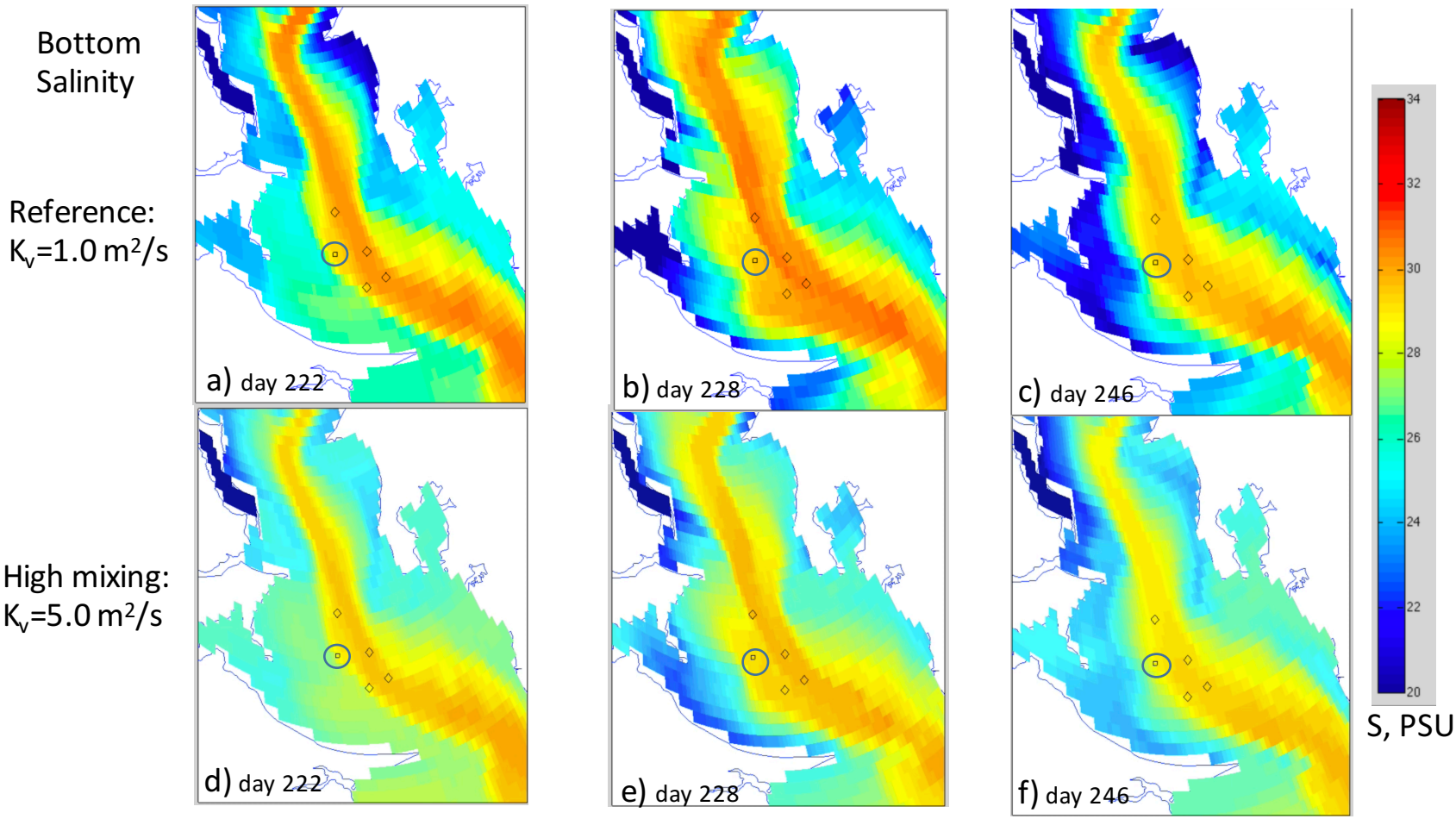

Figure 43. Similar to **Figure 42**, but for mapview plots of **salinity of near-bottom water**, for the reference (top row) and higher vertical mixing case (Kv=5 m²/s) (bottom row). Plots are for different days as labeled. As in Figure 42, enhanced vertical mixing can shift the locations of strong lateral hydrographic gradients/boundaries. In this instance, higher vertical mixing leads to lower salinity bottom water, creating a worse fit with data.

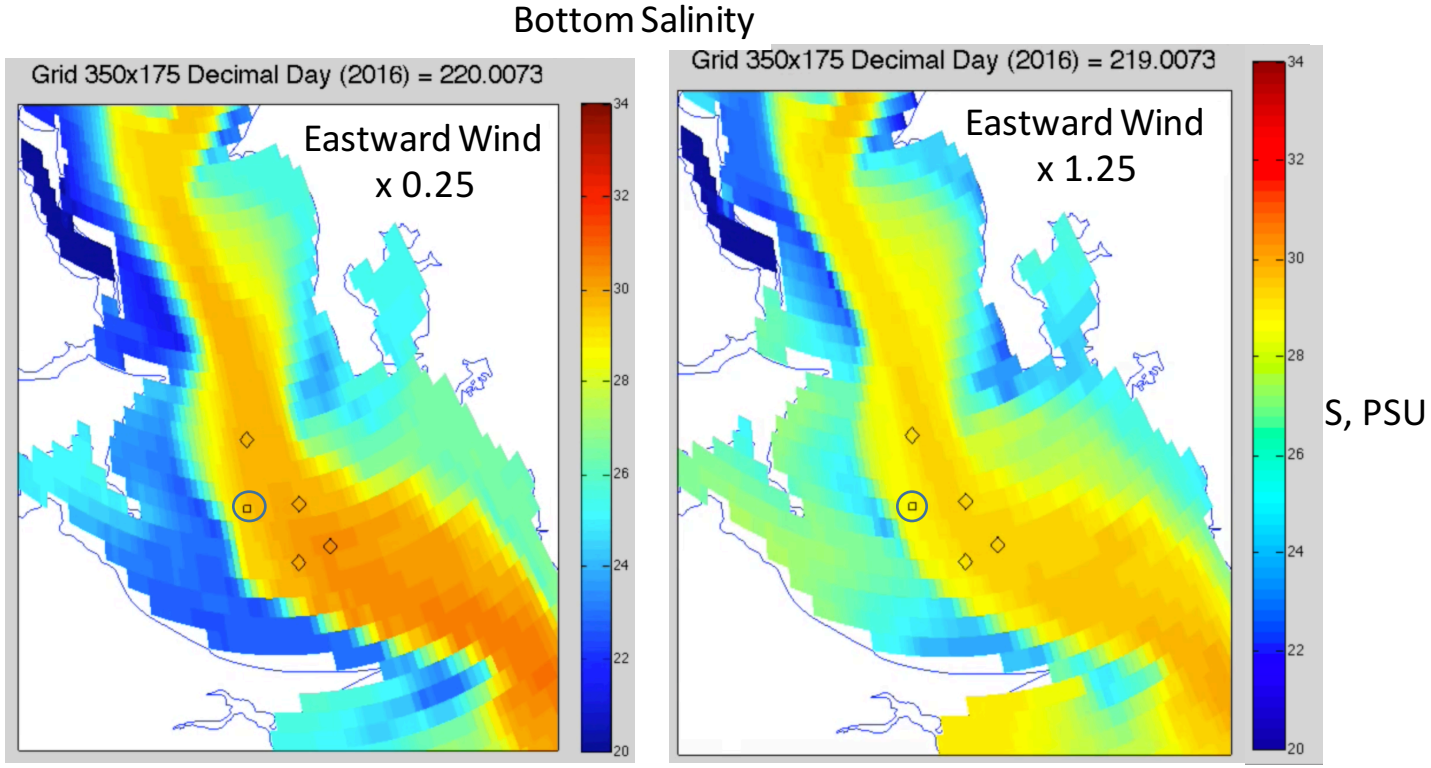

Figure 44. Mapview plots of bottom salinity in the Bullocks Reach region for two cases where eastward components of the applied wind are either reduced (a) or enhanced (b). Colors are in PSU. A weaker eastward wind results in higher salinity recorded at the ADCP site. In this region, it is expected that the narrow east-west orientation of the river should lead to a reduced eastward wind component, which could explain partly, why ROMS running with an artificially high eastward wind, reads fresher than observations.

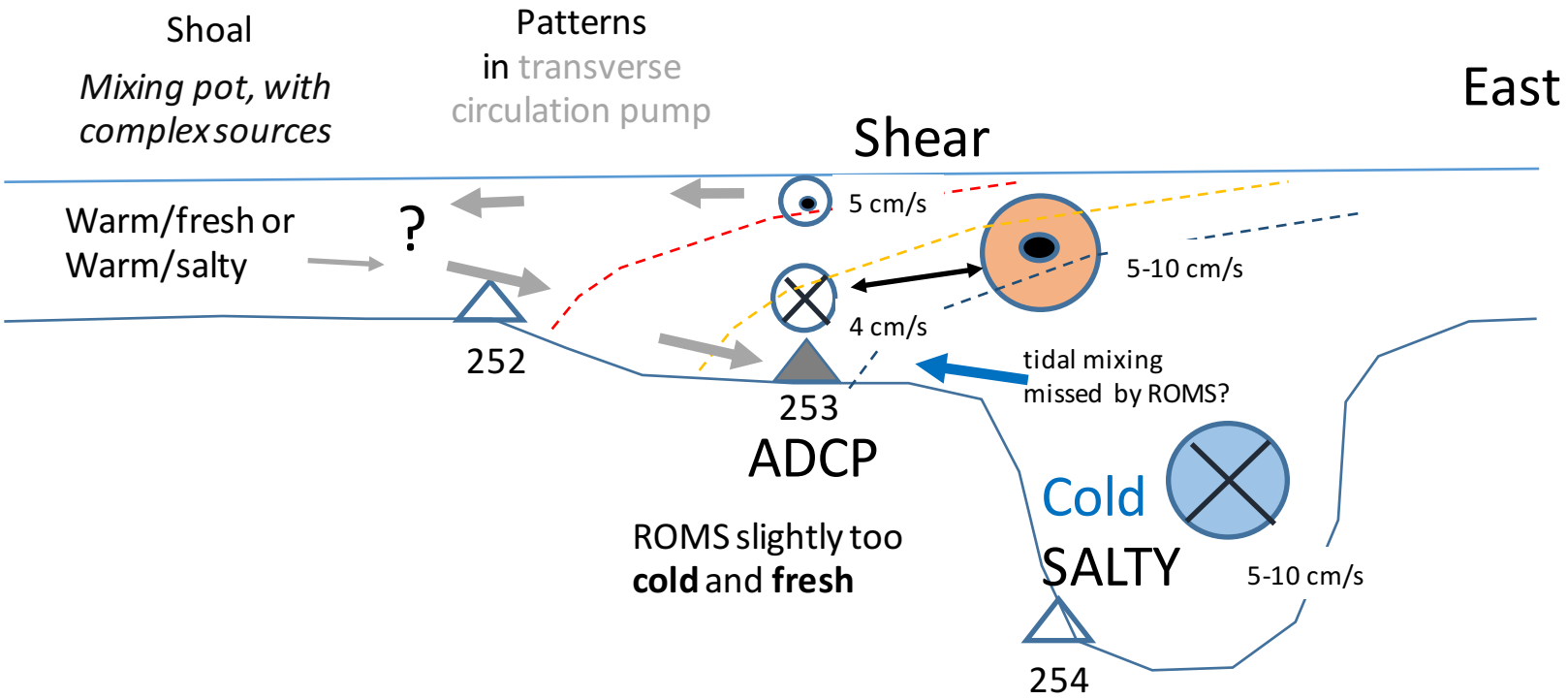

Figure 45. Schematic of flow/hydrography processes in Bullocks Reach area. Shown are stronger subtidal inflow/outflow patterns (channel-parallel flows) as warmer (red)/fresher arrow tips (outflow) and cooler (blue)/saltier arrow tails (inflow). Also shown are potential transverse flow arrows that can pump shoal water to/from the channel (shown as grey arrows). Station numbers discussed in text are shown for shoal (252), transition region (253) and channel locations (254). The shoal is an extremely complex mixing pot that can be fed from the north (south) by fresher (saltier) water. Dashed lines represent the strong lateral gradients in temperature/salinity that occur in the region of the ADCP and Bullocks Reach buoy. The colored, sub-horizontal dashed lines schematically represent a progression to warmer water moving from cooler channel to warmer shoal. A key point is that the Bullocks Buoy appears to be supplied by water heavily influenced by the shoal to the south of the station, and little is known about T-S conditions here.

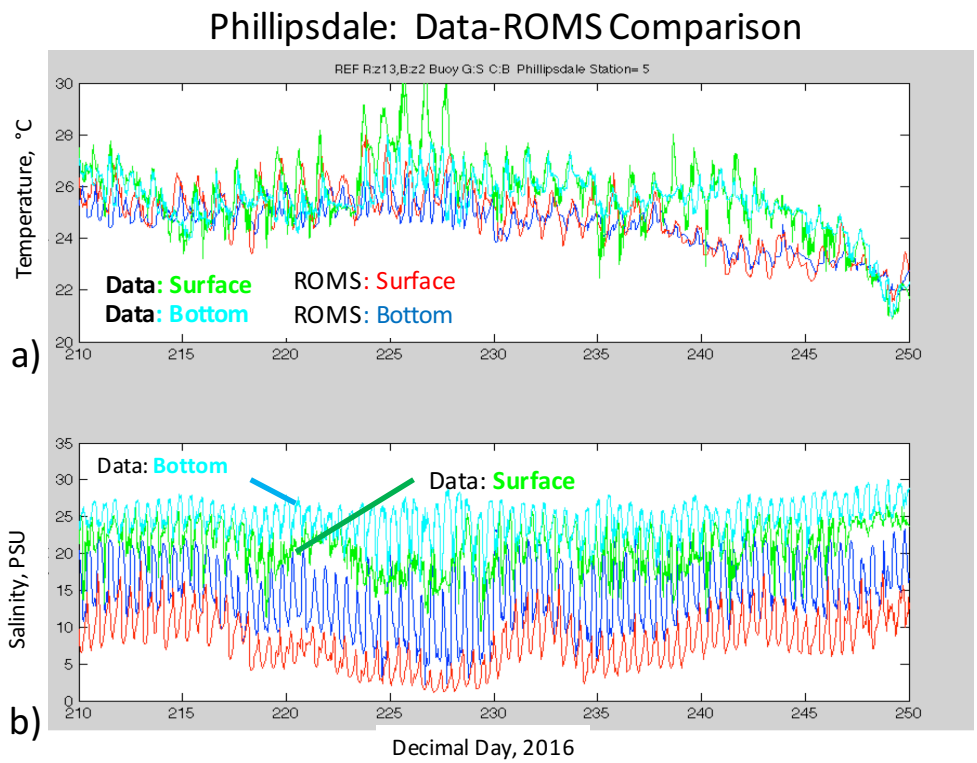

Figure 46. Data-model comparison time series plots of salinity and temperature at ROMS station 5, site of the Phillipsdale fixed-site station (see Figure 2 for location map). Line colors are labeled. Values shown are for the reference case (REF-R3), using actual ROMS forcing conditions from this period of 2016. a) Temperatures are close for the first 3rd of the period. After this buoy data becomes warmer than ROMS values. This may be a remnant of the larger warming event (days 224-228). On average, temperature data values are 2°C warmer than ROMS. b) The model salinities are significantly fresher than data values, by as much as 10 PSU, suggesting the return flow into the Seekonk, and the salt flux associated with this residual flow, are both too weak in the model.

Phillipsdale: Data-ROMS Comparison

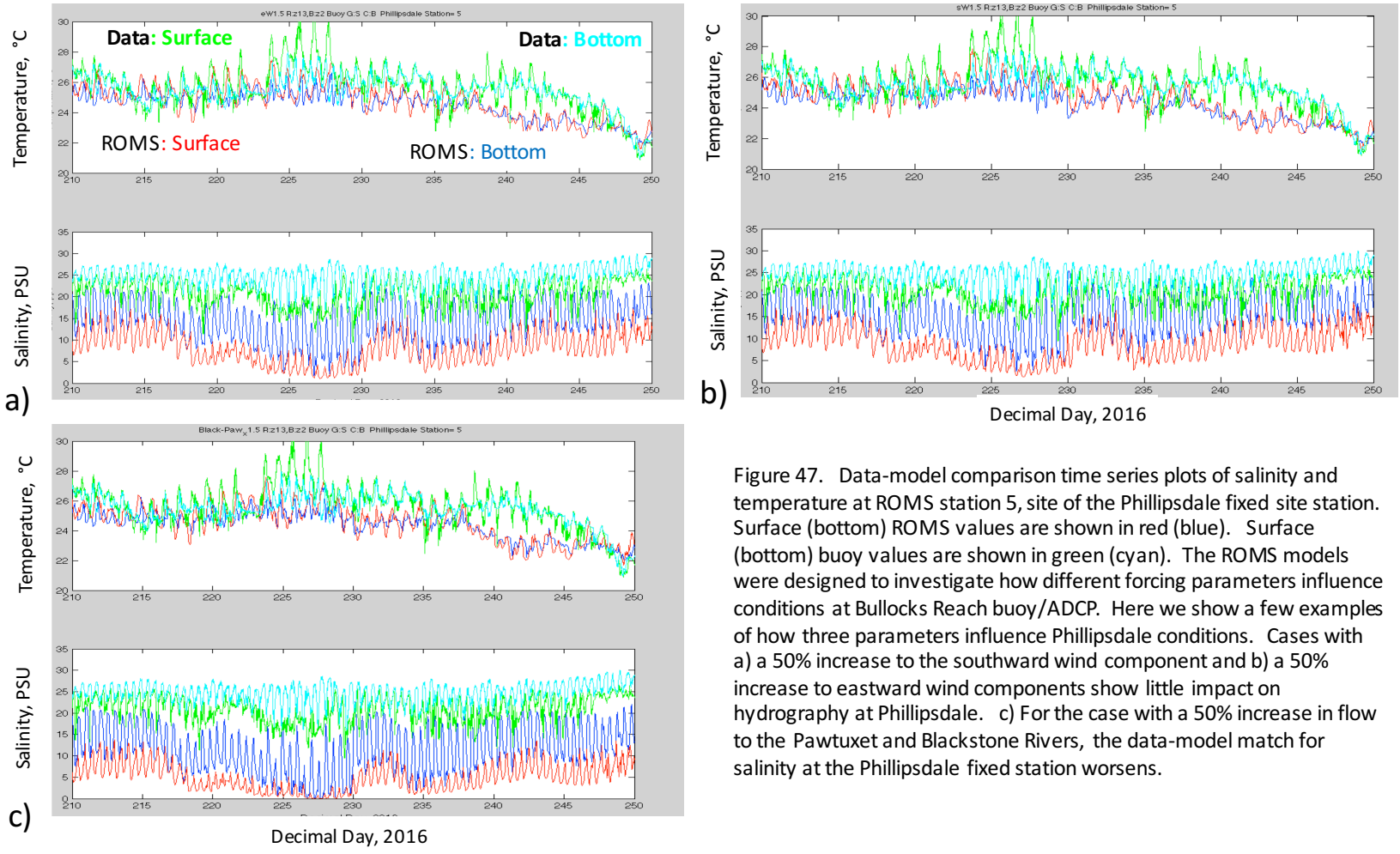

Figure 47. Data-model comparison time series plots of salinity and temperature at ROMS station 5, site of the Phillipsdale fixed site station. Surface (bottom) ROMS values are shown in red (blue). Surface (bottom) buoy values are shown in green (cyan). The ROMS models were designed to investigate how different forcing parameters influence conditions at Bullocks Reach buoy/ADCP. Here we show a few examples of how three parameters influence Phillipsdale conditions. Cases with a) a 50% increase to the southward wind component and b) a 50% increase to eastward wind components show little impact on hydrography at Phillipsdale. c) For the case with a 50% increase in flow to the Pawtuxet and Blackstone Rivers, the data-model match for salinity at the Phillipsdale fixed station worsens.